

# Exterior-point Operator Splitting for Nonconvex Learning

Shuvomoy Das Gupta <sup>\*1</sup>, Bartolomeo Stellato <sup>†2</sup>, and Bart P.G. Van Parys <sup>‡3</sup>

<sup>1</sup>Operations Research Center, Massachusetts Institute of Technology

<sup>2</sup>Department of Operations Research and Financial Engineering, Princeton University

<sup>3</sup>Sloan School of Management, Massachusetts Institute of Technology

## Abstract

In this paper, we present the *nonconvex exterior-point operator splitting* (NExOS) algorithm, a novel linearly convergent first-order algorithm tailored for constrained nonconvex learning problems. We consider the problem of minimizing a convex cost function over a nonconvex constraint set, where projection onto the constraint set is single-valued around local minima. A wide range of nonconvex learning problems have this structure including (but not limited to) sparse and low-rank optimization problems. By exploiting the underlying geometry of the constraint set, NExOS finds a locally optimal point by solving a sequence of penalized problems with strictly decreasing penalty parameters. NExOS solves each penalized problem by applying an outer iteration operator splitting algorithm, which converges linearly to a local minimum of the corresponding penalized formulation under regularity conditions. Furthermore, the local minima of the penalized problems converge to a local minimum of the original problem as the penalty parameter goes to zero. We implement NExOS in the open-source `Julia` package `NExOS.jl`, which has been extensively tested on many instances from a wide variety of learning problems. We study several examples of well-known nonconvex learning problems, and we show that in spite of being general purpose, NExOS is able to compute high quality solutions very quickly and is competitive with specialized algorithms.

## 1 Introduction

This paper considers optimization problems with convex cost functions over nonconvex sets that are *prox-regular* around local minima. A nonempty closed set is prox-regular at a point in the set if projection onto the set is single-valued in a neighborhood of that point [1]. We will indicate in this paper that many problems of practical interest in statistical learning and other fields are inherently nonconvex but enjoy this prox-regularity property. We present the *nonconvex exterior-point operator splitting* (NExOS) algorithm, which is a novel operator splitting algorithm tailored for optimizing over prox-regular sets. The optimization problem of interest here is of the form:

$$\begin{aligned} & \text{minimize} && f(x) + \frac{\beta}{2}\|x\|^2 \\ & \text{subject to} && x \in \mathcal{X}, \end{aligned} \tag{P}$$

where the decision variable  $x$  can be a vector in  $\mathbf{R}^d$  or a matrix in  $\mathbf{R}^{m \times d}$  or a combination of both. We consider a finite-dimensional vector space  $\mathbf{E}$  over the reals, where  $\mathbf{E}$  is equipped with inner

---

\*Corresponding Author: [sdgupta@mit.edu](mailto:sdgupta@mit.edu)

†[bstellato@princeton.edu](mailto:bstellato@princeton.edu)

‡[vanparys@mit.edu](mailto:vanparys@mit.edu)

product  $\langle \cdot | \cdot \rangle$  and norm  $\| \cdot \| = \sqrt{\langle x | x \rangle}$ . As stated previously, the cost function  $f$  is convex, and  $\beta > 0$  is a positive regularization parameter that can be arbitrarily small. The constraint set  $\mathcal{X}$  is nonconvex rendering the problem difficult to solve to global optimality. We only assume that our feasible set decomposes as  $\mathcal{X} = \mathcal{C} \cap \mathcal{N}$ , where  $\mathcal{C}$  is a convex compact set, and  $\mathcal{N}$  is a nonconvex set that is prox-regular around local minima. One can show (see Lemma 3 in §3) that the feasible set  $\mathcal{X}$  inherits the prox-regularity property around local minima from the set  $\mathcal{N}$ .

## 1.1 Applications

The algorithm and the subsequent convergence analysis presented in this paper are applicable to any optimization problem with a convex cost function over a constraint set that is prox-regular around local minima. We single out and discuss applications of particular significance below. Among different prox-regular sets, sparse and low-rank sets are perhaps the most prominent in machine learning and data mining because they allow for greater interpretability, higher speed-ups in computation, and reduced memory requirements [2]. Both sets are at the core of many modern methods dealing with high dimensional data.

**Sparse optimization problems.** Machine learning problems with sparsity constraints can be seen as particular instances of  $(\mathcal{P})$  with  $f$  acting as a loss function,  $\mathcal{C}$  representing a compact convex set, and

$$\mathcal{N} = \left\{ x \in \mathbf{R}^d \mid \mathbf{card}(x) \leq k \right\},$$

being the nonconvex part of the constraint set. Here,  $\mathbf{card}(x)$  counts the number of nonzero elements of the the decision variable  $x$  in  $\mathbf{R}^d$ . Cardinality or sparsity constraints have found applications in many practical settings, *e.g.*, gene expression analysis [3, pp. 2–4], sparse regression [2, pp. 155–157], signal transmission and recovery [4, 5], hierarchical sparse polynomial regression [6], and best subset selection [7], just to name a few.

**Low-rank optimization problems.** Low-rank optimization problems, which are at the core of many fundamental machine learning problems, are in the form  $(\mathcal{P})$  as well. In this case, we have a minimization problem over matrices with  $f$  as a convex cost function,  $\mathcal{C}$  representing a compact convex set, and

$$\mathcal{N} = \left\{ X \in \mathbf{R}^{m \times d} \mid \mathbf{rank}(X) \leq k \right\},$$

corresponding to the nonconvex constraint set. Such low-rank optimization models are critically used in many machine learning problems such as collaborative filtering [2, pp. 279–281], design of online recommendation systems [8, 9], manifold clustering [10], compression of text, image, and video data [11, 12, 13], and low rank kernel learning [14] *etc.*

**Other prox-regular sets.** Closed convex sets are prox-regular everywhere [15, page 612]. Examples of well-known prox-regular sets that are not convex include weakly convex sets [16], proximally smooth sets [17], strongly amenable sets [15, page 612], and sets with Shapiro property [18]. Also, a nonconvex set defined by a system of finitely many inequality and equality constraints for which a basic constraint qualification holds is prox-regular [19].

## 1.2 Related work

**Convex relaxations.** Due to the presence of the nonconvex set  $\mathcal{N}$ , the nonconvex problem ( $\mathcal{P}$ ) discussed previously is  $\mathcal{NP}$ -hard [20, 21]. Until very recently, a common way to deal with this issue in machine learning was to avoid this inherent nonconvexity altogether by carefully reformulating or simply convexifying the original problem. The relaxation of the sparsity constraint leads to the popular Lasso formulation and its many variants [3], whereas relaxation of the low-rank constraints produces the nuclear norm based convex models [22, 23]. The basic advantage of the convex relaxation technique is that, in general, a globally optimal solution to a convex problem can be computed reliably and efficiently [24, §1.1], whereas for nonconvex problems a local optimal solution is often the best one can hope for. Furthermore, if certain statistical assumptions on the data generating process are made, then it is possible to recover exact solutions to the original nonconvex problems with high probability by solving the convex relaxations (see [3] and the references therein). However, if these stringent assumptions do not hold, then solutions to the convex formulations can be of poor quality and may not scale very well [2, §6.3 and §7.8]. In this situation, the nonconvexity of the original problem must be confronted directly, because such nonconvex formulations capture the underlying problem structures far better than their convex counterparts.

**Nonconvex optimization methods in unconstrained setup.** For the reasons mentioned before, in the last few years, there has been significant interest in addressing the nonconvexity present in many learning problems directly. In this approach, the algorithms that are most frequently employed are first-order algorithms based on operator splitting. Examples of such operator splitting algorithms include projected gradient descent (a special case of forward-backward splitting), proximal point algorithm, alternating direction method of multipliers (ADMM), Douglas-Rachford splitting, alternating minimization, and variants thereof. Such operator splitting algorithms are favored by machine learning practitioners due to their low computational cost per iteration, parallelizability, and simplicity. Gradient descent and its stochastic variations are probably the most used algorithms in training unconstrained deep learning models [25, §8.3]. Closely related stochastic gradient descent algorithms with adaptive learning rates, *e.g.*, AdaGrad [26], RMSProp [25, §8.5], and Adam [27] are among the most widely known optimization methods due in no small part to their recent use in training deep neural networks. As the literature on unconstrained nonconvex optimization is quite large, we refer the interested readers to [28, Chapter 6] and the references therein.

**ADMM-based heuristics for constrained nonconvex problems.** When it comes to solving nonconvex problems with constraints, heuristics based on Douglas-Rachford splitting and ADMM have gained the most traction in the last few years. ADMM and Douglas-Rachford splitting are equivalent to each other subject to commutation of the underlying operators, hence we use the terms interchangeably [29]. Though ADMM was originally designed to solve convex optimization problems, since the idea of implementing this algorithm as a general purpose heuristic to solve nonconvex optimization problems was introduced in [30, §9.1-9.2], ADMM-based heuristics have been applied successfully to approximately solve nonconvex problems in many different application areas. Erseghe implements ADMM to solve the distributed optimal power flow problem in [31]. In [32], Wen *et al.* propose an ADMM-based algorithm to solve the classical and psychographic phase retrieval problems and empirically show that the algorithm outperforms convex relaxation based approaches. To solve clustering problems over partially observed networks, Aybat *et al.* investigate

the performance of an ADMM-based heuristic in [33] and show that under certain setups, their approach does better than the robust PCA method. Takapoui *et al.* introduce an ADMM-based heuristic in [34] and its extension in [35] to solve mixed-integer quadratic programming with applications in control and maximum-likelihood decoding problems. In [36], Diamond *et al.* extend the approach proposed in [34] to a broader class of nonconvex problems, and they integrate the method into the widely used optimization modeling language CVXPY [37]. Taylor *et al.* implement a scalable ADMM algorithm for training neural networks in [38].

The biggest drawback of the referenced ADMM-based heuristics comes from the fact that they take an algorithm designed to solve convex problems and apply it verbatim to a nonconvex setup. As a result, these algorithms often fail to converge, and even when they do, it need not be a local minimum, let alone a global one [39, §2.2]. Furthermore, empirical evidence suggests that the iterates of these algorithms may diverge even if they come arbitrarily close an optimal solution during some iteration. In addition, even when the iterates do converge to a limit point, these heuristics cannot identify this limit point as a saddle point, local minimum, or neither [36, §9.1-9.2]. The main reason behind this inability is that these ADMM-based heuristics do not establish a clear relationship between the local minimum of  $(\mathcal{P})$  and the fixed point set of the underlying operator that controls the iteration scheme.

**Convergence analysis for nonconvex ADMM.** Great progress has been made in the last few years on understanding convergence of ADMM and Douglas-Rachford splitting for certain nonconvex setups. In [40], Wang *et al.* study convergence analysis of ADMM for minimizing a nonconvex function over an affine set. Li and Pong investigate convergence analysis of ADMM for minimizing the sum of a smooth function with a bounded Hessian and a nonsmooth function with an easy-to-compute proximal operator [41]. Gao *et al.* consider ADMM applied to problems with multiaffine constraints and nonconvex cost function in [42]; they show that the algorithm, under mild technical conditions, converges to the set of constrained stationary points, which can be strengthened further to convergence to a single constrained stationary point if the Kurdyka-Łojasiewicz property holds. In [43], Boţ *et al.* propose two numerical algorithms based on ADMM in a fully nonconvex settings and establish convergence under mild conditions on the sequence of variable metrics and assuming the Kurdyka-Łojasiewicz property on a regularization of the augmented Lagrangian. Finally, in their recent paper [29], Themelis and Patrinos, considerably simplify the convergence analysis of nonconvex ADMM and Douglas-Rachford splitting using the *proximal-envelope* techniques [44, Chapter 3] and establish tight convergence results under less restrictive conditions.

Here we note that the goals and scope of our paper are somewhat different in contrast with [40, 41, 42, 43, 29]. Broadly speaking, these papers investigate convergence analysis of Douglas-Rachford splitting and ADMM applied to different nonconvex problems and provide deep insight into the qualitative behavior of the algorithms. On the contrary, we focus on  $(\mathcal{P})$  that encompasses many machine learning problems of significant current interest, design a tailored algorithm exploiting the problem structure based on operator splitting, provide a convergence analysis of the proposed algorithm, and finally implement and extensively test the algorithm on important nonconvex learning problems in the context of both synthetic and real-world datasets.

### 1.3 Contributions

The main contribution of this work is to propose the *nonconvex exterior-point operator splitting* (NExOS) algorithm: a novel first-order algorithm tailored for learning problems with convex cost functions over constraint sets that are prox-regular around local minima. The term *exterior-point* originates from the fact that the iterates approach a local minimum from outside of the feasible region; it is inspired by the convex exterior-point method first proposed by Fiacco and McCormick in the 1960s [45, §4].

By exploiting the prox-regularity of the constraint set around local minima, we construct an iterative method that finds a locally optimal point of the original problem by solving a sequence of penalized formulations with strictly decreasing penalty parameters. Each penalized problem is solved by applying an *outer iteration* algorithm that implements a variant of the Douglas-Rachford splitting algorithm. Beyond merely avoiding the drawbacks of the above-mentioned heuristics, our algorithm is shown to enjoy four main desirable characteristics:

1. Our penalization approach is *asymptotically exact*: the accuracy of the penalized problem can be made arbitrarily precise by reducing only one penalty parameter.
2. The penalized objective functions are locally strongly convex and smooth (hence differentiable) in the regions of interest.
3. With a controlled reduction in the penalty parameter, the local minimum of the penalized objective corresponding to a larger penalty parameter is designed to fall in the convex and smooth region associated with the smaller penalty parameter, thus ensuring (linear) convergence of the algorithm to the new local minimum under mild technical conditions.
4. As the penalty parameter goes to zero, the local minima of the penalized problems converge to a local minimum of the original problem.

We also implement NExOS in the open-source Julia package `NExOS.jl` available at

<https://github.com/Shuvomoy/NExOS.jl>

and test it extensively on many instances of different nonconvex learning problems that fit our setup with an emphasis on sparse and low-rank optimization problems. We find that NExOS can compute high quality solutions to these problems very quickly at a speed that is competitive with specialized algorithms.

### 1.4 Organization of the paper

The paper is organized as follows. In §2, we present the intuition behind and construction of NExOS. We provide convergence analysis of the algorithm in §3. In §4, we discuss how to initialize and select different parameters introduced in NExOS in practice. Then we demonstrate the performance of our algorithm on several nonconvex machine learning problems of significant current interest using `NExOS.jl` in §5. The concluding remarks are presented in §6.

## 2 Nonconvex exterior-point operator splitting algorithm

To develop our operator splitting algorithm, in §2.1, we introduce first an exact penalization formulation of  $(\mathcal{P})$ . Subsequently, we discuss how working with such a penalization formulation offers

several benefits both in theory and practice. Then in §2.2, we present Algorithm 1 that outlines NExOS. Broadly speaking, NExOS solves a sequence of the aforementioned penalized optimization problems with strictly decreasing penalty parameters, where each penalized problem is solved by applying an *outer iteration* algorithm implementing Algorithm 2—a variant of Douglas-Rachford splitting. Finally, we justify that in the context of our problem setup, Douglas-Rachford splitting is the most suitable algorithm to execute the outer iterations.

## 2.1 An asymptotically exact penalization of the original problem

We denote the indicator function of the constraint set  $\mathcal{X}$  as:

$$\iota(x) = \begin{cases} 0, & \text{if } x \in \mathcal{X} \\ \infty, & \text{else,} \end{cases}$$

which is nonconvex in our setup. The indicator function allows us to represent the constrained problem ( $\mathcal{P}$ ) as the unconstrained but equivalent problem:

$$\text{minimize } f(x) + \frac{\beta}{2}\|x\|^2 + \iota(x). \quad (\mathcal{P})$$

The shortcomings of the operator splitting heuristics, which we discussed in the §1.2, are mostly due to the ill-conditioned nature of the indicator function. In a convex setup, the indicator function of the constraint set is a convex function and has a well-defined subdifferential operator [46, Example 8.3, Theorem 21.2]. However, in a nonconvex setup, the indicator function is highly nonconvex and the subdifferential operator is difficult to work with. We instead describe an asymptotically exact penalization for ( $\mathcal{P}$ ), where we replace the indicator function  $\iota$  with its Moreau envelope, which, in presence of the regularizer  $(\beta/2)\|\cdot\|^2$ , is locally convex and differentiable at points where  $\mathcal{X}$  is prox-regular.

### 2.1.1 An approximation of $\iota$ via Moreau envelope

We define the Moreau envelope of the indicator function  $\iota$  as:

$$\begin{aligned} {}^\mu\iota(x) &= \min_y \left( \iota(y) + \frac{1}{2\mu}\|y - x\|^2 \right) \\ &= \min_{y \in \mathcal{X}} \frac{1}{2\mu}\|y - x\|^2 \\ &= \frac{1}{2\mu}d^2(x), \end{aligned} \quad (1)$$

where  $d(x)$  is the Euclidean distance of the point  $x$  from the set  $\mathcal{X}$ .

**Properties of  ${}^\mu\iota$ .** The function  ${}^\mu\iota$ , though nonconvex, has many desirable attributes that greatly simplify design and convergence analysis of our algorithm. We summarize these properties below; the first four follow from [46, Proposition 12.9] and [15, Theorem 1.25], and the last one is proved in Lemma 4 of §3.2.

1. **Bounded.** The function  ${}^\mu\iota$  is bounded on every compact set. In contrast,  $\iota$  is an extended valued function that takes the value  $+\infty$  outside the set  $\mathcal{X}$ .

2. **Finite and jointly continuous.** For every  $\mu > 0$  and  $x \in \mathbf{E}$ , the function  ${}^\mu\iota(x)$  is jointly continuous and finite. Therefore,  ${}^\mu\iota$  is continuous on  $\mathbf{E}$ . In contrast, the indicator function  $\iota$  is not continuous.
3. **Accuracy of approximation controlled by  $\mu$ .** With decreasing  $\mu$ , the approximation  ${}^\mu\iota$  monotonically increases to  $\iota$ , *i.e.*, for any positive  $\mu_1, \mu_2$  such that  $0 \leq \mu_1 \leq \mu_2$ , we have

$$0 \leq {}^{\mu_2}\iota(x) \leq {}^{\mu_1}\iota(x) \leq \iota(x)$$

for any  $x \in \mathbf{E}$ .

4. **Asymptotically equal to  $\iota$ .** The approximation  ${}^\mu\iota$  is asymptotically equal to  $\iota$  as  $\mu$  goes to zero, *i.e.*, we have the point-wise limit

$$\lim_{\mu \downarrow 0} {}^\mu\iota(x) = \iota(x)$$

for all  $x \in \mathbf{E}$ .

5. **Local convexity and differentiability around points of interest.** Adding any quadratic regularizer to  ${}^\mu\iota$  makes the sum locally convex and differentiable around points of interest. To be precise, if at  $x$ , the set  $\mathcal{X}$  is prox-regular, then for any value of  $\beta > 0$ , the function  ${}^\mu\iota(x) + \frac{\beta}{2}\|x\|^2$  is convex and differentiable on a neighborhood of  $x$ . We prove this result in Lemma 4 of §3.2.

### 2.1.2 Exterior-point minimization function

The features of  ${}^\mu\iota$  discussed above motivate us to consider the following penalization formulation of  $(\mathcal{P})$ :

$$\text{minimize } f(x) + \underbrace{\left( {}^\mu\iota(x) + \frac{\beta}{2}\|x\|^2 \right)}_{\equiv \mu_{\natural}(x)}, \quad (\mathcal{P}_\mu)$$

where  $x \in \mathbf{E}$  is the decision variable, and  $\mu$  is a positive *penalty parameter*. We call the cost function in  $(\mathcal{P}_\mu)$  an *exterior-point minimization function*; the term is inspired by [45, §4.1]. The notation  $\mu_{\natural} \equiv {}^\mu\iota + \frac{\beta}{2}\|\cdot\|^2$  introduced in  $(\mathcal{P}_\mu)$  not only reduces notational clutter, but also alludes to a specific way of splitting the objective into two summands  $f$  and  $\mu_{\natural}$ , which will ultimately allow us to establish linear convergence of our algorithm in §3.

In  $(\mathcal{P}_\mu)$ , the function  $\mu_{\natural}$  acts as a better-behaved version of  $\iota$ , which imposes a high penalty whenever a constraint is violated. Also,  $\mu_{\natural}$  acts as an asymptotically exact penalty function, *i.e.*, as  $\mu \rightarrow 0$ , we have

$$f(x) + \mu_{\natural}(x) \rightarrow f(x) + \frac{\beta}{2}\|x\|^2 + \iota(x)$$

for every  $x \in \mathbf{E}$ , and

$$f(x^*) + \mu_{\natural}(x^*) \rightarrow f(x^*) + \frac{\beta}{2}\|x^*\|^2,$$

where  $x^* \in \mathcal{X}$  is an optimal solution to  $(\mathcal{P})$ , which follows from [15, Theorem 1.25] and Theorem 2 that we prove in §3. Hence for a small enough value of the penalty parameter  $\mu$ , solving  $(\mathcal{P}_\mu)$  suffices for all practical purposes.

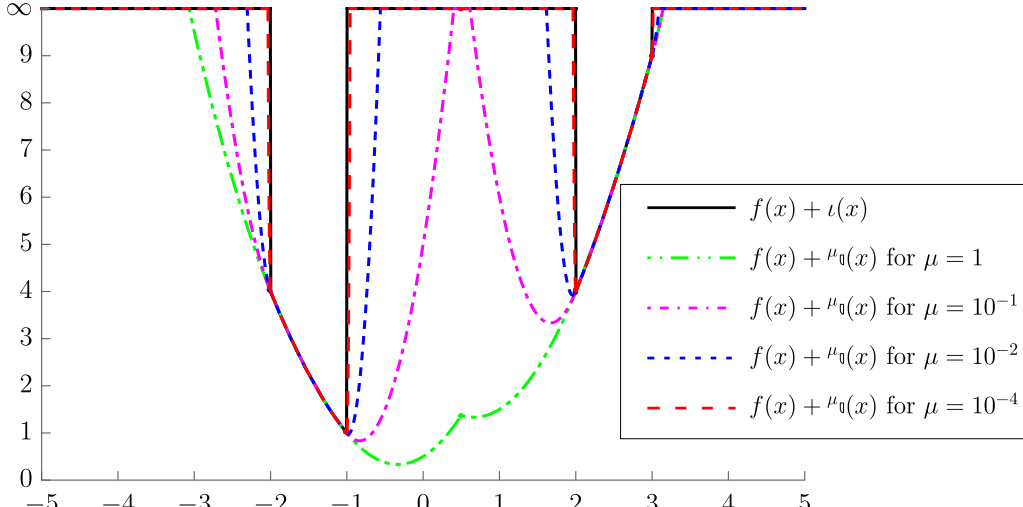


**Figure 1:** An illustration of how  $(\mathcal{P}_\mu)$  compares against  $(\mathcal{P})$  for different values of  $\mu$ .

**Illustrative example.** To provide intuition on how the exterior-point minimization function in  $(\mathcal{P}_\mu)$  compares against the original minimization function in  $(\mathcal{P})$ , we provide an illustrative one-dimensional example in Figure 1. Figure 1 captures all the key properties of the penalization scheme proven in §3. In this figure,  $f = (1/2)(\cdot)^2$ ,  $\beta = 1$ ,  $\mathcal{X} = [-2, -1] \cup [2, 3]$ , where  $\mathcal{X}$  is prox-regular everywhere. The problem has two local minima, one at  $-1$  and one at  $2$ . We see that for larger values of  $\mu$ ,  $(\mathcal{P}_\mu)$  is not a good approximation of  $(\mathcal{P})$ , but around each local minimum there is a relatively large region where  $f + \mu_0$  is strongly convex and smooth. As  $\mu$  gets smaller,  $(\mathcal{P}_\mu)$  becomes a more accurate approximation of  $(\mathcal{P})$ , though the regions of convexity and smoothness around local minima shrink. For  $\mu = 10^{-4}$ ,  $(\mathcal{P}_\mu)$  is identical to  $(\mathcal{P})$  for all practical purposes.

When  $\mu$  is large, the region of convexity and smoothness around a local minimum  $x_\mu$  of  $f + \mu_0$  is larger, and finding  $x_\mu$  is easier. However, at this stage  $x_\mu$  might be far from the corresponding local minimum  $\bar{x}$  of  $(\mathcal{P})$ . As  $\mu$  gets smaller,  $x_\mu$  gets closer to  $\bar{x}$ , but the region of convexity and smoothness around  $x_\mu$  shrinks, and it can be more challenging to compute  $x_\mu$ . However, we can circumvent this issue by applying the following intuition. Suppose we have a local minimum  $x_{\mu_1}$  for  $(\mathcal{P}_{\mu_1})$  when  $\mu_1$  is relatively large. Then for a controlled reduction in  $\mu$ , say  $\mu := \mu_2 < \mu_1$ , the previous solution  $x_{\mu_1}$  can be made to fall in the shrunken region of convexity and smoothness for  $(\mathcal{P}_{\mu_2})$  and finding the corresponding local minimum  $x_{\mu_2}$  will be computationally easy again. This controlled reduction of  $\mu$ , where the previous solution falls in the new region of convexity and smoothness, provides the core intuition to the development of our algorithm in the next section.

Now that we have justified the exact penalization  $(\mathcal{P}_\mu)$ , we are in a position to present NExOS.

## 2.2 Description of NExOS

Algorithm 1 outlines NExOS, which solves a sequence of penalized problems of the form  $(\mathcal{P}_\mu)$  with strictly decreasing penalty parameter  $\mu$ . Each outer iteration implements Algorithm 2 that solves  $(\mathcal{P}_\mu)$  for a fixed  $\mu > 0$ .

First, we briefly discuss the reasons for solving a sequence of penalized optimization problems which were foreshadowed in Figure 1. All the statements made here will be justified rigorously in our



convergence analysis presented in §3.

**Good initial point required for linear convergence.** Recall that  $\mu\iota$  is a global underestimator of the indicator function  $\iota$ , which improves with decreasing  $\mu$  and becomes asymptotically equal to  $\iota$  as  $\mu$  approaches 0 (§2.1.1). Hence, in principle, we could start with a very small value of  $\mu$  in  $(\mathcal{P}_\mu)$  and then focus on finding an approximate solution to  $(\mathcal{P})$ . However, in practice, such a one-shot approach may be problematic for the following reasons.

In our convergence analysis, we will show that as long as the initial point for the outer iteration algorithm lies in the region of convexity and smoothness mentioned earlier, our operator splitting algorithm will linearly converge to a locally optimal solution to  $(\mathcal{P}_\mu)$  under mild technical conditions, and roughly speaking, such regions can be called *regions of convergence*. Fortunately, such regions of convergence always exist for any positive value of  $\mu > 0$ . However, as  $\mu$  decreases, the diameter of this convergence zone *may* decrease. As a result, if we start our iteration with a very small positive value of  $\mu$ , and we are not careful, then the initial point may not lie in the convergence region. Hence, for a very small value of  $\mu$ , picking an initial point in the convergence zone requires some careful design choices.

**Need for solving a sequence of optimization problems.** This issue of picking a suitable initial point can be addressed by executing a sequence of *outer iterations*, where each step implements Algorithm 2 to  $(\mathcal{P}_\mu)$  for a fixed value of  $\mu$ . We will start the first outer iteration with a relatively large value of  $\mu$  and then gradually decrease  $\mu$  until a certain termination criterion is met. With the initial larger value of  $\mu$ ,  $(\mathcal{P}_\mu)$  is not a good approximation of the original problem, but it is easier to find a locally optimal solution to  $(\mathcal{P}_\mu)$ , because for a larger  $\mu$  the diameter of the convergence zone is larger. As we reduce  $\mu$ ,  $(\mathcal{P}_\mu)$  becomes a better and better proxy for  $(\mathcal{P})$ , but the diameter of the associated region of convergence *may* shrink, and the challenge is to keep the initial iterate in that smaller zone. In §3, we show that for a reasonable reduction in  $\mu$ , the solution found by the previous value of the penalty parameter does not go outside the new convergence region and acts as an a good initial point for the new outer iteration algorithm. This allows for linear convergence to the solution for the new value of the penalty parameter.

Here we note that conceptually this framework is similar to sequential unconstrained minimization technique (SUMT) [45]. However, the reason why our method requires the outer iterations is fundamentally different than SUMT. An algorithm based on SUMT, *e.g.*, the interior point method, requires multiple outer iterations not only to deal with convex inequality constraints present in the problem but also to avoid a situation where the Hessian varies rapidly near the boundary of the constraint set [24, page 564]. On the other hand, NExOS, which is designed for nonconvex problems, needs the outer iterations to keep the iterates in the shrinking regions of convergence and to ensure linear convergence.

**Synopsis of Algorithm 1.** Algorithm 1 requires the following input: the regularization parameter  $\beta$  that is fixed throughout, an initial point  $z_{\text{init}}$ , initial value of the penalty parameter  $\mu_{\text{init}}$ , the minimum value of the same parameter  $\mu_{\text{min}}$ , and a multiplicative factor  $\rho$  that is used to reduce the value of the penalty parameter gradually. The tolerance for the fixed point gap  $\epsilon$  is passed as a parameter into the outer iteration. The output of the algorithm is a locally optimal solution to  $(\mathcal{P}_{\mu_{\text{min}}})$ .

---

**Algorithm 1:** Nonconvex Exterior-point Operator Splitting (NExOS)

---

**given:** regularization parameter  $\beta > 0$ , an initial point  $z_{\text{init}}$ , initial penalty parameter  $\mu_{\text{init}}$ , minimum penalty parameter  $\mu_{\text{min}}$ , tolerance for the fixed point gap  $\epsilon$ , and multiplicative factor  $\rho \in (0, 1)$ .

- 1  $\mu := \mu_{\text{init}}$ .
- 2  $z^0 := z_{\text{init}}$ .
- 3 **while**  $\mu \geq \mu_{\text{min}}$  **do**
- 4     *Outer iteration.* Using the outer iteration algorithm (Algorithm 2), compute  $x_\mu, y_\mu$ , and  $z_\mu$  that solve  $(\mathcal{P}_\mu)$  with tolerance  $\epsilon$ , where  $z_\mu^0 := z^0$  is input as the initial point.
- 5     *Set initial point for next outer iteration.*  $z^0 := z_\mu$ .
- 6     *Update  $\mu$ .*  $\mu := \rho\mu$ .
- 7 **return**  $x_\mu, y_\mu$ , and  $z_\mu$

---

In lines 1-2 of Algorithm 1, we set the initial values for  $\mu$  and  $z_\mu^0$ , where the latter is the starting point for the very first outer iteration.

Line 4 refers to the outer iteration in Algorithm 1, which consists of the operator splitting algorithm (Algorithm 2) that solves  $(\mathcal{P}_\mu)$  for fixed  $\mu$ . Each outer iteration in turn runs a number of *inner iterations* of Algorithm 2 to compute the above-mentioned locally optimal solution to a given tolerance  $\epsilon$ .

In line 5 of the algorithm, we set  $z_\mu$ —solution corresponding to the third iterate for the present outer iteration—as the initial point for the next outer iteration. Line 6 reduces  $\mu$  by a factor of  $\rho$ .

**Constructing Algorithm 2 from Douglas-Rachford splitting.** We now discuss how to construct Algorithm 2 by applying Douglas-Rachford splitting to  $(\mathcal{P}_\mu)$ . If we apply Douglas-Rachford splitting [46, page 401] to  $(\mathcal{P}_\mu)$  with penalty parameter  $\mu$ , we have the following variant with three inner iterations:

$$\begin{aligned} x_\mu^{n+1} &= \mathbf{prox}_{\gamma f}(z_\mu^n) \\ y_\mu^{n+1} &= \mathbf{prox}_{\gamma \mu_0}(2x_\mu^{n+1} - z_\mu^n) \\ z_\mu^{n+1} &= z_\mu^n + y_\mu^{n+1} - x_\mu^{n+1}, \end{aligned} \tag{DRS}$$

where we have used the notion of a *proximal operator* that is defined as follows. For a function  $g$  (not necessarily convex), its proximal operator at point  $x$  with parameter  $\lambda > 0$  is defined as:

$$\mathbf{prox}_{\lambda g}(x) = \operatorname{argmin}_y \left( g(y) + \frac{1}{2\lambda} \|y - x\|^2 \right), \tag{2}$$

which may be set-valued. For a convex function, the proximal operator is always single-valued [47]. In (DRS),  $x_\mu^n, y_\mu^n$  and  $z_\mu^n$  are the iterates, the superscript  $n \in \mathbf{N}$  denotes the iteration counter, and the subscript  $\mu$  indicates the current value of the penalty parameter. With a slight abuse of notation, by  $\mathbf{prox}_{\gamma \mu_0}(2x_\mu^{n+1} - z_\mu^n)$  we denote one arbitrary solution in (DRS) rather than the entire set-valued map as in the original definition (2). This does not cause a problem technically, because our algorithm is guaranteed to operate at points where the above-mentioned map is single-valued by exploiting the prox-regularity of the constraint set.

Next, we discuss how to compute the inner iterations involving proximal operator explicitly.

**Computing  $\mathbf{prox}_{\gamma f}$ .** The function  $f$  is convex and computing the proximal map  $\mathbf{prox}_{\gamma f}$  is equivalent to solving a convex optimization problem, which often can be done in closed form for many relevant cost functions [47, Chapter 6].

**Computing  $\mathbf{prox}_{\gamma \mu_{\mathfrak{q}}}$ .** As the function  $\mu_{\mathfrak{q}}$  is nonconvex, the optimization problem to compute its proximal operator can have multiple solutions. The computational cost for  $\mathbf{prox}_{\gamma \mu_{\mathfrak{q}}}$  is the same as computing a projection onto the constraint set  $\mathcal{X}$ , as we will show in Lemma 1 below. Here, the notation  $\mathbf{\Pi}(x)$  denotes the *projection operator* of  $x$  onto the constraint set  $\mathcal{X}$ , defined as

$$\mathbf{\Pi}(x) = \operatorname{argmin}_{y \in \mathcal{X}} (\|y - x\|^2).$$

As  $\mathcal{X}$  is nonconvex, there can be multiple projections onto it from a point outside  $\mathcal{X}$ , hence,  $\mathbf{\Pi}$  can be set-valued. We stress again that, our algorithm is designed to ensure that  $\mathbf{\Pi}$  is single-valued at our iterates.

**Lemma 1** (Computing  $\mathbf{prox}_{\gamma \mu_{\mathfrak{q}}}(x)$ ). *Consider the nonconvex compact constraint set  $\mathcal{X}$  in (P). Denote*

$$\kappa = \frac{1}{\beta\gamma + 1} \in [0, 1], \text{ and } \theta = \frac{\mu}{\gamma\kappa + \mu} \in [0, 1].$$

*Then, for any  $x \in \mathbf{E}$ , and for any  $\mu, \beta, \gamma > 0$ , we have*

$$\mathbf{prox}_{\gamma \mu_{\mathfrak{q}}}(x) = \theta\kappa x + (1 - \theta) \mathbf{\Pi}(\kappa x).$$

*Proof.* See Appendix A.1. □

Combining (DRS), Lemma 8, and Lemma 1, we arrive at Algorithm 2.

---

**Algorithm 2:** Outer Iteration Algorithm for  $(\mathcal{P}_{\mu})$ .

---

**given:** starting point  $z_{\mu}^0$ , tolerance for the fixed point gap  $\epsilon$ , and proximal parameter  $\gamma > 0$ .

- 1  $n := 0$ .
  - 2  $\kappa := \frac{1}{\beta\gamma + 1}$ .
  - 3  $\theta := \frac{\mu}{\gamma\kappa + \mu}$ .
  - 4 **while**  $\|x_{\mu}^n - y_{\mu}^n\| > \epsilon$  **do**
  - 5     Compute  $x_{\mu}^{n+1} := \mathbf{prox}_{\gamma f}(z_{\mu}^n)$ .
  - 6     Compute  $\tilde{y}_{\mu}^{n+1} := \kappa(2x_{\mu}^{n+1} - z_{\mu}^n)$ .
  - 7     Compute  $y_{\mu}^{n+1} := \theta\tilde{y}_{\mu}^{n+1} + (1 - \theta)\mathbf{\Pi}(\tilde{y}_{\mu}^{n+1})$ .
  - 8     Compute  $z_{\mu}^{n+1} := z_{\mu}^n + y_{\mu}^{n+1} - x_{\mu}^{n+1}$ .
  - 9     Update  $n := n + 1$ .
- 
- 10 **return**  $x_{\mu}^n, y_{\mu}^n$ , and  $z_{\mu}^n$ .
-

**Synopsis of Algorithm 2.** We assume to have an initial point  $z_\mu^0$  to start the iteration. Also, we are given the proximal parameter  $\gamma > 0$ , and tolerance for fixed point gap  $\epsilon$ ; in §4 we will describe how to compute these parameters precisely. We initialize our iteration counter  $n$  at zero. We compute two parameters  $\kappa$  and  $\theta$  (introduced in Lemma 1), both in  $[0, 1]$ , which stay fixed throughout the algorithm. Lines 5-8 describe the inner iterations of our operator splitting algorithm until the termination criterion has been met or a maximum number of inner iterations is reached.

Line 5 of Algorithm 2, computes the proximal operator of the function  $f$  with parameter  $\gamma > 0$  at  $z_\mu^n$ .

In line 6, we compute an intermediate iterate  $\tilde{y}_\mu^{n+1}$  that is a scaled version of  $(2x_\mu^{n+1} - z_\mu^n)$  with the damping factor  $\kappa$ .

In line 7, the algorithm computes a convex combination of  $\tilde{y}_\mu^{n+1}$  and  $\Pi(\tilde{y}_\mu^{n+1})$ . In the context of our algorithm, the projection in line 7 will always be unique, a claim that will be apparent from §3 and §4.

Line 8 updates the main iterate  $z_\mu^n$  in terms of the already updated iterates  $x_\mu^{n+1}$  and  $y_\mu^{n+1}$ , and then in line 9 we update our iteration counter  $n$ .

In §3, we will show that, under mild technical assumptions, the iterates  $x_\mu^n, y_\mu^n$  both will linearly converge to a locally optimal solution to  $(\mathcal{P}_\mu)$ ,  $x_\mu^n - y_\mu^n$  will converge to zero, and  $z_\mu^n$  will linearly converge to a fixed point of the underlying operator that controls the iteration scheme.

**Why Douglas-Rachford splitting?** Problem  $(\mathcal{P}_\mu)$  involves minimizing the sum of two functions: a convex function  $f$  and a nonconvex function  $h$ . As the objective is split into two parts in  $(\mathcal{P}_\mu)$ , selecting any variant of some other two-operator splitting algorithm (*e.g.*, forward-backward splitting [48, page 25], Chambolle-Pock algorithm [48, page 32] *etc.*) to implement the outer iteration can work in principle. However, in the context of our problem setup, Douglas-Rachford splitting might be the most suitable choice. In his recent work [49], Ryu shows that Douglas-Rachford splitting is favorably unique in contrast with other two-operator splitting methods, as the former is the only two-operator splitting method that satisfies the following properties simultaneously:

- it converges unconditionally for maximally monotone operators,
- it is constructed only with scalar multiplication, addition, and proximal operators,
- it computes proximal operators only once every iteration, and
- it does not increase the problem size.

In §3, the last three of these desirable properties of Douglas-Rachford splitting are exploited to establish convergence.

### 3 Convergence analysis

This section is organized as follows. First, §3.1 provides a brief roadmap for our convergence analysis. We have made three assumptions in our convergence analysis; the first assumption (Assumption 1)—where  $f$  is taken to be strongly convex and smooth—is considered standard in optimization for machine learning, and the other two (Assumption 2 and Assumption 3) can be justified without incurring any loss of generality. In §3.2, we characterize the nature of the exterior-point minimization

function  $f + \mu \mathfrak{v}$  and how it influences the behavior of the underlying operators of our algorithm. In §3.3, we delineate how the local minima of  $(\mathcal{P}_\mu)$  correspond to the fixed point set of the foregoing operators, and how they relate to the local minima of the original problem  $(\mathcal{P})$ . Then, in §3.4, we present our main convergence results for NExOS. We also briefly discuss what convergence results can be established when Assumption 1 is relaxed.

**Notation.** In this section, we have used the following notation for an operator  $\mathbb{A}$ :

$$\mathbf{fix} \mathbb{A} = \{x \in \mathbf{E} \mid x \in \mathbb{A}(x)\},$$

and

$$\mathbf{zer} \mathbb{A} = \{x \in \mathbf{E} \mid 0 \in \mathbb{A}(x)\}.$$

Furthermore, for every  $x$ , addition of two operators  $\mathbb{A}_1, \mathbb{A}_2 : \mathbf{E} \rightrightarrows \mathbf{E}$ , denoted by  $\mathbb{A}_1 + \mathbb{A}_2$ , is defined as  $(\mathbb{A}_1 + \mathbb{A}_2)(x) = \mathbb{A}_1(x) + \mathbb{A}_2(x)$ , subtraction is defined analogously, and composition of these operators, denoted by  $\mathbb{A}_1 \mathbb{A}_2$ , is defined as  $\mathbb{A}_1 \mathbb{A}_2(x) = \mathbb{A}_1(\mathbb{A}_2(x))$ ; note that order matters for composition. Also, if  $\mathcal{S} \subseteq \mathbf{E}$  is a nonempty set, then  $\mathbb{A}(\mathcal{S}) = \bigcup_{x \in \mathcal{S}} \mathbb{A}(x)$ .

By  $B(x; r)$  and  $\overline{B}(x; r)$ , we denote an open ball and an closed ball of radius  $r$  and center  $x$ , respectively.

### 3.1 Synopsis of the convergence analysis

The convergence analysis of NExOS can be broken into two parts: (i) convergence of the individual outer iteration algorithm (Algorithm 2) and (ii) convergence of the sequence of outer iterations (Algorithm 1).

Convergence of an outer iteration algorithm (Algorithm 2) is controlled by the following operators defined as follows. The Douglas-Rachford operator for  $\mu > 0$  is defined as:

$$\mathbb{T}_\mu = \mathbf{prox}_{\gamma \mu \mathfrak{v}}(2\mathbf{prox}_{\gamma f} - \mathbb{I}) + \mathbb{I} - \mathbf{prox}_{\gamma f}, \quad (3)$$

where  $\mathbb{I}$  stands for the identity operator in  $\mathbf{E}$ , *i.e.*, for any  $x \in \mathbf{E}$ , we have  $\mathbb{I}(x) = x$ . Next, the reflection operator of  $\mathbb{T}_\mu$ , denoted by  $\mathbb{R}_\mu$ , is defined as:

$$\mathbb{R}_\mu = 2\mathbb{T}_\mu - \mathbb{I}, \quad (4)$$

where  $\mu > 0$ . The proximal parameter  $\gamma > 0$  is kept fixed throughout Algorithm 1.

Using these two operators the outer iteration algorithm—Algorithm 2—can be written very compactly in a single line as

$$z_\mu^{n+1} = \mathbb{T}_\mu(z_\mu^n) = \frac{1}{2}\mathbb{R}_\mu(z_\mu^n) + \frac{1}{2}z_\mu^n, \quad (\text{Compact-OI})$$

where  $\mu$  is the penalty parameter and the iterate  $z_\mu^n$  is initialized at the fixed point found in the previous outer iteration.

So, the convergence of Algorithm 2 to a locally optimal solution to  $(\mathcal{P}_\mu)$  requires investigating whether the equivalent scheme (Compact-OI) converges to a fixed point of  $\mathbb{T}_\mu$  and how the fixed point is related to a locally optimal solution. On the other hand, for the sequence of outer iterations,

we need to find out how the locally optimal solution to  $(\mathcal{P}_\mu)$  changes as  $\mu$  is varied and how it is connected to some locally optimal solution of the original problem  $(\mathcal{P})$ . In the following two subsequent sections, we outline what assumptions are imposed on the problem to facilitate establishing such a connection. We finally state our main convergence result in §3.4.

### 3.2 Characterization of $f + \mu \mathbb{0}$ and its effect on $\mathbb{T}_\mu$ and $\mathbb{R}_\mu$

**Assumption regarding strong convexity and smoothness of  $f$ .** We have the following assumption regarding strong convexity and smoothness of the function  $f$ .

**Assumption 1** (Strong convexity and smoothness of  $f$ ). *The function  $f$  in  $(\mathcal{P}_\mu)$  is  $\alpha$ -strongly convex and  $L$ -smooth where  $L > \alpha > 0$ , i.e.,  $f - (\alpha/2)\|\cdot\|^2$  is convex and  $f - (L/2)\|\cdot\|^2$  is concave.*

Assumption 1 is considered a standard assumption in proving convergence results in machine learning [2]. At the end of this section, we will discuss briefly what (weaker) convergence results can be stated when this assumption is relaxed. The  $L$ -smoothness in  $f$  is equivalent to its gradient  $\nabla f$  being  $L$ -Lipschitz everywhere on  $\mathbf{E}$  [46, Theorem 18.15]. This assumption helps us in establishing local convexity and smoothness of the exterior-point minimization function  $f + \mu \mathbb{0}$ .

**Contractive nature of  $2\text{prox}_{\gamma f} - \mathbb{I}$ .** Next, we record the following result from [50, Theorem 1] regarding the contractive nature of the operator  $2\text{prox}_{\gamma f} - \mathbb{I}$  under Assumption 1, which will be used later to prove contractive nature of the underlying operators  $\mathbb{T}_\mu$  and  $\mathbb{R}_\mu$  in Algorithm 2.

**Lemma 2** (The operator  $2\text{prox}_{\gamma f} - \mathbb{I}$  is contractive [50, Theorem 1]). *Under Assumption 1, the proximal operator  $2\text{prox}_{\gamma f} - \mathbb{I}$  associated with the  $\alpha$ -strongly convex and  $L$ -smooths function  $f$  is a contraction mapping for any  $\gamma > 0$  with the contraction factor*

$$\kappa = \max \left\{ \frac{\gamma L - 1}{\gamma L + 1}, \frac{1 - \gamma \alpha}{\gamma \alpha + 1} \right\} \in (0, 1).$$

**Prox-regularity of the constraint set  $\mathcal{X}$ .** We now describe the structure of the constraint set  $\mathcal{X} = \mathcal{C} \cap \mathcal{N}$ , where  $\mathcal{C}$  is compact and convex and  $\mathcal{X}$  is a prox-regular set. Recall that a prox-regular set is defined as follows.

**Definition 1** (Prox-regular set [51]). A nonempty closed set  $\mathcal{S} \subseteq \mathbf{E}$  is prox-regular at a point  $x \in \mathcal{S}$  if projection onto  $\mathcal{S}$  is single-valued on some neighborhood of  $x$ .

The key geometric property that we exploit in our algorithm design and subsequent convergence analysis is that when  $\mathcal{N}$  is a prox-regular set,  $\mathcal{X}$  too is prox-regular in our setup.

**Lemma 3** (Prox-regularity of  $\mathcal{X}$  when  $\mathcal{N}$  is prox-regular). *Consider the nonempty constraint set  $\mathcal{X} = \mathcal{C} \cap \mathcal{N} \subseteq \mathbf{E}$  where  $\mathcal{C}$  is compact and convex and  $\mathcal{N}$  is prox-regular at  $x \in \mathcal{X}$ . Then  $\mathcal{X}$  is prox-regular at  $x$ .*

*Proof.* See Appendix B.1. □

We now state two corollaries which establish the prox-regularity of two nonconvex sets encountered in the context of sparse and rank constrained optimization problems. Using Lemma 3 and the fact that  $\mathcal{N} = \{X \in \mathbf{R}^{m \times d} \mid \mathbf{rank}(X) \leq k\}$  is prox-regular at any point  $X \in \mathbf{R}^{m \times d}$  where  $\mathbf{rank}(X) = k$  [1, Proposition 3.8], we arrive at the following corollary.

**Corollary 1** (Prox-regularity of low-rank constraint set). *Consider the nonempty constraint set  $\mathcal{X} = \mathcal{C} \cap \mathcal{N}$  with matrix decision variable  $X \in \mathbf{R}^{m \times d}$  in  $(\mathcal{P})$ , where  $\mathcal{C}$  is compact and convex and*

$$\mathcal{N} = \left\{ X \in \mathbf{R}^{m \times d} \mid \mathbf{rank}(X) \leq k \right\}$$

*is the low-rank constraint set. Then  $\mathcal{X}$  is prox-regular at any feasible  $X \in \mathbf{R}^{m \times d}$  that satisfies  $\mathbf{rank}(X) = k$ .*

Next, note that we can write the sparsity constraint  $\mathbf{card}(x) \leq k$  for  $x \in \mathbf{R}^d$  as a special case of the low-rank constraint as follows. Define,  $X = \mathbf{diag}(x_1, \dots, x_d) \in \mathbf{R}^{d \times d}$ , i.e., we construct  $X$  by embedding the components of  $x$  in the diagonal entries of  $X$ . Then the sparsity constraint becomes a special case of the low-rank constraint, and we have the following corollary.

**Corollary 2** (Prox-regularity of sparsity constraint set). *Consider the nonempty constraint set  $\mathcal{X} = \mathcal{C} \cap \mathcal{N}$  with vector valued decision variable  $x \in \mathbf{R}^d$  in  $(\mathcal{P})$ , where  $\mathcal{C}$  is compact and convex and*

$$\mathcal{N} = \left\{ x \in \mathbf{R}^d \mid \mathbf{card}(x) \leq k \right\}$$

*is the sparsity constraint set. Then  $\mathcal{X}$  is prox-regular at any feasible  $x \in \mathbf{R}^d$ , that satisfies  $\mathbf{card}(x) = k$ .*

**Local strong convexity and smoothness of  $f + \mu_{\mathfrak{v}}$  and its implications.** We now present the result associated with the local convexity and smoothness of the exterior-point minimization function  $f + \mu_{\mathfrak{v}}$  in Lemma 4. Roughly speaking, this result says that if we are at a point that is not too far from  $\mathcal{X}$ , then around that point the function  $f + \mu_{\mathfrak{v}}$  behaves as a strongly convex and smooth (hence differentiable) function. We have used the concept of nonexpansiveness and firm-nonexpansiveness of an operator in Lemma 4, so we start with their definitions.

**Definition 2** (Nonexpansive and firmly nonexpansive operators). An operator  $\mathbb{A} : \mathbf{E} \rightarrow \mathbf{E}$  is nonexpansive on some set  $\mathcal{S}$  if it is Lipschitz continuous with Lipschitz constant 1 on  $\mathcal{S}$ . On the other hand,  $\mathbb{A}$  is firmly nonexpansive on  $\mathcal{S}$  if its reflection operator  $2\mathbb{A} - \mathbb{I}$  is nonexpansive. A firmly nonexpansive operator is always nonexpansive [46, page 59].

Now we present the result regarding local strong convexity and smoothness of  $f + \mu_{\mathfrak{v}}$  and its implications, which will be used later to establish convergence of our algorithm.

**Lemma 4** (Local strong convexity and smoothness of  $f + \mu_{\mathfrak{v}}$  and nonexpansiveness of  $2\mathbf{prox}_{\gamma\mu_{\mathfrak{v}}} - \mathbb{I}$ ). *Suppose that the constraint set  $\mathcal{X}$  is prox-regular at  $x$  and Assumption 1 holds. Then for any  $\mu > 0$ , there exists an open ball  $B(x; r_{\mu})$  with center  $x$  and radius*

$$r_{\mu} \geq c_x \frac{\beta\mu}{\beta\mu + 1}, \tag{5}$$

(where  $c_x > 0$  is the prox-regularity constant that depends on  $x$ ) such that on  $B(x; r_\mu)$ :

(i) the penalty function  $\mu_\mathfrak{v}$  is convex and differentiable,

(ii) the exterior-point minimization function  $f + \mu_\mathfrak{v}$  in  $(\mathcal{P}_\mu)$  is  $\alpha$ -strongly-convex and  $(L + 2\beta + \frac{2}{\mu})$ -smooth, and

(iii) the operator  $\mathbf{prox}_{\gamma\mu_\mathfrak{v}}$  is equal to  $\mathbb{J}_{\gamma\nabla(\mu_\mathfrak{v})}$ , and it is firmly nonexpansive and single-valued, and its reflection operator  $2\mathbf{prox}_{\gamma\mu_\mathfrak{v}} - \mathbb{I}$  is nonexpansive.

*Proof.* See Appendix B.2. □

In the rest of the paper, the ball  $B(x; r_\mu)$ , where  $f + \mu_\mathfrak{v}$  is strongly convex and smooth, is called the *region of convexity*.

**Contractive nature of the Douglas-Rachford operator  $\mathbb{T}_\mu$  and its reflection  $\mathbb{R}_\mu$ .** A consequence of Lemma 2 and Lemma 4 is that the Douglas-Rachford operator  $\mathbb{T}_\mu$  and its reflection  $\mathbb{R}_\mu$ , defined in (3) and (4), respectively, are contractive around a point of prox-regularity. This is made precise in the following proposition.

**Proposition 1** (Operators  $\mathbb{T}_\mu$  and  $\mathbb{R}_\mu$  are contractive in  $x$  and Lipschitz continuous in  $\mu$ ). *Suppose that the constraint set  $\mathcal{X}$  is prox-regular at  $x$  and Assumption 1 holds. Then for any  $\mu > 0$ , the operators  $\mathbb{T}_\mu$  and  $\mathbb{R}_\mu$  are contractive on the region of convexity  $B(x; r_\mu)$ .*

*Proof.* See Appendix B.3. □

Furthermore, the operators  $\mathbb{T}_\mu$  and  $\mathbb{R}_\mu$  are Lipschitz continuous in  $\mu$  for fixed argument, which is recorded in the following proposition.

**Lemma 5** (Lipschitz continuity of  $\mathbb{T}_\mu$  and  $\mathbb{R}_\mu$ ). *Let  $\mathcal{B}$  be a bounded set in  $\mathbf{E}$ . Then for any  $x \in \mathcal{B}$  and for any  $\gamma > 0$ , the operators  $\mathbb{T}_\mu(x)$  and  $\mathbb{R}_\mu(x)$  are Lipschitz continuous in  $\mu$ .*

*Proof.* See Appendix B.4. □

### 3.3 Relationship between local minima of $(\mathcal{P})$ and $(\mathcal{P}_\mu)$

**Local minima of  $(\mathcal{P})$ .** In this subsection, we indicate how the local minima of  $(\mathcal{P})$  and  $(\mathcal{P}_\mu)$  are related to the operators  $\mathbb{T}_\mu$  and  $\mathbb{R}_\mu$ .

**Definition 3** (Local minimum of  $(\mathcal{P})$ ). A point  $\bar{x} \in \mathcal{X}$  is a local minimum of  $(\mathcal{P})$  if there exists a closed ball  $\overline{B}(\bar{x}; r)$  such that for all  $y \in \mathcal{X} \cap \overline{B}(\bar{x}; r) \setminus \{\bar{x}\}$ , we have

$$f(\bar{x}) + \frac{\beta}{2}\|\bar{x}\|^2 < f(y) + \frac{\beta}{2}\|y\|^2.$$

In the definition above, the strict inequality is due to the strongly convex nature of the objective  $f + \frac{\beta}{2}\|\cdot\|^2$  and follows from [52, Proposition 2.1] and [15, Theorem 6.12].



**Regularity condition on local minimum.** Next, we make the following assumption regarding the geometry of such a local minimum  $\bar{x}$ . In this assumption, we denote by  $G > 0$  an upper bound on the norm of the gradients of  $f$  over  $\bar{B}(\bar{x}; r)$ , which always exists due to [53, Lemma 1, §1.4.2], and let  $M = \|\bar{x}\|$ .

**Assumption 2** (Regularity assumption on local minimum). *At local minimum  $\bar{x} \in \mathcal{X}$  for  $(\mathcal{P})$ , the constraint set  $\mathcal{X}$  is prox-regular, and there exists some  $\eta > 1$  such that the prox-regularity constant  $c_{\bar{x}}$  (as defined in Lemma 4) satisfies the following condition:*

$$c_{\bar{x}} \geq \eta \left( \frac{G}{\beta} + M \right). \quad (6)$$

**Justification for Assumption 2.** Now we justify the assumption above in the context of our problem setup. In our paper, where the focus is on prox-regular constraint sets, the constraint set  $\mathcal{X}$  is prox-regular at a local minimum  $\bar{x} \in \mathcal{X}$  due to Lemma 3. In this case, due to Lemma 4, around the local minimum  $\bar{x}$  of  $(\mathcal{P})$ , for any  $\mu > 0$ , the exterior-point minimization function  $f + \mu \iota$  for the penalized problem  $(\mathcal{P}_\mu)$  is strongly convex and smooth on the region of convexity  $B(\bar{x}; r_\mu)$  and  $r_\mu \geq c_{\bar{x}}\beta\mu/(\beta\mu + 1)$ .

Imposing the lower bound on the prox-regularity constant  $c_{\bar{x}}$  in (6) means that  $r_\mu$ —the radius of convexity of  $f + \mu \iota$  around the local minimum  $\bar{x}$ —is not too small for a larger value of  $\mu$ . This condition is not too stringent, because when  $\mu$  is large,  $(\mathcal{P}_\mu)$  has more weight on  $f + (\beta/2)\|\cdot\|^2$ —the convex part of  $(\mathcal{P})$  and less weight on  $\mu \iota = (1/2\mu)d^2$ —the nonconvex part, so the corresponding minimum  $\bar{x}$  will have larger radius of convexity  $r_\mu$ . As a sanity check, if we make  $\mu \rightarrow \infty$  or if  $\mathcal{X}$  were a convex set, then the prox-regularity constant  $c_{\bar{x}}$  would have been  $+\infty$  around the minimum  $\bar{x}$ , thus satisfying condition (6).

Furthermore, as  $G, M$ , and  $\beta$  are constants that are independent of the problem dimension, by suitably rescaling the problem, it is always possible to ensure that (6) is satisfied. That being said, we may not know in practice what the particular rescaling is.

**Assumption regarding  $(\mathcal{P})$  not being trivial.** Finally, we impose the assumption that a local minimum of  $(\mathcal{P})$  is not the global minimum of its unconstrained convex relaxation. Then we discuss why this assumption does not incur a loss of generality.

**Assumption 3** (Problem  $(\mathcal{P})$  is not trivial). *The unique solution to the unconstrained strongly convex problem*

$$\text{minimize } f(x) + \frac{\beta}{2}\|x\|^2 \quad (7)$$

*does not lie in  $\mathcal{X}$ .*

**Justification for Assumption 3.** This assumption does not incur any loss of generality, because we can solve the unconstrained strongly convex optimization problem (7) and check if the corresponding minimizer lies in  $\mathcal{X}$ ; if that is the case, then that minimizer is also the global minimizer of  $(\mathcal{P})$ , and there is no point in solving the nonconvex problem. As this case that can be easily checked by

solving an unconstrained convex optimization problem (7), imposing Assumption 3 does not cause any loss of generality.

**Attainment of local minimum by the exterior point minimization function.** We next present the following lemma regarding the  $f + \mu_0$  attaining a local minimum over a ball around  $\bar{x}$  and its implications. This result can be used to select the parameters  $\mu_{\min}$  and  $\mu_{\max}$  in NExOS in the context of our convergence analysis.

**Lemma 6** (Attainment of local minimum by  $f + \mu_0$ ). *Let  $\bar{x} \in \mathcal{X}$  be a local minimum to  $(\mathcal{P})$ , where Assumptions 1, 2, and 3 hold. Then the following hold.*

(i) *There exist  $\check{\mu} > 0$  and  $\check{r} > 0$  such that for any  $\mu \in (0, \check{\mu}]$ , the exterior point minimization function  $f + \mu_0$  in  $(\mathcal{P}_\mu)$  will be differentiable in the open ball  $B(\bar{x}; \check{r})$  and will attain a local minimum of  $f + \mu_0$  in this ball denoted by  $x_\mu$ .*

(ii) *As  $\mu \rightarrow 0$ , this local minimum  $x_\mu$  will go to  $\bar{x}$  in limit, i.e.,  $x_\mu \rightarrow \bar{x}$ .*

(iii) *Let  $\xi \in (0, \check{\mu}]$ ,  $\eta' \in (1, \eta)$ , and  $\alpha \in \left(0, \frac{1}{\eta'} - \frac{1}{\eta}\right)$  with  $\eta > 1$  being the constant defined in Assumption 2. Then there exists some  $\hat{\mu} \in (0, \check{\mu}]$  such that for any  $\mu \in (0, \hat{\mu}]$ , we have*

$$\|\mathbf{\Pi}(x_\mu) - \bar{x}\| < \alpha \min_{\mu \in [\xi, \hat{\mu}]} r_\mu, \quad (8)$$

where  $r_\mu$  is the radius of convexity for the open ball  $B(\bar{x}; r_\mu)$ .

*Proof.* See Appendix B.5. □

*Remark 1* (Selecting  $\mu_{\min}$  and  $\mu_{\max}$ ). We now use Lemma 6 to select the parameters  $\mu_{\min}$  and  $\mu_{\max}$  for our convergence analysis. Define,

$$\mathfrak{M} = [\mu_{\min}, \mu_{\max}]. \quad (9)$$

First, we select a  $\check{\mu}$  that satisfies property (i) of Lemma 6, such a  $\check{\mu}$  exists due to this lemma. Now, we pick  $\xi \in (0, \check{\mu}]$ ,  $\eta' \in (1, \eta)$ , and  $\alpha \in \left(0, \frac{1}{\eta'} - \frac{1}{\eta}\right)$  with  $\eta > 1$  being the constant defined in Assumption 2. For this value of  $\xi, \eta'$ , and  $\alpha$ , we finally pick a  $\hat{\mu}$  that satisfies property (iii) of Lemma 6, which exists because the same lemma. We have two cases:

1. If  $\xi \geq \hat{\mu}$ , then select  $\mu_{\min} := \hat{\mu}$  and  $\mu_{\max} := \hat{\mu}$ . In this case, we have a singleton for  $\mathfrak{M}$ , i.e.,  $\mathfrak{M} = \{\hat{\mu}\}$ .
2. If  $\xi < \hat{\mu}$ , then select  $\mu_{\min} := \xi$  and  $\mu_{\max} = \hat{\mu}$ . In this case, we have an interval for  $\mathfrak{M}$  with  $\mathfrak{M} = [\xi, \hat{\mu}]$ .

Note that by considering different  $\check{\mu}, \xi, \eta', \alpha$ , and  $\hat{\mu}$ , we can construct different  $\mathfrak{M}$ .

**Relationship between local minima of  $(\mathcal{P})$ , local minima of  $(\mathcal{P}_\mu)$ , and the fixed point set of  $\mathbb{T}_\mu$ .** The next result connects local minimum  $x_\mu$  of  $(\mathcal{P}_\mu)$  over the region of convexity  $B(\bar{x}; r_\mu)$  and the fixed point set of  $\mathbb{T}_\mu$ .

**Lemma 7** (Relationship between local minima of  $(\mathcal{P})$  and  $\mathbf{fix} \mathbb{T}_\mu$ ). *Let  $\bar{x} \in \mathcal{X}$  be a local minimum to  $(\mathcal{P})$ , where Assumptions 1, 2, and 3 hold and  $\mu > 0$ . Let a local minimum  $x_\mu$  of  $(\mathcal{P}_\mu)$  over the region of convexity  $B(\bar{x}; r_\mu)$  is attained. Then*

$$x_\mu = \mathbf{zer}(\nabla f + \nabla^{\mu_0}) = \mathbf{prox}_{\gamma f}(\mathbf{fix} \mathbb{T}_\mu), \quad (10)$$

where the sets  $\mathbf{zer}(\nabla f + \nabla^{\mu_0})$ ,  $\mathbf{fix} \mathbb{T}_\mu$ , and  $\mathbf{prox}_{\gamma f}(\mathbf{fix} \mathbb{T}_\mu)$  are singletons over  $B(\bar{x}; r_\mu)$ . In other words,  $x_\mu$  is the unique local minimum over  $B(\bar{x}; r_\mu)$ .

*Proof.* See Appendix B.6. □

The next theorem shows how the distance between  $x_\mu$  and  $\bar{x}$  changes as  $\mu$  is varied over the sequence of outer iterations in Algorithm 1. This result establishes that for any  $\mu \in \mathfrak{M}$ , the local minimum  $x_\mu$  of  $(\mathcal{P}_\mu)$  is unique and is attained over the region of convexity  $B(\bar{x}; r_\mu)$ ; this will be used to establish convergence of NEXOS in §3.4.

**Proposition 2** (Relationship between local minima of  $(\mathcal{P})$  with local minima of  $(\mathcal{P}_\mu)$ ). *Let  $\bar{x} \in \mathcal{X}$  be a local minimum to  $(\mathcal{P})$ , where Assumptions 1, 2, and 3 hold. Let  $\mathfrak{M} = [\mu_{\min}, \mu_{\max}]$  as defined in Remark 1 and consider the case  $\mu_{\min} < \mu_{\max}$ . Then the following hold.*

(i) *For any  $\mu \in \mathfrak{M}$ , the local minimum  $x_\mu$  of  $(\mathcal{P}_\mu)$  over the region of convexity  $B(\bar{x}; r_\mu)$  is attained and is unique. More precisely, for any  $\mu \in \mathfrak{M}$ ,*

$$\|x_\mu - \bar{x}\| < \frac{1}{\eta'} r_\mu,$$

where  $\eta' > 1$ .

(ii) *Let  $z_\mu$  be the unique fixed point of  $\mathbb{T}_\mu$  corresponding to  $x_\mu$ . Then there exist  $\phi > 0$  and  $\psi > 0$  such that for any  $\mu \in \mathfrak{M}$ , we have*

$$r_\mu - \|x_\mu - \bar{x}\| > \phi,$$

and

$$r_\mu - \|z_\mu - \bar{x}\| > \psi,$$

where the proximal parameter  $\gamma$  is taken to satisfy

$$0 < \gamma < \frac{\phi}{\max_{\mu \in \mathfrak{M}} \|\nabla f(x_\mu)\|}. \quad (11)$$

*Proof.* See Appendix B.7. □

### 3.4 Main convergence results

We now present our main convergence results for NEXOS. Recall from Remark 1 while selecting  $\mu_{\min}, \mu_{\max}$ , we have two cases:  $\mu_{\min} < \mu_{\max}$  and  $\mu_{\min} = \mu_{\max}$ . First, in Theorem 1 we present convergence results for the case  $\mu_{\min} < \mu_{\max}$ , and then in Proposition 3 we consider the case when  $\mu_{\min} = \mu_{\max}$ .

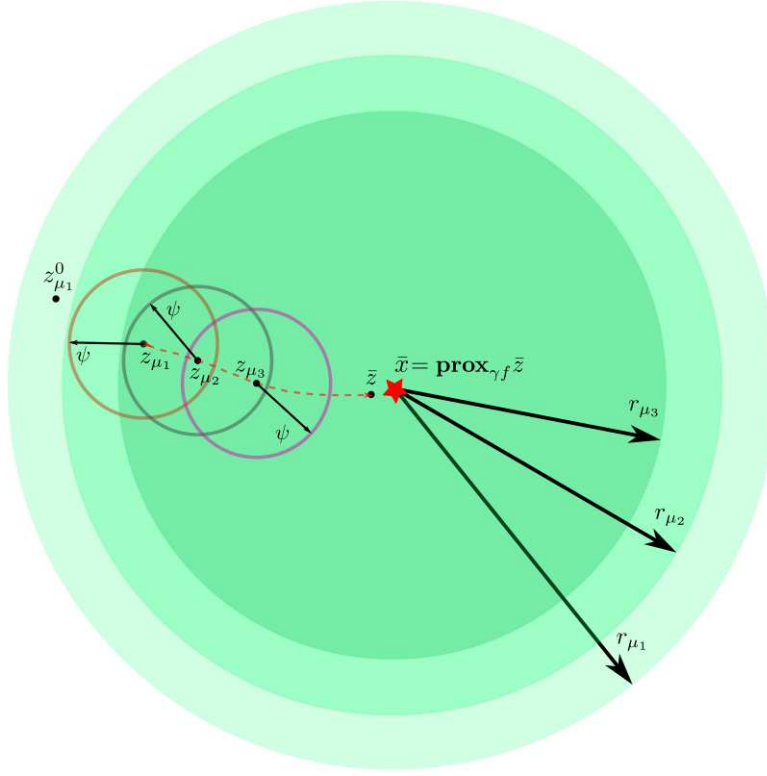


**Figure 2:** This figure shows the intuition behind the proof to Theorem 1. Here,  $\bar{x}$  is the associated local minimum to  $(\mathcal{P})$  and  $\bar{z} = \bar{x} + \gamma \nabla f(\bar{x})$ . For the chosen initial point  $z_{\mu_1}^0$  that lies in  $B(\bar{x}, r_{\mu_1})$ , the first outer iteration linearly converges to  $z_{\mu_1}$ , which is the unique fixed point of  $\mathbb{T}_{\mu_1}$  in  $B(\bar{x}, r_{\mu_1})$ . The point  $x_{\mu_1} = \mathbf{prox}_{\gamma f}(z_{\mu_1})$  is the unique local minimum of  $(\mathcal{P}_{\mu_1})$ . Next, we pick  $\mu_2$  by using (42), and we construct an open ball  $B(z_{\mu_1}, \psi)$  where  $\psi$  is the constant defined in Proposition 2(ii). For solving  $(\mathcal{P}_{\mu_2})$ , we set our initial point of the new outer iteration to  $z_{\mu_1}$ . This initialization process ensures that the outer iteration algorithm linearly converges to  $z_{\mu_2}$ —the unique fixed point of  $\mathbb{T}_{\mu_2}$ . Similarly, point  $x_{\mu_2} = \mathbf{prox}_{\gamma f}(z_{\mu_2})$  is the unique local minimum of  $(\mathcal{P}_{\mu_2})$ . We repeat this process until we reduce  $\mu$  to  $\mu_{\min}$ .

**Convergence result for NExOS when  $\mu_{\min} < \mu_{\max}$ .** The following theorem provides convergence result for NExOS for the case  $\mu_{\min} < \mu_{\max}$ . The intuition behind the proof is captured in Figure 2.

**Theorem 1** (Convergence result for NExOS). *Let  $\bar{x} \in \mathcal{X}$  be a local minimum to  $(\mathcal{P})$ , where Assumptions 1, 2, and 3 hold. Let  $\mathfrak{M} = [\mu_{\min}, \mu_{\max}]$  (as defined in Remark 1) and consider the case  $\mu_{\min} < \mu_{\max}$ . Suppose that Algorithm 2 for penalty parameter  $\mu_{\max}$  produces an exact or approximate fixed point  $z_{\mu_{\max}}$  of  $\mathbb{T}_{\mu_{\max}}$  over  $B(\bar{x}; r_{\mu_{\max}})$ . The proximal parameter  $\gamma$  is selected to satisfy (11).*

Then we can construct a finite sequence of strictly decreasing penalty parameters

$$\{\mu_1 := \mu_{\max}, \mu_2, \dots, \mu_N := \mu_{\min}\} \subseteq \mathfrak{M},$$

such that for each  $m \in \{1, 2, \dots, N\}$  Algorithm 2 has the following convergence properties:

- the iterates  $z_{\mu_m}^n$  linearly converges to  $z_{\mu_m}$ —the unique fixed point of  $\mathbb{T}_{\mu_m}$  over the region of convexity  $B(\bar{x}, r_{\mu_m})$ ,
- the iterates  $x_{\mu_m}^n, y_{\mu_m}^n$  linearly converge to  $x_{\mu_m} = \mathbf{prox}_{\gamma f}(z_{\mu_m})$ —the unique local minimum to  $(\mathcal{P}_{\mu})$  over  $B(\bar{x}; r_{\mu_m})$ ), and
- $x_{\mu_{\min}} \rightarrow \bar{x}$  as  $\mu_{\min} \rightarrow 0$ .

*Proof.* See Appendix B.8. □

*Remark 2* (Selecting  $\rho$ ). The proof to Theorem 1 shows that the multiplicative factor  $\rho \in (0, 1)$  in Algorithm 1 can be selected using

$$\rho \in \left( 0, 1 - \frac{(1 - \kappa')\psi}{\ell\mu_{\max}} \right), \quad (12)$$

where  $0 < (1 - \kappa')\psi/(\ell\mu_{\max}) < 1$ . Any value of  $\rho$  that satisfies (12) can be used as the multiplicative factor to tune  $\mu$  and construct the strictly decreasing sequence of penalty parameters  $\{\mu_1 := \mu_{\max}, \mu_2 = \rho\mu_1, \mu_3 = \rho\mu_2, \dots, \mu_N := \mu_{\min}\} \subseteq \mathfrak{M}$ , where  $N = \lceil \log(\mu_{\min}/\mu_{\max}) / \log \rho \rceil$ .

**Convergence result for NExOS when  $\mu_{\min} = \mu_{\max}$ .** The following proposition provides convergence result for NExOS for the case  $\mu_{\min} = \mu_{\max}$ . This also provides a standalone convergence result for the outer iteration algorithm for one value of the penalty parameter as well.

**Proposition 3** (Convergence result for the outer iteration algorithm for a fixed value of  $\mu$ ). *Let  $\bar{x} \in \mathcal{X}$  be a local minimum to  $(\mathcal{P})$ , where Assumptions 1, 2, and 3 hold. Let the value of the penalty parameter be  $\mu > 0$ . Let  $B(\bar{x}; r_{\mu})$  be the region of convexity around  $\bar{x}$ , and  $x_{\mu}$  be the unique local minimum to  $(\mathcal{P}_{\mu})$  over  $B(\bar{x}; r_{\mu})$ , and  $z_{\mu}$  be the corresponding unique fixed point of  $\mathbb{T}_{\mu}$ . Let  $z_{\mu}^0$  be the chosen initial point such that  $\bar{B}(z_{\mu}; \|z_{\mu}^0 - z_{\mu}\|) \subseteq B(\bar{x}; r_{\mu})$ .*

*Then, in Algorithm 2,  $z_{\mu}^n$  linearly converges to  $z_{\mu}$ , and both  $x_{\mu}^n$  and  $y_{\mu}^n$  linearly converge to the unique local minimum  $x_{\mu}$  of  $(\mathcal{P}_{\mu})$  over  $B(\bar{x}; r_{\mu})$ . Finally,  $x_{\mu} \rightarrow \bar{x}$  as  $\mu \rightarrow 0$ .*

*Proof.* See Appendix B.9. □

In the development of our convergence results, we made three assumptions, where Assumption 2 and Assumption 3 can be justified without incurring a loss of generality. While Assumption 1 is a standard assumption in proving convergence results in machine learning [2], the reader may wonder how the convergence results would change if this particular assumption is removed. Instead of Assumption 1, if we assume that the function  $f$  is just convex, then all the convergence results stay the same, except the convergence rate would be sublinear with a rate

$$\|z_{\mu_m}^{n+1} - z_{\mu_m}^n\|^2 \leq O\left(\frac{1}{n+1}\right).$$

The extension is straightforward based on our previous analysis but quite tedious with very little new insight, so rather than proving the new results in detail, we provide pointers regarding how to achieve them in Appendix C.

## 4 Initialization and parameter selection

In this section, we discuss how to select different parameters introduced in the algorithms in §2 in practice.

### 4.1 Picking initial penalty parameter $\mu_{\text{init}}$

From the proof to Theorem 1 (see Appendix B.8), we see that any  $\mu_{\text{init}} \leq \mu_{\text{max}}$  (where  $\mu_{\text{max}}$  was defined in Theorem 2) will work. Unfortunately, the precise value of  $\mu_{\text{max}}$  depends on several constants that we do not know in practice. However, in our empirical studies we have found to  $\mu_{\text{init}} = 2$  to be a good choice for this parameter.

### 4.2 Picking the first initial point $z_{\text{init}}$

Let  $\tilde{z}$  be a point where  $\mathcal{X}$  is prox-regular. From Lemma 4, we know that, there is a convex neighborhood around  $\tilde{z}$ , where the objective function in  $(\mathcal{P}_\mu)$  is locally convex. The distance function  $d(\cdot)$  is continuous [15, Example 9.6], and at  $\mu := \mu_{\text{init}}$ , the diameter of the convex neighborhood around  $\tilde{z}$  is at its largest compared to the subsequent smaller values of  $\mu$  chosen. Thus, for  $\mu := \mu_{\text{init}}$ , around any point that is close to  $\tilde{z}$ , the objective function in  $(\mathcal{P}_\mu)$  is approximately equal to  $f + (\beta/2)\|\cdot\|^2$ : a strongly convex function. Hence, setting  $z_{\text{init}}$  close to such a point  $\tilde{z}$  can serve as a good initialization point for NExOS.

In practice, we have found that, besides the method described above, selecting  $z_{\text{init}}$  randomly or to be any point in (or near)  $\mathcal{X}$  works very well too. The intuition is that any closed set in  $\mathbf{E}$  is prox-regular almost everywhere (follows from [54, Proposition 7.39]).

### 4.3 Picking the final penalty parameter $\mu_{\text{min}}$

The final and smallest value of the penalty parameter  $\mu_{\text{min}}$  is chosen to be close to zero, so that the corresponding problem  $(\mathcal{P}_{\mu_{\text{min}}})$  is a good approximation to the original problem  $(\mathcal{P})$  from a practical point of view. In most of our numerical experiments, we take  $\mu_{\text{min}}$  to be in the order of  $10^{-8}$ .

### 4.4 Tuning the penalty parameter $\mu$

As discussed in Remark 2, any value of  $\rho$  that satisfies (12) can be used as the multiplicative factor to tune  $\mu$ . Unfortunately, in practice, we do not know the numerical values for the constants  $\kappa'$ ,  $\psi$ ,  $\mu_{\text{max}}$ , and  $\ell$  appearing in (12). In our empirical studies, we have found  $\rho = 1/2$  to be a good choice that have worked for all the problems that we have tested our algorithm to.

## 5 Numerical experiments

In this section, we apply NExOS to nonconvex machine learning problems of substantial current interest fitting our setup. We have implemented NExOS in NExOS.jl solver, which is an open-source software package written in the Julia programming language. NExOS.jl can solve any optimization problem of the form  $(\mathcal{P})$ . The code and documentation are available online at:

<https://github.com/Shuvomoy/NExOS.jl>.

To compute the proximal operator of a function  $f$  that has closed form or easy-to-compute solution, `NExOS.jl` uses the open-source Julia package `ProximalOperators.jl` [55]. When  $f$  is a constrained convex function (i.e., a convex function over some convex constraint set) with no closed form proximal map, `NExOS.jl` computes the proximal operator by using the open-source Julia package `JuMP` [56] and any of the commercial or open-source solver supported by it. The set  $\mathcal{X}$  can be any prox-regular nonconvex set fitting our setup. Our implementation is readily extensible using Julia abstract types so that the user can add support for additional convex functions and prox-regular sets.

The numerical study is executed on a computer with Intel Core i5-8250U CPU with 8 GB RAM running Windows 10 Pro operating system. The datasets considered in this section, unless specified otherwise, are available online at:

[https://github.com/Shuvomoy/NExOS\\_Numerical\\_Experiments\\_Datasets](https://github.com/Shuvomoy/NExOS_Numerical_Experiments_Datasets).

In applying `NExOS`, we use the following values for the parameters unless otherwise stated. We take the starting value of  $\mu$  to be 2, the minimum value of  $\mu$  to be  $10^{-8}$  with a multiplicative factor of 0.5. The value of  $\gamma$  is chosen to be cubic root of the minimum value of  $\mu$ . We initialize our iterates at  $\mathbf{0}$ . Maximum number of inner iterations for a fixed value of  $\mu$  is taken to be 1000. The tolerance for the fixed point gap is taken to be  $10^{-4}$ . Fixed point gap and distance from the constraint set are measured in infinity norm.

## 5.1 Regressor selection

**Problem description.** The regressor selection problem is concerned with approximating a vector  $b \in \mathbf{R}^m$  with a linear combination of at most  $k$  columns of a matrix  $A \in \mathbf{R}^{m \times d}$  with bounded coefficients. The problem can be written as:

$$\begin{aligned} & \text{minimize} && \|Ax - b\|_2^2 + \frac{\beta}{2}\|x\|_2^2 \\ & \text{subject to} && \mathbf{card}(x) \leq k \\ & && \|x\|_\infty \leq \Gamma, \end{aligned} \tag{REG-SEL}$$

where  $x \in \mathbf{R}^d$  is the decision variable, and  $A \in \mathbf{R}^{m \times d}$ ,  $b \in \mathbf{R}^m$ , and  $\Gamma > 0$  are problem data.

In **(REG-SEL)**, we set  $\mathcal{X} := \{x \mid \|x\|_\infty \leq \Gamma, \mathbf{card}(x) \leq k\}$ , and  $f(x) := \|Ax - b\|_2^2$  with  $\beta = 10^{-8}$ . A projection onto  $\mathcal{X}$  can be computed using the formula in [2, §2.2], whereas the proximal operator for  $f$  can be computed using the formula in [47, §6.1.1]. Now we are in a position to apply `NExOS` to this problem.

### 5.1.1 Synthetic dataset: comparison with Lasso

We compare the solution found by `NExOS` with the solution found by an algorithm based on Lasso (least absolute shrinkage and selection operator).

**Lasso.** Lasso is perhaps the most well-known method for solving the regressor selection problem, that computes an approximate solution as follows. First, Lasso solves:

$$\begin{aligned}
& \text{minimize} && \|Ax - b\|_2^2 + \lambda \|x\|_1 + \frac{\beta}{2} \|x\|_2^2 \\
& \text{subject to} && x \in \mathbf{R}^d,
\end{aligned} \tag{CVX-REG-SEL}$$

where  $\lambda$  is a parameter that is related to the sparsity of the decision variable  $x$ . To solve this problem, we have used `glmnet`, which is one of the most popular packages to implement Lasso [57, pp. 50-52].

To compute the value of  $\lambda$  corresponding to a desired  $k$  such that  $\mathbf{card}(x) \leq k$  we follow the method proposed in [58, §3.4] and [24, Example 6.4]. We solve the problem (CVX-REG-SEL) for different values of  $\lambda$ , and find the smallest value of  $\lambda$  for which we have  $\mathbf{card}(x) \leq k$ , and we consider the sparsity pattern of the corresponding solution  $\tilde{x}$ . Let the index set of zero elements of  $\tilde{x}$  be  $\mathcal{Z}$ , where  $\mathcal{Z}$  has  $d - k$  elements. Then the Lasso-based algorithm solves the following optimization problem:

$$\begin{aligned}
& \text{minimize} && \|Ax - b\|_2^2 + \frac{\beta}{2} \|x\|_2^2 \\
& \text{subject to} && (\forall j \in \mathcal{Z}) \quad x_j = 0 \\
& && x \in \mathbf{R}^d,
\end{aligned} \tag{13}$$

where  $x$  is the decision variable. To solve (13), we have used Gurobi's quadratic optimization solver.

**Data generation process and setup.** The data generation procedure is similar to [36]. In this numerical experiment, we vary  $m$  from 50 to 150, and for each value of  $m$ , we generate 50 random instances. For a certain value of  $m$ , the matrix  $A \in \mathbf{R}^{m \times 2m}$  is generated from an independent and identically distributed normal distribution with  $\mathcal{N}(0, 1)$  entries. We choose  $b = A\tilde{x} + v$ , where  $\tilde{x}$  is drawn uniformly from the set of vectors satisfying  $\mathbf{card}(\tilde{x}) \leq \lfloor \frac{m}{5} \rfloor$  and  $\|\tilde{x}\|_\infty \leq 1$ . The vector  $v$  corresponds to noise, and is drawn from the distribution  $\mathcal{N}(0, \sigma^2 I)$ , where  $\sigma^2 = \|A\tilde{x}\|_2^2 / (400/m)$ , which keeps the signal to noise ratio to approximately 20.

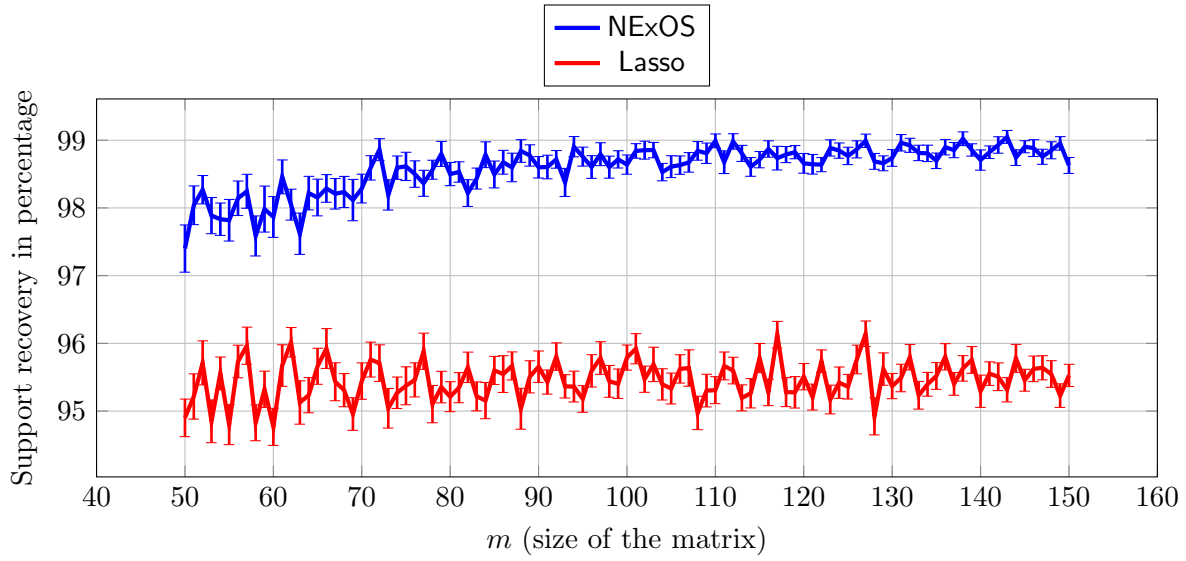
**Results.** The results displayed in the figures are averaged over 50 simulations for each value of  $m$ , and also show one-standard-error bands that represent one standard deviation confidence interval around the mean. For each instance, NExOS is able to find a locally optimal solution.

Figure 3 shows the support recovery (%) of the solutions found by NExOS and Lasso. We see that NExOS always recovers most of the original signal's support, and it does it better than Lasso consistently. On average the support recovery by NExOS is 4% more than Lasso.

Figure 4 compares the quality of the solutions found by both algorithms in terms of objective values. We see that the objective value found by Lasso is much larger than the objective value found by NExOS in all the cases averaged over all the 50 instances for each size of the problem.

Finally, in Figure 5, we compare the solution times of NExOS to that of `glmnet`. Note that, to compare only with `glmnet`, we have only considered the solution time to compute one solution to (CVX-REG-SEL) by `glmnet` and have excluded the solution time to solve (13). We see that `glmnet` is slightly faster than Algorithm 1. This slower performance is due to the fact that our algorithm is a general purpose method to solve nonconvex optimization problem applicable to any convex loss function over a prox-regular constraint set, whereas `glmnet` is specifically optimized for the convexified sparse regression problem with a very specific objective function. Furthermore, by choosing a slightly larger value of  $\mu_{\min}$ , we can make our algorithm as fast as `glmnet`, though the precision of the solution may not be very high.





**Figure 3:** Support recovery (%) by Lasso and NExOS vs  $m$  for the sparse regression problem.

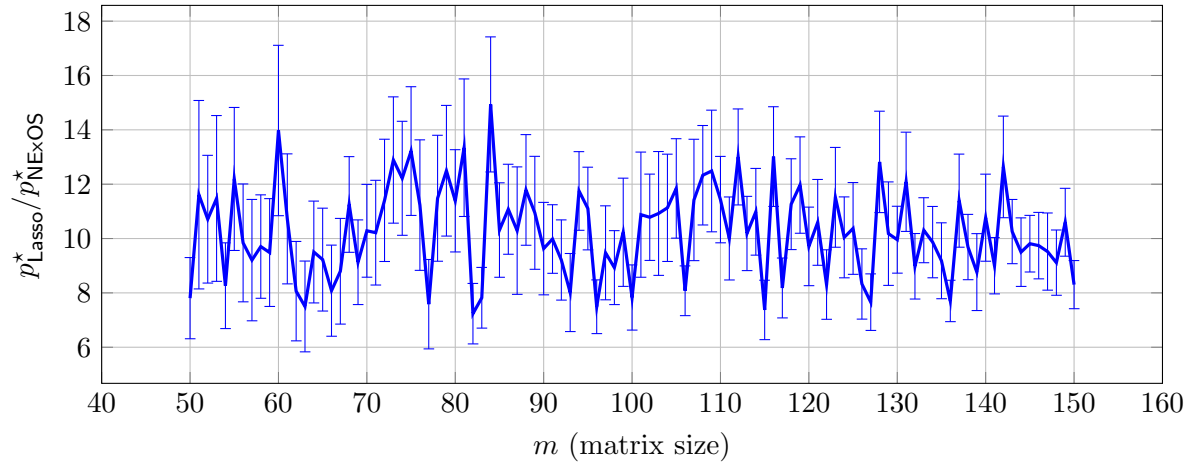


**Figure 4:** Ratio of objective value of the solution found by Lasso and NExOS vs  $m$  for the sparse regression problem. The objective values of the solutions computed by NExOS and Lasso are denoted by  $p_{\text{NExOS}}^*$  and  $p_{\text{Lasso}}^*$ , respectively.

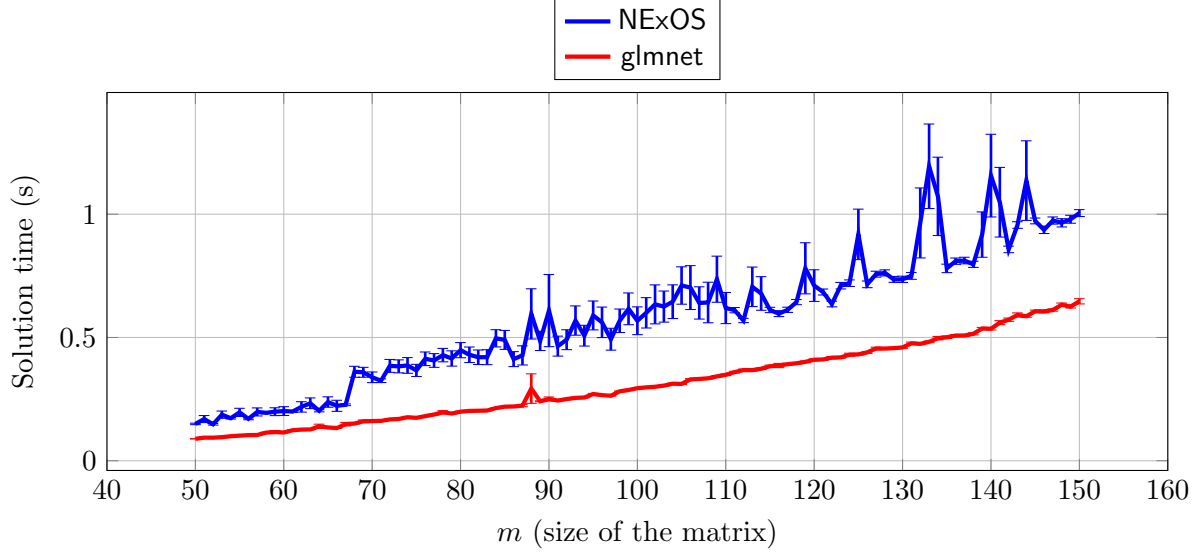


**Figure 5:** Solution time by Lasso and NExOS vs  $m$  for the sparse regression problem.

Here we note that, if we consider the total solution time to solve both (CVX-REG-SEL) and (13), then NExOS is faster; but we omit this timing result as Gurobi is not in particular optimized to solve (13) and increases the solution time disproportionately.

To summarize, the experiments with the synthetic datasets suggest that the solution found by NExOS is consistently of higher quality in terms of support recovery and objective value than that of Lasso.

### 5.1.2 Synthetic dataset: comparison with Gurobi

The next experiment we perform is to see how well NExOS does in getting close to the absolute optimal value of the original problem. NExOS is guaranteed to provide a locally optimal solution under regularity conditions; however, if we are interested in reducing the objective value as much as possible to investigate how close we get to the absolute minimum value, then it is reasonable to initialize NExOS for different random points and take the solution associated with the least objective value.

**Formulation for Gurobi.** The sparse regression problem (REG-SEL) can be modeled as the following mixed integer quadratic optimization problem:

$$\begin{aligned}
 & \text{minimize} && \|Ax - b\|_2^2 + \frac{\beta}{2}\|x\|_2^2 \\
 & \text{subject to} && |x_i| \leq \Gamma y_i, \quad i = 1, \dots, d \\
 & && \sum_{i=1}^d y_i \leq k \\
 & && x \in \mathbf{R}^d, y \in \{0, 1\}^d,
 \end{aligned}$$

where  $\Gamma$  is a large number that can be chosen based on the problem data [7]. This mixed integer quadratic optimization problem can be solved exactly using Gurobi.

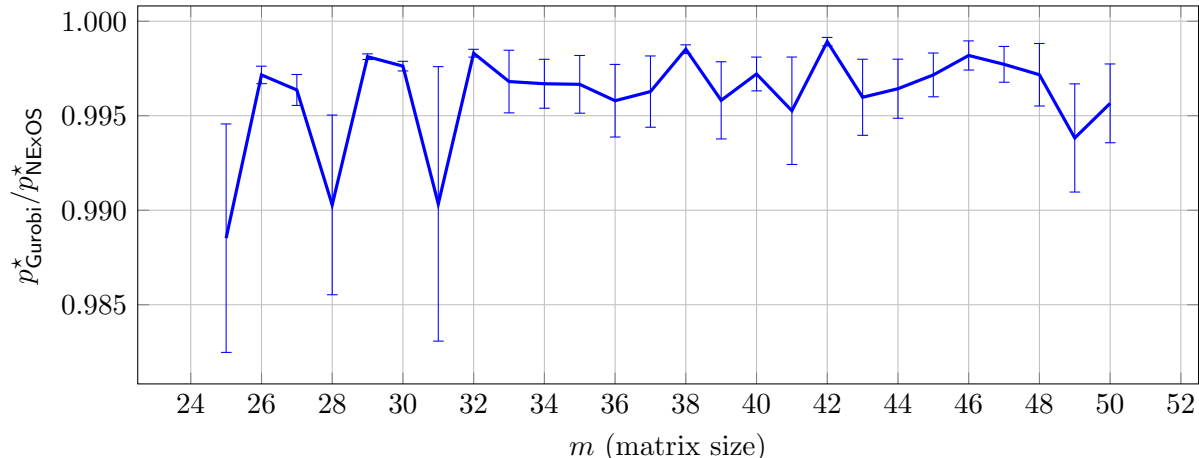


**Figure 6:** Ratio of objective value found by Gurobi and NExOS vs  $m$  for the sparse regression problem synthetic datasets.

**Data generation process and setup.** We vary  $m$  from 25 to 50, and for each value of  $m$ , we generate 50 instances like before. We limit the size of the problems because the solution time by Gurobi becomes too large for comparison if we go beyond the aforesaid size.

For each of the instances, we generate 100 random instances from the uniform distribution over the interval  $[-\Gamma, \Gamma]$ . We speed up the calculation by running NExOS for different initializations by using multi-threading capability in Julia, each thread running NExOS for a different random initialization parallelly. Number of threads for this experiment was 4. All the parameter values are kept same as §5.1.1.

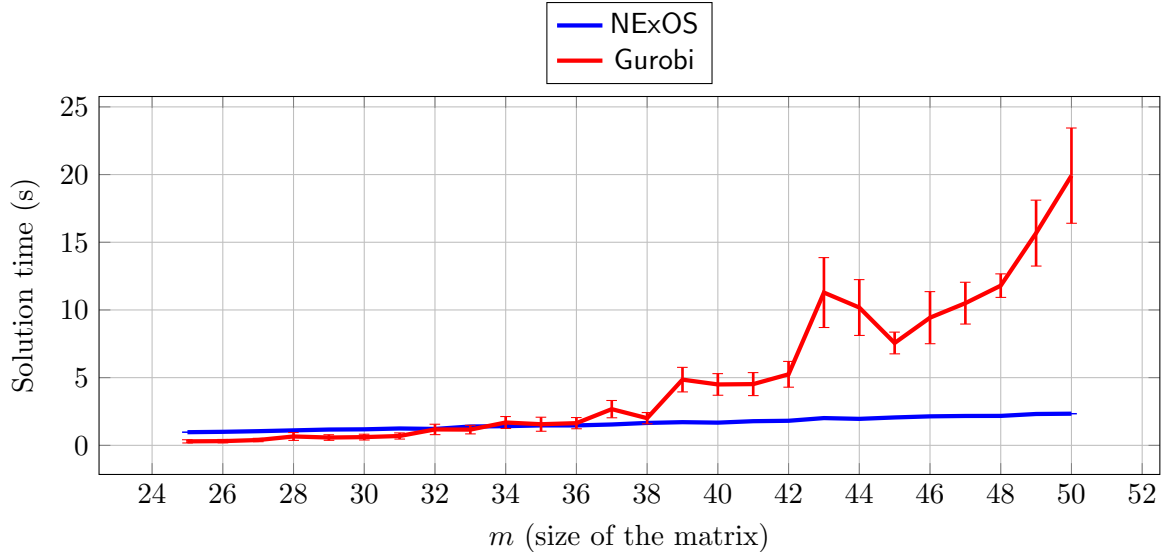
**Results.** The results displayed in Figure 6 and Figure 7 are averaged over 50 simulations for each value of  $m$ , and also show one-standard-error bands.

Figure 6 shows the ratio between the objective value found by NExOS and Gurobi. The closer it is to 1, the better is the quality of the solution found by NExOS in terms of minimizing the objective value. We see that in most cases NExOS is able to find a solution that is very close to the optimal solution.

In Figure 7, we compare the solution times of NExOS to that of Gurobi. For smaller problems, Gurobi is somewhat faster than NExOS, however once we go beyond  $m \geq 34$ , the solution time by Gurobi starts to increase in an exponential fashion whereas NExOS scales linearly. Beyond  $m \geq 50$ , comparing the runtimes is not meaningful as Gurobi cannot find a solution in 2 minutes.

### 5.1.3 Experiments and results for real-world dataset

**Description of the dataset.** To investigate the performance of our algorithm on a real-world dataset, we consider the problem of murder rate detection per 100,000 people comprising of  $m = 2215$  communities in the United States with  $d = 101$  attributes. By preprocessing the data, we remove some of the columns with missing entries, and for 101 attributes, no data is missing. Then we standardize the data matrix  $\bar{A}$  so that each column of  $\bar{A}$  has a zero mean and unit standard deviation. The dataset is from UCI machine learning repository, and it is available at the url:



**Figure 7:** Solution time by Gurobi and NExOS vs  $m$  for the sparse regression problem synthetic datasets.

<http://archive.ics.uci.edu/ml/datasets/Communities+and+Crime+Unnormalized>.

Our goal is to predict the murder rate per 100,000 people as a linear function of the attributes, where at most  $k$  attributes can be nonzero. We include a bias term in our model, *i.e.*, in (REG-SEL) we set  $A = [\bar{A} \mid \mathbf{1}]$ . We use 10-fold cross-validation and vary  $k$  from 2 to 20.

In this experiment, we take the the minimum value of  $\mu$  to be  $10^{-15}$  and maximum number of inner iterations for a fixed value of  $\mu$  is taken to be 20,000. All the other parameters are kept at their default values as stated in the beginning of §5.

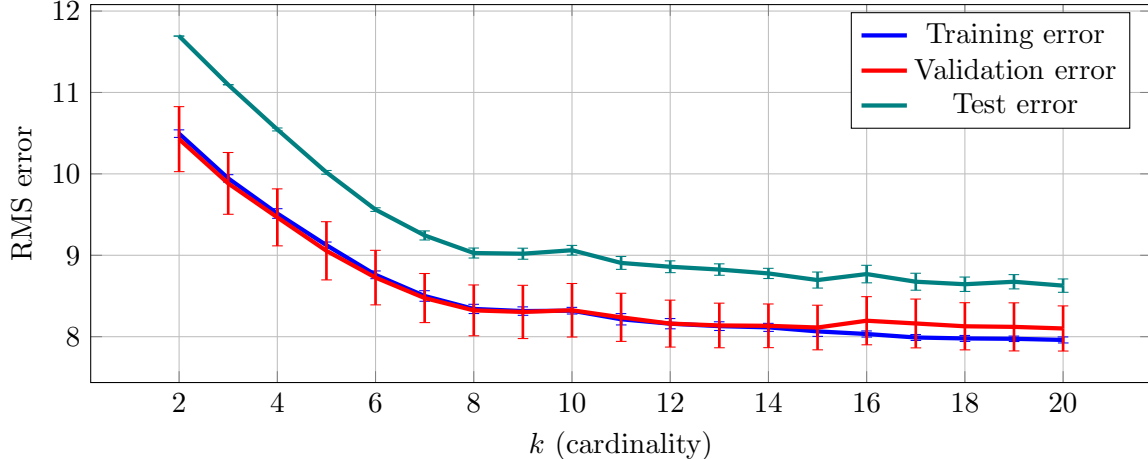
**Results.** For each instance, NExOS is able to find a locally optimal solution.

Figure 8 shows the RMS error for the training datasets, validation datasets, and the test dataset along with one-standard-error bands. The results for training, validation, and test datasets are reasonably similar for each value of  $k$ . This gives us confidence that the sparse regression model will have similar performance on new and unseen data. This also suggests that our model does not suffer from over-fitting. We also see that, for  $k \geq 10$ , none of the errors drop significantly. Scanning the RMS error on the test sets in Figure 8, we can expect that our prediction error on new data will be around 10.

## 5.2 Affine rank minimization problem

**Problem description.** The affine rank minimization can be written as:

$$\begin{aligned}
 & \text{minimize} && \| \mathcal{A}(X) - b \|_2^2 + \frac{\beta}{2} \| X \|_F^2 \\
 & \text{subject to} && \mathbf{rank}(X) \leq r \\
 & && \| X \|_2 \leq \Gamma \\
 & && X \in \mathbf{R}^{m \times d},
 \end{aligned} \tag{ARM}$$



**Figure 8:** RMS error vs  $k$  (cardinality) for the murder rate detection problem.

where  $X \in \mathbf{R}^{m \times d}$  is the decision variable,  $b \in \mathbf{R}^k$  is a noisy measurement data, and  $\mathcal{A} : \mathbf{R}^{m \times d} \rightarrow \mathbf{R}^k$  is a linear map. The parameter  $\Gamma > 0$  denotes the upper bound for the spectral norm of  $X$ . The affine map  $\mathcal{A}$  can be determined by  $k$  matrices  $A_1, \dots, A_k$  in  $\mathbf{R}^{m \times d}$  such that

$$\mathcal{A}(X) = (\text{tr}(A_1^T X), \dots, \text{tr}(A_k^T X)).$$

In (REG-SEL), we set  $\mathcal{X} := \{X \in \mathbf{R}^{m \times d} \mid \text{rank}(X) \leq r, \|X\|_2 \leq \Gamma\}$ , and  $f(X) := \|\mathcal{A}(X) - b\|_2^2$ . To compute the proximal operator of  $f$ , we use the formula in [47, §6.1.1]. Finally, we use the formula in [36, page 14] for projecting onto  $\mathcal{X}$ . Now we are in a position to apply the NExOS to this problem. We have taken  $\beta = 10^{-10}$ .

**Summary of the experiments performed.** First, we apply NExOS to solve (ARM) for synthetic datasets, where we observe how the algorithm performs in recovering a low-rank matrix given noisy measurements.

Second, we apply NExOS to a real-world dataset to see how our algorithm performs in solving a matrix-completion problem (which is a special case of (ARM)).

### 5.2.1 Experiments and results for synthetic dataset

**Data generation process and setup.** We generate the data as follows, which is similar to [36]. We vary  $m$  (number of rows of the decision variable  $X$ ) from 50 to 75 with a linear spacing of 5, where we take  $d = 2m$ , and rank to be equal to  $m/10$  rounded to the nearest integer. For each value of  $m$ , we create 25 random instances as follows. The operator  $\mathcal{A}$  is drawn from a iid normal distribution with  $\mathcal{N}(0, 1)$  entries. Similarly, we create the low rank matrix  $X_{\text{True}}$  with rank  $r$ , first drawn from a iid normal distribution with  $\mathcal{N}(0, 1)$  entries, and then truncating the singular values that exceed  $\Gamma$  to 0. Signal to noise ratio is taken to be around 20 by following the same method described for the sparse regression problem.

**Results.** The results displayed in the figures are averaged over 50 simulations for each value of  $m$ , and also show one-standard-error bands. For each instance, the solution found by NExOS is locally

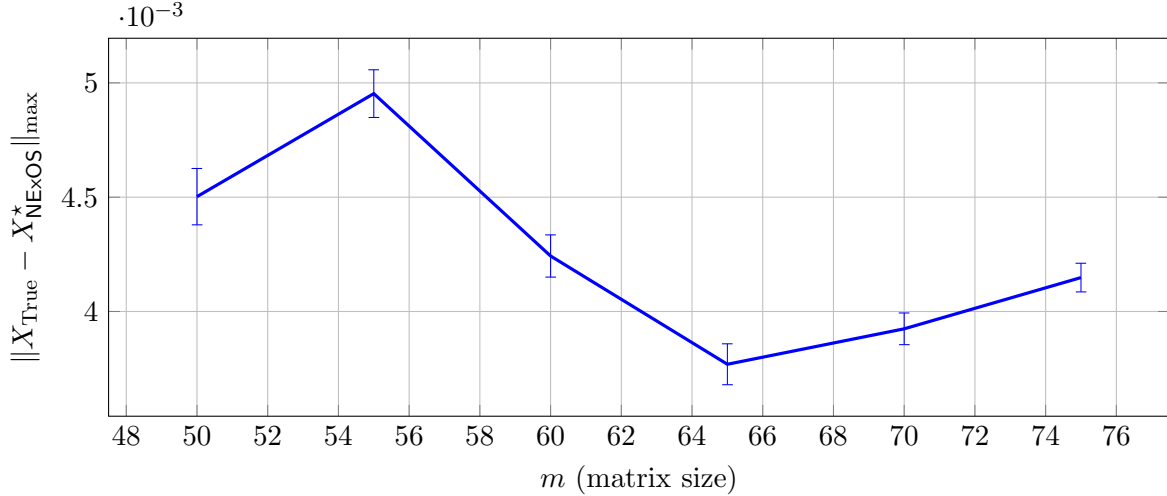


**Figure 9:** Maximum absolute error in recovering the original matrix vs  $m$  for the affine rank minimization problem.

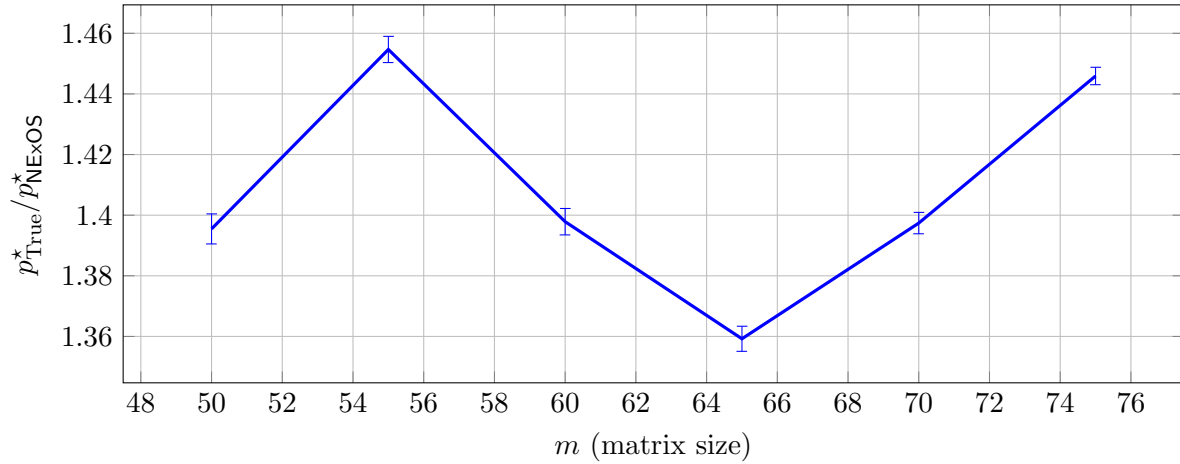


**Figure 10:** Ratio of objective values of the true matrix  $X_{\text{True}}$  and the solution found by NExOS vs  $m$  for the affine rank minimization problem.

optimal.

Figure 9 shows how well NExOS does in recovering the original matrix  $X^{\text{True}}$ . To quantify the recovery, we compute the max norm of the difference matrix  $\|X_{\text{True}} - X_{\text{NExOS}}^*\|_{\max} = \max_{i,j} |X_{\text{True}}(i,j) - X_{\text{NExOS}}^*(i,j)|$ , where the solution found by NExOS is denoted by  $X_{\text{NExOS}}^*$ . We see that the worst case component-wise error is very small in all the cases.

Finally, we show how the objective value of the solution  $X_{\text{NExOS}}^*$  computed by NExOS compares with the original matrix  $X_{\text{True}}$  in Figure 10. Note that the ratio is larger than one in most cases, *i.e.*, NExOS finds a solution that has a smaller value compared to  $X_{\text{True}}$ . This is due to the fact that under the quite high signal to noise ratio the problem data can be explained better by another matrix with a lower objective value. That being said,  $X_{\text{NExOS}}^*$  is not too far from  $X_{\text{True}}$  component-wise as we saw in Figure 9.

### 5.2.2 Experiments and results for real-world dataset: matrix completion problem

**Description of the dataset.** To investigate the performance of our problem on a real-world dataset, we consider the MovieLens 1M Dataset, which is available at the url:

<https://grouplens.org/datasets/movielens/1m/>.

This dataset contains 1,000,023 ratings for 3,706 unique movies (the dataset contains some repetitions in movie ratings and we have ignored them); these recommendations were made by 6,040 MovieLens users. The rating is on a scale of 1 to 5. If we construct a matrix of movie ratings by the users (also called the preference matrix), denoted by  $Z$ , then it is a matrix of 6,040 rows (each row corresponds to a user) and 3,706 columns (each column corresponds to a movie) with only 4.47% of the total entries are observed, while the rest of the entries are missing. We standardize the preference matrix  $Z$  (ignoring the missing entries) so that each column has a zero mean and unit standard deviation. Our goal is to complete this matrix, under the assumption that the matrix is low-rank. For more details about the model, we refer the reader to the discussion in [2, §8.1].

To gain confidence in the generalization ability of this model, we use an out-of-sample validation process. By random selection, we split the available data into a training set (80% of the total data) and a test set (20% of the total data). We use the training set as the input data for solving the underlying optimization process, and the held-out test set is used to compute the test error for each value of  $r$ , which is indicative of the generalization ability of the model. The best rank  $r$  corresponds to the point beyond which the improvement in the test error is rather minor. We tested rank values  $r$  ranging in  $\{1, 3, 5, 7, 10, 20, 25, 30, 35\}$ .

**Matrix completion problem.** The underlying optimization problem in this case is called a matrix completion problem. A matrix completion problem can be formulated as:

$$\begin{aligned} & \text{minimize} && \sum_{(i,j) \in \Omega} (X_{ij} - Z_{ij})^2 + \frac{\beta}{2} \|X\|_F^2 \\ & \text{subject to} && \mathbf{rank}(X) \leq r \\ & && \|X\|_2 \leq \Gamma \\ & && X \in \mathbf{R}^{m \times d}, \end{aligned} \tag{MAT-CMPLT}$$

where  $Z \in \mathbf{R}^{m \times d}$  is the matrix whose entries  $Z_{ij}$  are observable for  $(i, j) \in \Omega$ . Based on these observed entries, our goal is to construct a matrix  $X \in \mathbf{R}^{m \times d}$  that has rank  $r$ . We have taken  $\beta = 10^{-10}$ . The problem above can be written as a special case of affine rank minimization problem (ARM). Hence, computing projection onto the constraint set and the proximal operator is the same as in problem (ARM). The upper bound  $\Gamma$  for  $\|X\|_2$  is computed as follows. We construct a virtual matrix  $Y$  by filling each missing entries of standardized matrix  $Z$  with the absolute maximum of the available entries, which results in the maximum possible Frobenius norm of any preference matrix in our setup. Then we compute the Frobenius norm  $\|Y\|_F$  and set  $\Gamma = \|Y\|_F$ . As the spectral norm of a matrix is always less than its Frobenius norm, this gives a valid upper bound on  $\|X\|_2$ .

**Results.** For each instance, NExOS finds a locally optimal solution.

Figure 11 shows the RMS error for the training dataset and test dataset for each value of rank  $r$ . The results for training and test datasets are reasonably similar for each value of  $r$ . We observe that beyond rank 15, the reduction in the test error is rather minor and going beyond this rank

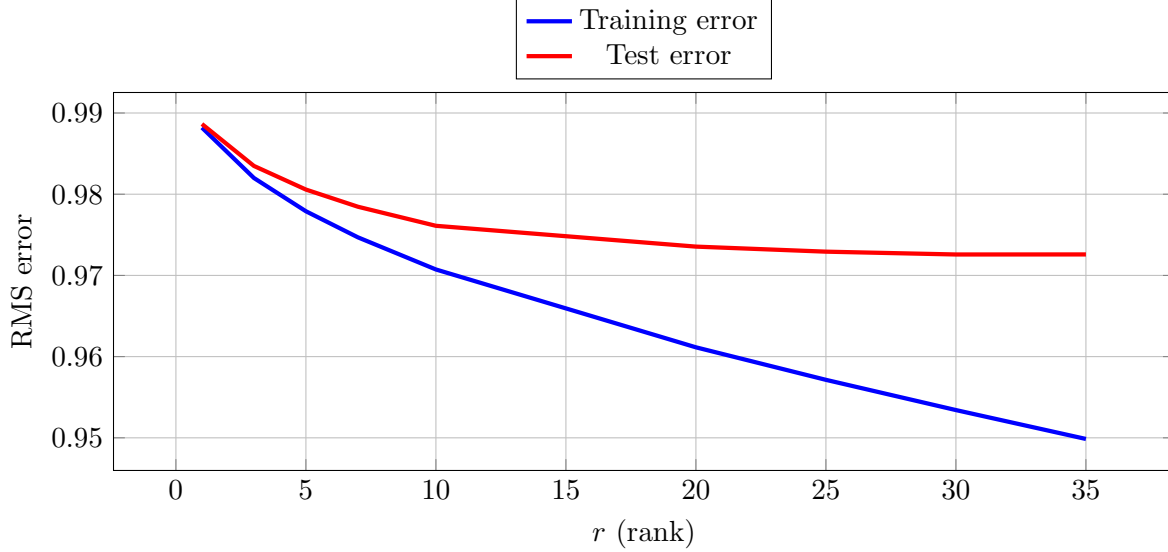


**Figure 11:** RMS error vs  $r$  (rank) for the matrix completion problem.

provides only diminishing return, which is a common occurrence for low-rank matrix approximation [59, §7.1]. Thus we can choose the optimal rank to be 15 for all practical purposes.

### 5.3 Factor analysis problem

**Problem description.** The factor analysis model with sparse noise (also known as low-rank factor analysis model) involves decomposing a given positive semidefinite matrix as a sum of a low-rank positive semidefinite matrix and a diagonal matrix with nonnegative entries [3, page 191]. It can be posed as the following optimization problem [60]:

$$\begin{aligned}
& \text{minimize} && \|\Sigma - X - D\|_F^2 + \frac{\beta}{2} (\|X\|_F^2 + \|D\|_F^2) \\
& \text{subject to} && D = \mathbf{diag}(d) \\
& && d \geq 0 \\
& && X \succeq 0 \\
& && \mathbf{rank}(X) \leq r \\
& && \Sigma - D \succeq 0 \\
& && \|X\|_2 \leq \Gamma,
\end{aligned} \tag{FACT-ANA}$$

where  $X \in \mathbf{S}^p$  and the diagonal matrix  $D \in \mathbf{S}^p$  with nonnegative entries are the decision variables, and  $\Sigma \in \mathbf{S}_+^p$ ,  $r \in \mathbf{Z}_+$ , and  $\Gamma \in \mathbf{R}_{++}$  are the problem data. We have taken  $\beta = 10^{-10}$ .

A proper solution for (FACT-ANA) requires that both  $X$  and  $D$  are positive semidefinite. The covariance matrix for the common parts of the variables, *i.e.*,  $\Sigma - D$  has to be positive semidefinite, as otherwise statistical interpretations of the solution will be troublesome if not impossible [61, page 326].

In (FACT-ANA), we set  $\mathcal{X} := \{(X, D) \in \mathbf{S}^p \times \mathbf{S}^p \mid \|X\|_2 \leq \Gamma, \mathbf{rank}(X) \leq r, D = \mathbf{diag}(d), d \geq 0\}$ , and

$$f(X, D) := \|\Sigma - X - D\|_F^2 + I_{\mathcal{P}}(X, D),$$



where  $I_{\mathcal{P}}$  denotes the indicator function of the convex set

$$\mathcal{P} = \{(X, D) \in \mathbf{S}^p \times \mathbf{S}^p \mid X \succeq 0, D = \mathbf{diag}(d), d \geq 0, d \in \mathbf{R}^p\}.$$

To compute the projection onto  $\mathcal{X}$ , we use the formula in [36, page 14] and the fact that  $\mathbf{II}_{\{y|y \geq 0\}}(x) = \max\{x, 0\}$ , where pointwise max is used. The proximal operator for  $f$  at  $(X, D)$  can be computed by solving the following convex optimization problem:

$$\begin{aligned} & \text{minimize} && \left\| \Sigma - \tilde{X} - \tilde{D} \right\|_F^2 + \frac{1}{2\gamma} \|\tilde{X} - X\|_F^2 + \frac{1}{2\gamma} \|\tilde{D} - D\|_F^2 \\ & \text{subject to} && \tilde{X} \succeq 0 \\ & && \tilde{D} = \mathbf{diag}(\tilde{d}) \\ & && \Sigma - \tilde{D} \succeq 0 \\ & && \tilde{d} \geq 0 \end{aligned}$$

where  $\tilde{X} \in \mathbf{S}_+^p$ , and  $\tilde{d} \in \mathbf{R}_+^p$  (*i.e.*,  $\tilde{D} = \mathbf{diag}(\tilde{d})$ ) are the optimization variables. Now we are in a position to apply NExOS to this problem.

**Comparison with nuclear norm heuristic.** We compare the solution provided by NExOS to that of the nuclear norm heuristic, which is perhaps the most well-known heuristic to approximately solve (FACT-ANA) [62]. This heuristic considers the following convex relaxation of (FACT-ANA):

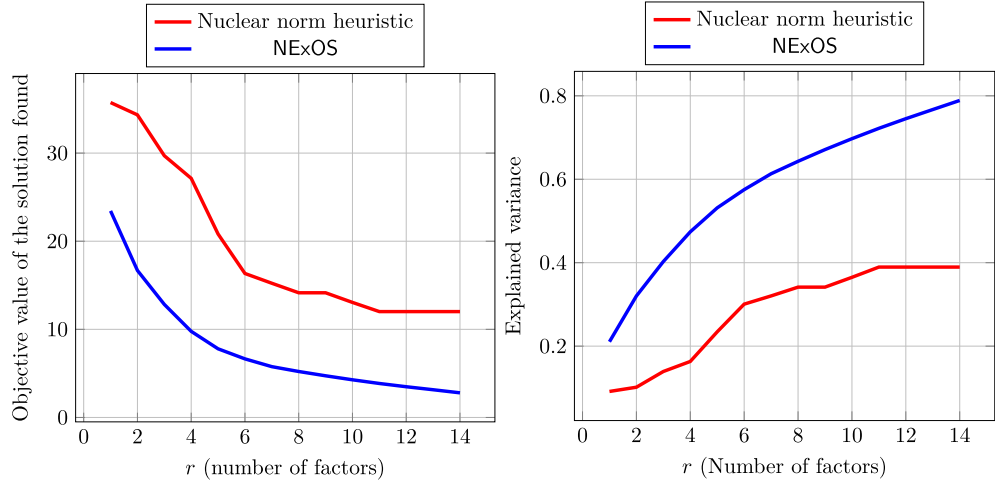
$$\begin{aligned} & \text{minimize} && \|\Sigma - X - D\|_F^2 + \lambda \|X\|_* \\ & \text{subject to} && D = \mathbf{diag}(d) \\ & && d \geq 0 \\ & && X \succeq 0 \\ & && \Sigma - D \succeq 0 \\ & && \|X\|_2 \leq \Gamma, \end{aligned} \tag{14}$$

where  $\lambda$  is a positive parameter that is related to the rank of the decision variable  $X$ . Note that, as  $X$  is positive semidefinite, we have its nuclear norm  $\|X\|_* = \mathbf{tr}(X)$ ; for this reason this heuristic is also called minimum trace factor analysis. The nuclear norm heuristic is similar to Lasso because it solves the relaxed problem (14) for different values of  $\lambda$ , and find the smallest value of  $\lambda$  for which solution to (14) satisfies  $\mathbf{rank}(X) \leq r$ .

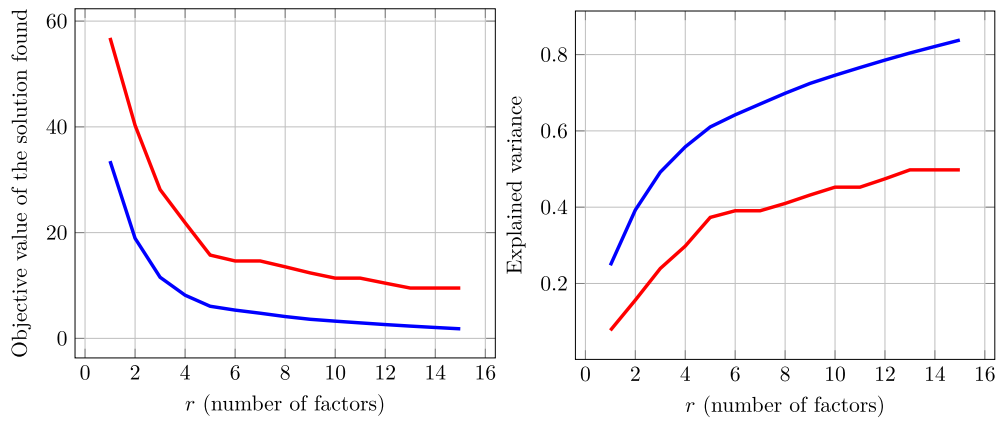
**Performance measures.** We consider two performance measures. First, we compare the objective value  $\|\Sigma - X - D\|_F^2$  of the solutions found by NExOS and the nuclear norm heuristic. As both NExOS and the nuclear norm heuristic provide a point from the feasible set of (FACT-ANA), such a comparison of objective values tells us which algorithm is providing a better quality solution.

Second, we compute the *proportion of explained variance*, which represents how well the  $r$ -common factors explain the residual covariance, *i.e.*,  $\Sigma - D$ . For a given  $r$ , input proportion of variance explained by the  $r$  common factors is given by:

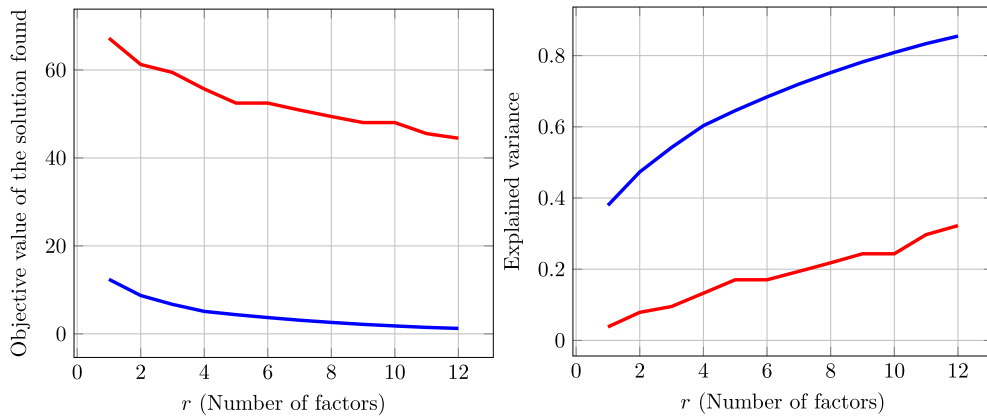
$$\frac{\sum_{i=1}^r \sigma_i(X)}{\sum_{i=1}^p \sigma_i(\Sigma - D)},$$



(a) bfi dataset



(b) neo dataset



(c) Harman74 dataset

**Figure 12:** Figure showing performance of NExOS in solving factor analysis problem for different datasets. Each row represents one dataset. The first and second column compares objective value and proportion of the variance explained of the solutions found by NExOS and the nuclear norm heuristic.

where  $X, D$  are inputs, that correspond to solutions found by NExOS or the nuclear norm heuristic. As  $r$  increases, the explained variance increases to 1. The higher the value of the explained variance for a certain solution, the better is the quality of the solution from a statistical point of view.

**Description of the datasets.** We consider three different real-world bench-mark datasets that are popularly used for factor analysis. These datasets can be found in the R libraries `datasets`, and `psych`.

- The `bfi` dataset contains 2800 observations with 28 variables (25 personality self-reported items and 3 demographic variables) and is available at:  
<https://www.rdocumentation.org/packages/psych/versions/1.0-93/topics/bfi>.
- The `neo` dataset has 1000 measurements for 30 variables and is available at:  
<https://www.rdocumentation.org/packages/psych/versions/1.8.12/topics/neo>.
- The `Harman74` dataset has 145 observations on 24 variables and is available at:  
<https://rdr.io/r/datasets/Harman74.cor.html>.

**Setup.** In applying NExOS for the factor analysis problem, we initialize our iterates with  $Z_0 := \Sigma$  and  $z_0 := \mathbf{0}$ . All the other parameters are kept at their default values as stated in the beginning of §5. For each dataset, we vary the number of factors from 1 to  $\lfloor p/2 \rfloor$ , where  $p$  is the size of the underlying matrix  $\Sigma$ .

**Results.** Figure 12 shows performance of NExOS in solving the factor analysis problem for different datasets, with each row representing one dataset. For each instance, NExOS is able to find a locally optimal solution.

The first column compares the objective value of the solution found by NExOS and the nuclear norm heuristic. We see that for all the datasets, NExOS finds a solution with a better objective value that is considerably lower than that of the nuclear norm heuristic.

The second column shows the proportion of variance explained by the algorithms considered for the datasets considered (higher is better). We see that in terms of the proportion of explained variance, NExOS delivers larger values than that of the nuclear norm heuristic for different values of  $r$ , which is indeed desirable. NExOS consistently provides solutions with better objective value and explained variance compared to the nuclear norm heuristic.

## 6 Conclusions

In this paper, we have presented NExOS, a novel algorithm to solve optimization problems with strongly convex cost functions over nonconvex constraint sets that are prox-regular around local minima – a problem structure that is satisfied by a wide range of nonconvex machine learning problems including sparse and low-rank optimization. We have shown that, under certain regularity conditions, NExOS is able find a locally optimal point of the original problem by solving a sequence of penalized problems with strictly decreasing penalty parameters. Each penalized problem is solved by applying an outer iteration algorithm based on the Douglas-Rachford splitting algorithm. Under mild technical conditions, this outer iteration algorithm converges linearly to a local minimum of the corresponding penalization formulation, and as the penalty parameter goes to zero, the local

minimum of the penalized problem converges to a local minimum of the original problem. We have implemented NExOS in the open-source Julia package `NExOS.jl` and have extensively tested its performance on a wide variety of learning problems. We have found that NExOS is able to compute high quality solutions at a speed that is competitive with tailored algorithms.

## Acknowledgments

We thank Kevin Hu, Miles Lubin, Ian Ruffolo, and Andreas Themelis for careful reading of the manuscript and constructive feedback. We thank Ernest Ryu for fruitful discussions that materially improved this paper.

## References

- [1] D. R. Luke, “Prox-regularity of rank constraint sets and implications for algorithms,” *Journal of Mathematical Imaging and Vision*, vol. 47, no. 3, pp. 231–238, Nov 2013.
- [2] P. Jain and P. Kar, “Non-convex optimization for machine learning,” *Foundations and Trends® in Machine Learning*, vol. 10, no. 3-4, pp. 142–336, 2017.
- [3] T. Hastie, R. Tibshirani, and M. Wainwright, *Statistical learning with sparsity: The lasso and generalizations*. Taylor & Francis, 2015.
- [4] E. Candès, M. B. Wakin, and S. Boyd, “Enhancing sparsity by reweighted l1 minimization,” *Journal of Fourier Analysis and Applications*, 2008.
- [5] J. A. Tropp, “Just relax: Convex programming methods for identifying sparse signals in noise,” *IEEE Transactions on Information Theory*, 2006.
- [6] D. Bertsimas and B. Van Parys, “Sparse hierarchical regression with polynomials,” *Machine Learning*, 2020.
- [7] D. Bertsimas, A. King, and R. Mazumder, “Best subset selection via a modern optimization lens,” *Annals of Statistics*, 2016.
- [8] R. Mazumder, T. Hastie, and R. Tibshirani, “Spectral regularization algorithms for learning large incomplete matrices,” *Journal of Machine Learning Research*, 2010.
- [9] E. Candès and B. Recht, “Exact matrix completion via convex optimization,” *Foundations of Computational Mathematics*, 2009.
- [10] R. Souvenir and R. Piess, “Manifold clustering,” in *Proceedings of the IEEE International Conference on Computer Vision*, 2005.
- [11] A. Gress and I. Davidson, “A flexible framework for projecting heterogeneous data,” in *CIKM 2014 - Proceedings of the 2014 ACM International Conference on Information and Knowledge Management*, 2014.
- [12] T. Mikolov, I. Sutskever, K. Chen, G. Corrado, and J. Dean, “Distributed representations of words and phrases and their compositionality,” in *Advances in Neural Information Processing Systems*, 2013.

- [13] V. Srikumar and C. D. Manning, “Learning distributed representations for structured output prediction,” in *Advances in Neural Information Processing Systems*, 2014.
- [14] F. Bach, “Sharp analysis of low-rank kernel matrix approximations,” in *Journal of Machine Learning Research*, 2013.
- [15] R. T. Rockafellar and R. J.-B. Wets, *Variational analysis*. Springer Science & Business Media, 2009, vol. 317.
- [16] J.-P. Vial, “Strong and weak convexity of sets and functions,” *Mathematics of Operations Research*, vol. 8, no. 2, pp. 231–259, 1983.
- [17] F. H. Clarke, R. J. Stern, and P. R. Wolenski, “Proximal smoothness and the lower- $\mathcal{C}^2$  property,” *Journal of Convex Analysis*, vol. 2, no. 1-2, pp. 117–144, 1995.
- [18] A. Shapiro, “Existence and differentiability of metric projections in Hilbert spaces,” *SIAM Journal on Optimization*, vol. 4, no. 1, pp. 130–141, 1994.
- [19] R. T. Rockafellar, “Characterizing firm nonexpansiveness of prox mappings both locally and globally,” 2020, <http://sites.math.washington.edu/~rtr/papers/rtr254-ProxMaps.pdf>.
- [20] A. Anandkumar and R. Ge, “Efficient approaches for escaping higher order saddle points in non-convex optimization,” in *Journal of Machine Learning Research*, 2016.
- [21] M. Hardt, R. Meka, P. Raghavendra, and B. Weitz, “Computational limits for Matrix Completion,” in *Journal of Machine Learning Research*, 2014.
- [22] M. Fazel, E. Candès, B. Recht, and P. Parrilo, “Compressed sensing and robust recovery of low rank matrices,” in *Conference Record - Asilomar Conference on Signals, Systems and Computers*, 2008.
- [23] M. Fazel, “Matrix Rank Minimization with Applications,” Ph.D. dissertation, Stanford University, 2002.
- [24] S. Boyd and L. Vandenberghe, *Convex Optimization*. Cambridge University Press, 2004.
- [25] I. Goodfellow, Y. Bengio, and A. Courville, *Deep Learning*. MIT Press, 2016, <http://www.deeplearningbook.org>.
- [26] J. Duchi, E. Hazan, and Y. Singer, “Adaptive subgradient methods for online learning and stochastic optimization,” *Journal of Machine Learning Research*, 2011.
- [27] D. P. Kingma and J. L. Ba, “Adam: A method for stochastic optimization,” in *3rd International Conference on Learning Representations, ICLR 2015 - Conference Track Proceedings*, 2015.
- [28] G. Lan, *First-order and Stochastic Optimization Methods for Machine Learning*. Springer, 2020.
- [29] A. Themelis and P. Patrinos, “Douglas-Rachford splitting and ADMM for nonconvex optimization: Tight convergence results,” *SIAM Journal on Optimization*, vol. 30, no. 1, pp. 149–181, 2020.

- [30] S. Boyd, N. Parikh, E. Chu, B. Peleato, and J. Eckstein, “Distributed optimization and statistical learning via the alternating direction method of multipliers,” *Foundations and Trends® in Machine learning*, vol. 3, no. 1, pp. 1–122, 2011.
- [31] T. Erseghe, “Distributed optimal power flow using ADMM,” *IEEE transactions on power systems*, vol. 29, no. 5, pp. 2370–2380, 2014.
- [32] Z. Wen, C. Yang, X. Liu, and S. Marchesini, “Alternating direction methods for classical and ptychographic phase retrieval,” *Inverse Problems*, 2012.
- [33] N. S. Aybat, S. Zarmehri, and S. Kumara, “An ADMM algorithm for clustering partially observed networks,” in *SIAM International Conference on Data Mining 2015, SDM 2015*, 2015.
- [34] R. Takapoui, N. Moehle, S. Boyd, and A. Bemporad, “A simple effective heuristic for embedded mixed-integer quadratic programming,” in *American Control Conference (ACC), 2016*. IEEE, 2016, pp. 5619–5625.
- [35] —, “A simple effective heuristic for embedded mixed-integer quadratic programming,” *International Journal of Control*, pp. 1–11, 2017.
- [36] S. Diamond, R. Takapoui, and S. Boyd, “A general system for heuristic minimization of convex functions over non-convex sets,” *Optimization Methods and Software*, vol. 33, no. 1, pp. 165–193, 2018.
- [37] S. Diamond and S. Boyd, “CVXPY: A Python-embedded modeling language for convex optimization,” *The Journal of Machine Learning Research*, vol. 17, no. 1, pp. 2909–2913, 2016.
- [38] G. Taylor, R. Burmeister, Z. Xu, B. Singh, A. Patel, and T. Goldstein, “Training neural networks without gradients: A scalable ADMM approach,” in *International conference on machine learning*, 2016, pp. 2722–2731.
- [39] R. Takapoui, “The alternating direction method of multipliers for mixed-integer optimization applications,” Ph.D. dissertation, Stanford University, 2017.
- [40] Y. Wang, W. Yin, and J. Zeng, “Global convergence of ADMM in nonconvex nonsmooth optimization,” *Journal of Scientific Computing*, pp. 1–35, 2015.
- [41] G. Li and T. K. Pong, “Global convergence of splitting methods for nonconvex composite optimization,” *SIAM Journal on Optimization*, vol. 25, no. 4, pp. 2434–2460, 2015.
- [42] W. Gao, D. Goldfarb, and F. E. Curtis, “ADMM for multiaffine constrained optimization,” *Optimization Methods and Software*, vol. 35, no. 2, pp. 257–303, 2020.
- [43] R. I. Boţ and D.-K. Nguyen, “The proximal alternating direction method of multipliers in the nonconvex setting: convergence analysis and rates,” *Mathematics of Operations Research*, vol. 45, no. 2, pp. 682–712, 2020.
- [44] A. Themelis, “Proximal algorithms for structured nonconvex optimization,” Ph.D. dissertation, IMT Lucca, 2018.
- [45] A. V. Fiacco and G. P. McCormick, *Nonlinear programming: sequential unconstrained minimization techniques*. SIAM, 1990.

- [46] H. H. Bauschke and P. L. Combettes, *Convex analysis and monotone operator theory in Hilbert spaces*. Springer, 2011, vol. 408.
- [47] N. Parikh and S. Boyd, “Proximal algorithms,” *Foundations and Trends® in Optimization*, vol. 1, no. 3, pp. 127–239, 2014.
- [48] E. K. Ryu and S. Boyd, “Primer on monotone operator methods,” *Appl. Comput. Math.*, vol. 15, no. 1, pp. 3–43, 2016.
- [49] E. K. Ryu, “Uniqueness of DRS as the 2 operator resolvent-splitting and impossibility of 3 operator resolvent-splitting,” *Mathematical Programming*, vol. 182, no. 1, pp. 233–273, 2020.
- [50] P. Giselsson and S. Boyd, “Linear convergence and metric selection for douglas-rachford splitting and ADMM,” *IEEE Transactions on Automatic Control*, vol. 62, no. 2, pp. 532–544, Feb 2017.
- [51] R. Poliquin, R. T. Rockafellar, and L. Thibault, “Local differentiability of distance functions,” *Transactions of the American Mathematical Society*, vol. 352, no. 11, pp. 5231–5249, 2000.
- [52] A. Auslender, “Stability in mathematical programming with nondifferentiable data,” *SIAM Journal on Control and Optimization*, vol. 22, no. 2, pp. 239–254, 1984.
- [53] B. T. Polyak, “Introduction to optimization. Translations series in mathematics and engineering,” *Optimization Software*, 1987.
- [54] F. H. Clarke, *Functional analysis, calculus of variations and optimal control*. Springer Science & Business Media, 2013, vol. 264.
- [55] L. Stella, N. Antonello, M. Fält, D. Volodin, D. Hecceg, E. Saba, F. B. Carlson, T. Kelman, P. Sotasakis, and P. Patrinos, “Proximaloperators.jl,” Sep. 2020. [Online]. Available: <https://doi.org/10.5281/zenodo.4020559>
- [56] I. Dunning, J. Huchette, and M. Lubin, “JuMP: A modeling language for mathematical optimization,” *SIAM Review*, vol. 59, no. 2, pp. 295–320, 2017.
- [57] J. Friedman, T. Hastie, and R. Tibshirani, “glmnet: Lasso and elastic-net regularized generalized linear models,” 2009.
- [58] ———, *The elements of statistical learning*. Springer series in statistics New York, 2001, vol. 1, no. 10.
- [59] J. Lee, S. Kim, G. Lebanon, Y. Singer, and S. Bengio, “LLORMA: Local low-rank matrix approximation,” *The Journal of Machine Learning Research*, vol. 17, no. 1, pp. 442–465, 2016.
- [60] D. Bertsimas, M. S. Copenhaver, and R. Mazumder, “Certifiably optimal low rank factor analysis,” *The Journal of Machine Learning Research*, vol. 18, no. 1, pp. 907–959, 2017.
- [61] J. M. ten Berge, “Some recent developments in factor analysis and the search for proper communalities,” in *Advances in data science and classification*. Springer, 1998, pp. 325–334.
- [62] J. Saunderson, V. Chandrasekaran, P. Parrilo, and A. S. Willsky, “Diagonal and low-rank matrix decompositions, correlation matrices, and ellipsoid fitting,” *SIAM Journal on Matrix Analysis and Applications*, vol. 33, no. 4, pp. 1395–1416, 2012.

- [63] A. Beck, *First-Order Methods in Optimization*. SIAM, 2017, vol. 25.
- [64] F. Bernard, L. Thibault, and N. Zlateva, “Prox-regular sets and epigraphs in uniformly convex Banach spaces: various regularities and other properties,” *Transactions of the American Mathematical Society*, vol. 363, no. 4, pp. 2211–2247, 2011.
- [65] W. Rudin, *Principles of Mathematical Analysis*. McGraw-hill New York, 1986.
- [66] A. L. Dontchev and R. T. Rockafellar, *Implicit functions and solution mappings*. Springer, 2009, vol. 543.
- [67] E. K. Ryu and W. Yin, *Large-Scale Convex Optimization via Monotone Operators*, 2020, <https://large-scale-book.mathopt.com/LSCOMO.pdf>.



## A Proofs to the results in §1

### A.1 Proof to Lemma 1

To prove this result, we use the following helper Lemma.

**Lemma 8** (Computing  $\mathbf{prox}_{\gamma(g+\frac{\beta}{2}\|\cdot\|^2)}(x)$ ). *For any proper (not necessarily convex) function  $g : \mathbf{E} \rightarrow \mathbf{R} \cup \{+\infty\}$ , for any  $x \in \mathbf{E}$ , and for any  $\beta, \gamma > 0$ , we have*

$$\mathbf{prox}_{\gamma(g+\frac{\beta}{2}\|\cdot\|^2)}(x) = \mathbf{prox}_{\gamma\kappa g}(\kappa x),$$

where  $\kappa = \frac{1}{\beta\gamma+1} \in [0, 1]$ .

*Proof.* This result follows from [63, Theorem 6.13]. □

Now, we start the proof to Lemma 1 with the proof sketch as follows. First we prove that, the proximal operator of  ${}^\mu\iota$ —the Moreau envelope of  $\iota$ —is:

$$\mathbf{prox}_{\gamma\mu\iota}(x) = \frac{\mu}{\gamma + \mu}x + \frac{\gamma}{\gamma + \mu}\mathbf{\Pi}(x),$$

and then using Lemma 8 we arrive at the claim.

Using the definition of proximal operator, we have,

$$\mathbf{prox}_{\gamma\mu\iota}(x) = \operatorname{argmin}_z ({}^\mu\iota(z) + \frac{1}{2\gamma}\|z - x\|^2), \quad (15)$$

hence we are interested in solving the following minimization problem, which can be subsequently modified as follows

$$\begin{aligned} & \min_z \left( {}^\mu\iota(z) + \frac{1}{2\gamma}\|z - x\|^2 \right) \\ & \stackrel{a)}{=} \min_z \left\{ \min_y \left( \iota(y) + \frac{1}{2\mu}\|z - y\|^2 \right) + \frac{1}{2\gamma}\|z - x\|^2 \right\} \\ & \stackrel{b)}{=} \min_z \left\{ \min_y \left( \iota(y) + \frac{1}{2\mu}\|z - y\|^2 + \frac{1}{2\gamma}\|z - x\|^2 \right) \right\} \\ & \stackrel{c)}{=} \min_y \min_z \left( \iota(y) + \frac{1}{2\mu}\|z - y\|^2 + \frac{1}{2\gamma}\|z - x\|^2 \right) \\ & \stackrel{d)}{=} \min_y \left\{ \iota(y) + \min_z \left( \frac{1}{2\mu}\|z - y\|^2 + \frac{1}{2\gamma}\|z - x\|^2 \right) \right\}, \end{aligned} \quad (16)$$

where in *a*) we have used the definition of Moreau envelope, in *b*) we have included the term  $\frac{1}{2\gamma}\|z - x\|^2$  in the inner minimization w.r.t.  $y$ , in *c*) we have switched the order of the minimization which is an allowed operation due to [15, Proposition 1.35] and in *d*) we have separated the term  $\iota(y)$  from the inner minimization w.r.t.  $z$ . Now first note that, the inner minimization problem attains its minimum at

$$z^*(y) = \frac{\gamma y + \mu x}{\gamma + \mu}$$

for any value of  $y$ . Hence the optimal value of the inner minimization problem

$$\min_z \left( \frac{1}{2\mu} \|z - y\|^2 + \frac{1}{2\gamma} \|z - x\|^2 \right)$$

is  $\frac{1}{\gamma+\mu} \frac{1}{2} \|x - y\|^2$ , and (16) is equal to

$$\begin{aligned} & \min_y \left( \iota(y) + \frac{1}{\gamma + \mu} \frac{1}{2} \|x - y\|^2 \right) \\ &= \min_{y \in \mathcal{C}} \left( \frac{1}{\gamma + \mu} \frac{1}{2} \|x - y\|^2 \right), \end{aligned}$$

i.e., the inner minimization is solved by any element of the projection map  $\mathbf{\Pi}(x)$  onto  $\mathcal{X}$ . Thus using [15, Proposition 1.35], an optimal solution of (15) is given by  $z^*(y) = \frac{\gamma y + \mu x}{\gamma + \mu}$ , where  $y = \mathbf{\Pi}(x)$ . Thus we have shown that,

$$\mathbf{prox}_{\gamma\mu\iota}(x) = \frac{\mu}{\gamma + \mu} x + \frac{\gamma}{\gamma + \mu} \mathbf{\Pi}(x). \quad (17)$$

Now we compute the proximal operator of  $\mu_{\natural} \equiv \mu_{\natural} + \frac{\beta}{2} \|\cdot\|^2$  using (17) and Lemma 8 as follows:

$$\begin{aligned} \mathbf{prox}_{\gamma\mu_{\natural}}(x) &= \mathbf{prox}_{\frac{\gamma}{\beta\gamma+1}\mu_{\natural}} \left( \frac{x}{\beta\gamma+1} \right) \\ &\stackrel{a)}{=} \frac{\mu}{\frac{\gamma}{\beta\gamma+1} + \mu} \frac{x}{\beta\gamma+1} + \frac{\frac{\gamma}{\beta\gamma+1}}{\frac{\gamma}{\beta\gamma+1} + \mu} \mathbf{\Pi} \left( \frac{x}{\beta\gamma+1} \right) \\ &= \frac{\mu}{\frac{\gamma}{\beta\gamma+1} + \mu} \frac{x}{\beta\gamma+1} + \left( 1 - \frac{\mu}{\frac{\gamma}{\beta\gamma+1} + \mu} \right) \mathbf{\Pi} \left( \frac{x}{\beta\gamma+1} \right), \end{aligned}$$

where  $a)$  uses (17). Thus we have arrived at the claim.

## B Proofs to the results in §3

### B.1 Proof to Lemma 3

In this proof, we are going to use the following result from [64], where by  $d_{\mathcal{S}}(x)$  we denote the Euclidean distance of a point  $x$  from the set  $\mathcal{S}$ , and  $\overline{\mathcal{S}}$  denotes closure of a set  $\mathcal{X}$ .

**Lemma 9** (Intersection of prox-regular sets [64, Corollary 7.3(a)]). *Let  $\mathcal{S}_1, \mathcal{S}_2$  be two closed sets in  $\mathbf{E}$ , such that  $\mathcal{S} = \mathcal{S}_1 \cap \mathcal{S}_2 \neq \emptyset$  and both  $\mathcal{S}_1, \mathcal{S}_2$  are prox-regular at  $x \in \mathcal{S}$ . If  $\mathcal{S}$  is metrically calm at  $x$  i.e., if there exist some  $\varsigma > 0$  and some neighborhood of  $x$  denoted by  $\mathcal{B}$  such that*

$$d_{\mathcal{S}}(y) \leq \varsigma (d_{\mathcal{S}_1}(y) + d_{\mathcal{S}_2}(y)) \quad (18)$$

for all  $y \in \mathcal{B}$ , then  $\mathcal{S}$  is prox-regular at  $x$ .

Now, we start the proof. The set  $\mathcal{N}$  is prox-regular at  $x$  by assumption. Now, a set is prox-regular at a point if and only if projection onto that set is single-valued on some neighborhood of that point

[51, Theorem 1.3]. From this result, projection onto  $\mathcal{N}$  is single-valued on some open ball  $B(x; a)$  with center  $x$  and radius  $a > 0$ . Also, the set associated with the convex constraints  $\mathcal{C}$  is compact and convex, hence projection onto  $\mathcal{C}$  is single-valued around every point, hence single-valued on  $B(x; a)$  as well [46, Theorem 3.14, Remark 3.15]. Note that for any  $y \in B(x; a)$ ,  $d_{\mathcal{X}}(y) = 0$  if and only if both  $d_{\mathcal{C}}(y)$  and  $d_{\mathcal{N}}(y)$  are zero. Hence, for any  $y \in B(x; a) \cap \mathcal{X}$ , the metrically calmness condition (18) is trivially satisfied. Next, recalling that the distance from a closed set is continuous [15, Example 9.6], over the compact set  $\overline{B(x; a) \setminus \mathcal{X}}$ , the ratio

$$\frac{d_{\mathcal{X}}(y)}{d_{\mathcal{C}}(y) + d_{\mathcal{N}}(y)}$$

is continuous over  $y$ , hence it will attain a maximum  $\varsigma > 0$  over  $\overline{B(x; a) \setminus \mathcal{X}}$  [65, Theorem 4.16], thus satisfying the metrically calmness condition (18) on  $B(x; a) \setminus \mathcal{X}$  as well. Hence, using Lemma 9, the constraint set  $\mathcal{X}$  is prox-regular at  $x$ .

## B.2 Proof to Lemma 4

(i): For any  $\mu, \beta > 0$ , and for any  $y \in \mathbf{E}$ , we can write

$$\begin{aligned} \mu_{\natural}(y) &= \mu_{\iota}(y) + \frac{\beta}{2} \|y\|^2 \\ &\stackrel{a)}{=} \frac{1}{2\mu} d^2(y) + \frac{\beta}{2} \|y\|^2 \\ &= \frac{1}{2\mu} (d^2(y) + \beta\mu \|y\|^2), \end{aligned}$$

where  $a)$  follows from (1). From the proof to [51, Proposition 3.1 (iii)], it follows that the function  $d^2 + \beta\mu \|\cdot\|^2$  is convex and differentiable on an open ball  $B(x; r_{\mu})$  with center  $x$  and radius  $r_{\mu} \geq c_x \frac{\beta\mu}{\beta\mu+1}$ , where  $c_x > 0$  is a constant that depends on  $x$  only. Thus, for any  $\mu, \beta > 0$ , the function  $\mu_{\natural}$  is locally convex and differentiable on  $B(x; r_{\mu})$ .

(ii): The function  $f + \mu_{\natural}$  is  $\alpha$ -strongly convex and differentiable on  $B(x; r_{\mu})$ , because its summands  $f$  is  $\alpha$ -strongly convex and differentiable everywhere, and  $\mu_{\natural}$  is locally convex and differentiable on  $B(x; r_{\mu})$  as shown in (i). Now let us show smoothness of  $f + \mu_{\natural}$  on  $B(x; r_{\mu})$ . On  $B(x; r_{\mu})$ , the function  $f + \mu_{\natural}$  is differentiable with derivative

$$\begin{aligned} \nabla (f + \mu_{\natural})(x) &= \nabla \left( f + \frac{\beta}{2} \|\cdot\|^2 + \mu_{\iota} \right) (x) \\ &= \nabla f(x) + \beta x + \frac{1}{2\mu} \nabla d^2(x) \\ &\stackrel{a)}{=} \nabla f(x) + \beta x + \frac{1}{\mu} (x - \mathbf{\Pi}(x)) \\ &= \nabla f(x) + \left( \beta + \frac{1}{\mu} \right) x - \frac{1}{\mu} \mathbf{\Pi}(x), \end{aligned} \tag{19}$$

where  $a)$  uses (i) and the following fact from [51, Theorem 1.3(e)]:  $\nabla d^2(x) = 2(x - \mathbf{\Pi}(x))$  whenever  $d^2$  is differentiable [51, page 5240]. Thus, for any  $x_1, x_2 \in B(x; r_{\mu})$  we have

$$\begin{aligned}
& \left\| \nabla \left( f + \frac{\beta}{2} \|\cdot\|^2 + \mu \iota \right) (x_1) - \nabla \left( f + \frac{\beta}{2} \|\cdot\|^2 + \mu \iota \right) (x_2) \right\| \\
&= \left\| \nabla f(x_1) + \left( \beta + \frac{1}{\mu} \right) x_1 - \frac{1}{\mu} \mathbf{\Pi}(x_1) - \nabla f(x_2) - \left( \beta + \frac{1}{\mu} \right) x_2 + \frac{1}{\mu} \mathbf{\Pi}(x_2) \right\| \\
&\stackrel{a)}{\leq} \underbrace{\left\| \nabla f(x_1) - \nabla f(x_2) \right\|}_{\leq L \|x_1 - x_2\|} + \left( \beta + \frac{1}{\mu} \right) \|x_1 - x_2\| + \frac{1}{\mu} \underbrace{\left\| \mathbf{\Pi}(x_1) - \mathbf{\Pi}(x_2) \right\|}_{\leq (1+\beta\mu) \|x_1 - x_2\|} \\
&\leq \left( L + 2\beta + \frac{2}{\mu} \right) \|x_1 - x_2\|,
\end{aligned}$$

where we have used the following in a):  $\nabla f$  is  $L$ -Lipschitz everywhere due to  $f$  being an  $L$ -smooth function in  $\mathbf{E}$  ([46, Theorem 18.15]), and on  $B(x; r_\mu)$  the projection operator  $\mathbf{\Pi}$  is  $(1+\beta\mu)$ -Lipschitz continuous ([51, page 5239]).

(iii): Let  $\overline{B}(x; r_\mu)$  be the closure of the open ball  $B(x; r_\mu)$ . Define the function  $g$  as follows:

$$g(y) = \begin{cases} \mu_0(y), & \text{if } y \in B(x; r_\mu) \\ \liminf_{\tilde{y} \rightarrow y} \mu_0(\tilde{y}), & \text{if } \|y - x\| = r_\mu \\ +\infty, & \text{else.} \end{cases}$$

which is CPC everywhere due to [46, Lemma 1.31 and Corollary 9.10]. As  $g$  is CPC, we have  $\mathbf{prox}_{\gamma g} = \mathbb{J}_{\gamma \partial g}$  on  $\mathbf{E}$  and  $\mathbf{prox}_{\gamma g}$  is firmly nonexpansive and single-valued everywhere, which follows from [46, Proposition 12.27, Proposition 16.34, and Example 23.3]. But, for  $y \in B(x; r_\mu)$ , we have  $\mu_0(y) = g(y)$  and  $\nabla \mu_0(y) = \partial g(y)$ . Thus, on  $B(x; r_\mu)$ , the operator  $\mathbf{prox}_{\gamma \mu_0} = \mathbb{J}_{\gamma \nabla \mu_0}$ , and it is firmly nonexpansive and single-valued.

Any firmly nonexpansive operator has a nonexpansive reflection operator on its domain of firm nonexpansiveness [46, Proposition 4.2]. Hence, on  $B(x; r_\mu)$ , the reflection operator  $2\mathbf{prox}_{\gamma \mu_0} - \mathbb{I}$  is nonexpansive.

### B.3 Proof to Proposition 1

First, we show that the reflection operator can be represented as

$$\mathbb{R}_\mu = \left( 2\mathbf{prox}_{\gamma \mu_0} - \mathbb{I} \right) \left( 2\mathbf{prox}_{\gamma f} - \mathbb{I} \right), \tag{20}$$

which will then be used to show the contractive nature of  $\mathbb{R}_\mu$  over the region of convexity  $B(x; r_\mu)$ . To show the previous equality, first note that, for every  $x \in \mathbf{E}$ ,

$$\begin{aligned}
\mathbb{T}_\mu(x) &= \left( \mathbf{prox}_{\gamma \mu_0} \left( 2\mathbf{prox}_{\gamma f} - \mathbb{I} \right) + \mathbb{I} - \mathbf{prox}_{\gamma f} \right) (x) \\
&= \mathbf{prox}_{\gamma \mu_0} \left( 2\mathbf{prox}_{\gamma f}(x) - x \right) + x - \mathbf{prox}_{\gamma f}(x).
\end{aligned} \tag{21}$$

Furthermore, for every  $x \in \mathbf{E}$ ,

$$\mathbb{R}_\mu(x) = \left( 2\mathbb{T}_\mu - \mathbb{I} \right) (x)$$

$$\stackrel{a)}{=} 2\mathbf{prox}_{\gamma\mu_0}(2\mathbf{prox}_{\gamma f}(x) - x) + x - 2\mathbf{prox}_{\gamma f}(x), \quad (22)$$

where  $a)$  uses (21). Hence, for every  $x \in \mathbf{E}$ ,

$$\begin{aligned} (2\mathbf{prox}_{\gamma\mu_0} - \mathbb{I})(2\mathbf{prox}_f - \mathbb{I})(x) &= (2\mathbf{prox}_{\gamma\mu_0} - \mathbb{I}) \underbrace{(2\mathbf{prox}_f(x) - x)}_{=y \text{ (let)}} \\ &= 2\mathbf{prox}_{\gamma\mu_0}(y) - y \\ &= 2\mathbf{prox}_{\gamma\mu_0}(2\mathbf{prox}_f(x) - x) - 2\mathbf{prox}_f(x) + x \\ &\stackrel{a)}{=} \mathbb{R}_\mu(x), \end{aligned}$$

where  $a)$  uses (22). Thus we have shown (20).

Now, we start the proof to Proposition 1. Using (20), for every  $x_1, x_2 \in B(x; r_\mu)$  we have

$$\begin{aligned} &\|\mathbb{R}_\mu(x_1) - \mathbb{R}_\mu(x_2)\| \\ &= \left\| \left( (2\mathbf{prox}_{\gamma\mu_0} - \mathbb{I})(2\mathbf{prox}_{\gamma f} - \mathbb{I})(x_1) \right) - \left( (2\mathbf{prox}_{\gamma\mu_0} - \mathbb{I})(2\mathbf{prox}_{\gamma f} - \mathbb{I})(x_2) \right) \right\| \quad (23) \\ &= \left\| (2\mathbf{prox}_{\gamma\mu_0} - \mathbb{I}) \left( (2\mathbf{prox}_{\gamma f} - \mathbb{I})(x_2) \right) - (2\mathbf{prox}_{\gamma\mu_0} - \mathbb{I}) \left( (2\mathbf{prox}_{\gamma f} - \mathbb{I})(x_2) \right) \right\| \\ &\stackrel{a)}{\leq} \left\| (2\mathbf{prox}_{\gamma f} - \mathbb{I})(x_1) - (2\mathbf{prox}_{\gamma f} - \mathbb{I})(x_2) \right\| \\ &\stackrel{b)}{\leq} \kappa \|x_1 - x_2\|, \quad (24) \end{aligned}$$

where  $\kappa \in [0, 1)$  is the contraction factor. In the equations above,  $a)$  uses the fact that  $2\mathbf{prox}_{\gamma\mu_0} - \mathbb{I}$  is nonexpansive over  $B(x; r_\mu)$  from Lemma 4(iii),  $b)$  uses the  $\kappa$ -contractiveness of the operator  $2\mathbf{prox}_{\gamma f} - \mathbb{I}$  from Lemma 2, where  $\kappa \in (0, 1)$ . Thus we have proved that  $\mathbb{R}_\mu$  acts as a contractive operator over the set  $B(x; r_\mu)$ .

Similarly, for any  $x_1, x_2 \in B(x; r_\mu)$  we have

$$\begin{aligned} \|\mathbb{T}_\mu(x_1) - \mathbb{T}_\mu(x_2)\| &\stackrel{a)}{=} \left\| \frac{1}{2}\mathbb{R}_\mu(x_1) + \frac{1}{2}x_1 - \frac{1}{2}\mathbb{R}_\mu(x_2) - \frac{1}{2}x_2 \right\| \\ &= \left\| \frac{1}{2}(x_1 - x_2) + \frac{1}{2}(\mathbb{R}_\mu(x_1) - \mathbb{R}_\mu(x_2)) \right\| \\ &\stackrel{b)}{\leq} \frac{1}{2}\|x_1 - x_2\| + \frac{1}{2} \underbrace{\|\mathbb{R}_\mu(x_1) - \mathbb{R}_\mu(x_2)\|}_{\leq \kappa \|x_1 - x_2\|} \\ &\leq \underbrace{\left( \frac{1 + \kappa}{2} \right)}_{\in [0, 1)} \|x_1 - x_2\|, \quad (25) \end{aligned}$$

where  $a)$  uses (Compact-OI), and  $b)$  uses triangle inequality and (24). As the factor  $\kappa' = (1 + \kappa)/2 \in [0, 1)$ ; the operator  $\mathbb{T}_\mu$  is  $\kappa'$ -contractive on  $B(x; r_\mu)$ .

## B.4 Proof to Lemma 5

First, recall that,

$$\mathbb{T}_\mu = \frac{1}{2}\mathbb{R}_\mu + \frac{1}{2}\mathbb{I}$$

For any  $x \in \mathbf{E}$  and  $\mu, \tilde{\mu} > 0$ , we have

$$\begin{aligned}
\|\mathbb{T}_\mu(x) - \mathbb{T}_{\tilde{\mu}}(x)\| &= \left\| \frac{1}{2}\mathbb{R}_\mu x + \frac{1}{2}x - \frac{1}{2}\mathbb{R}_{\tilde{\mu}}x - \frac{1}{2}x \right\| \\
&= \frac{1}{2}\|\mathbb{R}_\mu x - \mathbb{R}_{\tilde{\mu}}x\| \\
&= \frac{1}{2}\left\| \left(2\mathbf{prox}_{\gamma\mu_0} - \mathbb{I}\right) \underbrace{\left(2\mathbf{prox}_{\gamma f} - \mathbb{I}\right)x}_{=y \text{ (say)}} - \left(2\mathbf{prox}_{\gamma\tilde{\mu}_0} - \mathbb{I}\right) \underbrace{\left(2\mathbf{prox}_{\gamma f} - \mathbb{I}\right)x}_{=y} \right\| \\
&= \frac{1}{2}\left\| \left(2\mathbf{prox}_{\gamma\mu_0} - \mathbb{I}\right)y - \left(2\mathbf{prox}_{\gamma\tilde{\mu}_0} - \mathbb{I}\right)y \right\| \\
&= \frac{1}{2}\|2\mathbf{prox}_{\gamma\mu_0}y - y - 2\mathbf{prox}_{\gamma\tilde{\mu}_0}y + y\| \\
&= \frac{1}{2}\|2\mathbf{prox}_{\gamma\mu_0}y - 2\mathbf{prox}_{\gamma\tilde{\mu}_0}y\| \\
&= \|\mathbf{prox}_{\gamma\mu_0}y - \mathbf{prox}_{\gamma\tilde{\mu}_0}y\| \\
&\stackrel{a)}{=} \left\| \frac{\mu}{\gamma + \mu(\beta\gamma + 1)}y + \frac{\gamma}{\gamma + \mu(\beta\gamma + 1)}\mathbf{\Pi}\left(\frac{y}{\beta\gamma + 1}\right) \right. \\
&\quad \left. - \frac{\tilde{\mu}}{\gamma + \tilde{\mu}(\beta\gamma + 1)}y - \frac{\gamma}{\gamma + \tilde{\mu}(\beta\gamma + 1)}\mathbf{\Pi}\left(\frac{y}{\beta\gamma + 1}\right) \right\| \\
&= \left\| \left( \frac{\mu}{\gamma + \mu(\beta\gamma + 1)} - \frac{\tilde{\mu}}{\gamma + \tilde{\mu}(\beta\gamma + 1)} \right) y \right. \\
&\quad \left. + \left( \frac{\gamma}{\gamma + \mu(\beta\gamma + 1)} - \frac{\gamma}{\gamma + \tilde{\mu}(\beta\gamma + 1)} \right) \mathbf{\Pi}\left(\frac{y}{\beta\gamma + 1}\right) \right\| \\
&\leq \left\| \left( \frac{\mu}{\gamma + \mu(\beta\gamma + 1)} - \frac{\tilde{\mu}}{\gamma + \tilde{\mu}(\beta\gamma + 1)} \right) \right\| \|y\| \\
&\quad + \left\| \left( \frac{\gamma}{\gamma + \mu(\beta\gamma + 1)} - \frac{\gamma}{\gamma + \tilde{\mu}(\beta\gamma + 1)} \right) \right\| \left\| \mathbf{\Pi}\left(\frac{y}{\beta\gamma + 1}\right) \right\|, \tag{26}
\end{aligned}$$

where  $a)$  uses Lemma 1. Note that in line 3 we have set

$$y = 2\mathbf{prox}_{\gamma f}(x) - x \tag{27}$$

to avoid notational clutter.

Now,

$$\begin{aligned}
\left\| \frac{\mu}{\gamma + \mu(\beta\gamma + 1)} - \frac{\tilde{\mu}}{\gamma + \tilde{\mu}(\beta\gamma + 1)} \right\| &= \left\| \frac{\gamma(\mu - \tilde{\mu})}{(\gamma + \mu(\beta\gamma + 1))(\gamma + \tilde{\mu}(\beta\gamma + 1))} \right\| \\
&= \left\| \frac{\frac{1}{\gamma}(\mu - \tilde{\mu})}{\frac{1}{\gamma^2}(\gamma + \mu(\beta\gamma + 1))(\gamma + \tilde{\mu}(\beta\gamma + 1))} \right\|
\end{aligned}$$

$$\begin{aligned}
&= \left\| \frac{\frac{1}{\gamma}(\mu - \tilde{\mu})}{\left(1 + \mu(\beta + \frac{1}{\gamma})\right) \left(1 + \tilde{\mu}(\beta + \frac{1}{\gamma})\right)} \right\| \\
&\leq \frac{1}{\gamma} \|\mu - \tilde{\mu}\|,
\end{aligned}$$

and similarly,

$$\begin{aligned}
\left\| \left( \frac{\gamma}{\gamma + \mu(\beta\gamma + 1)} - \frac{\gamma}{\gamma + \tilde{\mu}(\beta\gamma + 1)} \right) \right\| &= \left\| -\frac{\gamma(\beta\gamma + 1)(\mu - \tilde{\mu})}{(\gamma + \mu(\beta\gamma + 1))(\gamma + \tilde{\mu}(\beta\gamma + 1))} \right\| \\
&\leq \left( \beta + \frac{1}{\gamma} \right) \|\mu - \tilde{\mu}\|.
\end{aligned}$$

Putting the last two inequalities in (26), we have for any  $x \in \mathcal{B}$ , and for any  $\mu, \tilde{\mu} \in \mathbf{R}_{++}$ ,

$$\begin{aligned}
\|\mathbb{T}_\mu(x) - \mathbb{T}_{\tilde{\mu}}(x)\| &= \frac{1}{2} \|\mathbb{R}_\mu x - \mathbb{R}_{\tilde{\mu}} x\| \\
&\leq \frac{1}{\gamma} \|\mu - \tilde{\mu}\| \|y\| + \left( \beta + \frac{1}{\gamma} \right) \|\mu - \tilde{\mu}\| \left\| \mathbf{\Pi} \left( \frac{y}{\beta\gamma + 1} \right) \right\|
\end{aligned} \tag{28}$$

$$\begin{aligned}
&= \left( \frac{1}{\gamma} \|y\| + \left( \beta + \frac{1}{\gamma} \right) \left\| \mathbf{\Pi} \left( \frac{y}{\beta\gamma + 1} \right) \right\| \right) \|\mu - \tilde{\mu}\| \\
&\stackrel{a)}{=} \left( \frac{1}{\gamma} \|2\mathbf{prox}_{\gamma f}(x) - x\| + \left( \beta + \frac{1}{\gamma} \right) \left\| \mathbf{\Pi} \left( \frac{2\mathbf{prox}_{\gamma f}(x) - x}{\beta\gamma + 1} \right) \right\| \right) \|\mu - \tilde{\mu}\|,
\end{aligned} \tag{29}$$

where  $a)$  uses (27). Now, as  $\mathcal{B}$  is a bounded set and  $x \in \mathcal{B}$ , norm of the vector  $y = 2\mathbf{prox}_{\gamma f}(x) - x$  can be upper-bounded over  $\mathcal{B}$  because  $2\mathbf{prox}_{\gamma f} - \mathbf{I}$  is continuous (in fact contractive) from Lemma 2. Also as  $\mathcal{X}$  is a compact set, for any  $x$ ,  $\left\| \mathbf{\Pi} \left( (2\mathbf{prox}_{\gamma f}(x) - x)/(\beta\gamma + 1) \right) \right\|$  is upper-bounded. Combining the last two-statements, it follows that there exists some  $\ell > 0$  such that

$$\sup_{x \in \mathcal{B}} \left( \frac{1}{\gamma} \|2\mathbf{prox}_{\gamma f}(x) - x\| + \left( \beta + \frac{1}{\gamma} \right) \left\| \mathbf{\Pi} \left( \frac{2\mathbf{prox}_{\gamma f}(x) - x}{\beta\gamma + 1} \right) \right\| \right) \leq \ell,$$

and putting the last inequality in (29), we get

$$\|\mathbb{T}_\mu(x) - \mathbb{T}_{\tilde{\mu}}(x)\| \leq \ell \|\mu - \tilde{\mu}\|$$

for any  $x \in \mathcal{B}$ .

## B.5 Proof to Lemma 6

To prove (i), we are going to use the following lemma regarding differentiability of  ${}^\mu\iota$ .

**Lemma 10** (Differentiability of  ${}^\mu\iota$ ). *Let  $\bar{x} \in \mathcal{X}$  be a local minimum to  $(\mathcal{P})$ , where Assumptions 1, 2, and 3 hold. Then there exists some  $r_0 > 0$  such that for any  $\mu > 0$ ,*

(i) *the function  ${}^\mu\iota$  is differentiable on  $\overline{\mathcal{B}}(\bar{x}; r_0)$  with derivative*

$$\nabla {}^\mu\iota = \frac{1}{\mu}(\mathbf{I} - \mathbf{\Pi}),$$

and

(ii) *projection operator  $\mathbf{\Pi}$  onto  $\mathcal{X}$  is single-valued and continuous on  $\overline{\mathcal{B}}(\bar{x}; r_0)$ .*

*Proof.* From [51, Theorem 1.3(e)], there exists some  $r_0 > 0$  such that the function  $d^2$  is differentiable on  $\overline{B}(\bar{x}; r_0)$ . As  ${}^\mu\iota = (1/2\mu)d^2$  from 1, it follows that for any  $\mu > 0$ ,  ${}^\mu\iota$  is differentiable on  $\overline{B}(\bar{x}; r_0)$  which proves the first part of (i). The second part of (i) follows from the fact that  $\nabla d^2(x) = 2(x - \mathbf{\Pi}(x))$  whenever  $d^2$  is differentiable at  $x$  [51, page 5240]. Finally, from [51, Lemma 3.2], whenever  $d^2$  is differentiable at a point, projection  $\mathbf{\Pi}$  is single-valued and continuous at that point, and this proves (ii).  $\square$

(i): Now we start proving (i) earnestly. As point  $\bar{x} \in \mathcal{X}$  is a local minimum of  $(\mathcal{P})$ , from Definition 3, there is some  $r > 0$  such that for all  $y \in \overline{B}(\bar{x}; r)$ , we have

$$f(\bar{x}) + \frac{\beta}{2}\|\bar{x}\|^2 < f(y) + \frac{\beta}{2}\|y\|^2 + \iota(y).$$

As  $f + {}^\mu\iota$  is a global underestimator of and approximates the function  $f + \frac{\beta}{2}\|\cdot\|^2 + \iota$  with arbitrary precision as  $\mu \rightarrow 0$  (§2.1.1), due to Lemma 10(i), we can find some  $r_0 > 0$  such that for any  $\mu > 0$  the function  $f + {}^\mu\iota$  will be differentiable in the open ball  $B(\bar{x}; r_0)$ . The previous statement and [15, Theorem 1.25] imply that there exist some  $\check{\mu} > 0$  and some  $\check{r} \leq \min\{r, r_0\}$  such that for any  $\mu \in (0, \check{\mu}]$ , the function  $f + {}^\mu\iota$  will achieve a local minimum  $x_\mu$  over  $B(\bar{x}; \check{r})$  where the  $\nabla(f + {}^\mu\iota)$  vanishes, *i.e.*,

$$\nabla(f + {}^\mu\iota)(x_\mu) = \nabla f(x_\mu) + \beta x_\mu + \frac{1}{\mu}(x_\mu - \mathbf{\Pi}(x_\mu)) = 0 \quad (30)$$

$$\Rightarrow x_\mu = \frac{1}{\beta\mu + 1}(\mathbf{\Pi}(x_\mu) - \mu\nabla f(x_\mu)). \quad (31)$$

This proves (i).

(ii): Using [15, Theorem 1.25], as  $\mu \rightarrow 0$ , we have

$$x_\mu \rightarrow \bar{x}, \text{ and } (f + {}^\mu\iota)(x_\mu) \rightarrow f(\bar{x}) + \frac{\beta}{2}\|\bar{x}\|^2.$$

Note that  $x_\mu$  reaches  $\bar{x}$  only in limit, as otherwise Assumption 3 will be violated.

(iii): In (ii)  $x_\mu \rightarrow \bar{x}$  as  $\mu \rightarrow 0$ , and the projection operator is continuous over  $B(\bar{x}; \check{r})$  from Lemma 10(ii), so

$$\mathbf{\Pi}(x_\mu) \rightarrow \mathbf{\Pi}(\bar{x}) = \bar{x}, \quad (32)$$

as  $\mu \rightarrow 0$ . This means that for any  $\epsilon > 0$ , there exist some  $\hat{\mu} \in (0, \check{\mu}]$  such that for any  $\mu \in (0, \hat{\mu}]$ , we have  $\|\mathbf{\Pi}(x_\mu) - \bar{x}\| < \epsilon$ . As  $\alpha > 0$  by construction and  $\min_{\mu \in [\xi, \check{\mu}]} r_\mu > 0$  due to (5), setting  $\epsilon := \alpha \min_{\mu \in [\xi, \check{\mu}]} r_\mu > 0$ , we must have some  $\hat{\mu} \in (0, \check{\mu}]$  such that for any  $\mu \in (0, \hat{\mu}]$ ,

$$\|\mathbf{\Pi}(x_\mu) - \bar{x}\| < \alpha \min_{\mu \in [\xi, \check{\mu}]} r_\mu,$$

thus arriving at the claim.



## B.6 Proof to Lemma 7

The structure of the proof follows that of [46, Proposition 25.1(ii)]. For notational convenience, we have used  $\mathbb{J}_{\gamma\nabla f} = \mathbf{prox}_{\gamma f}$ ,  $\mathbb{R}_{\gamma\nabla f} = \mathbb{J}_{\gamma\nabla f} - \mathbb{I}$  and  $\mathbb{R}_{\gamma\mu_0} = 2\mathbb{J}_{\gamma\mu_0} - \mathbb{I}$ . Then  $x_\mu \in B(\bar{x}; r_\mu)$  satisfies

$$\begin{aligned}
& x_\mu \in \mathbf{zer}(\nabla f + \nabla^{\mu_0}) \\
& \Leftrightarrow (\exists y \in \mathbf{E}) \ x_\mu - y \in \gamma\nabla^{\mu_0}(x_\mu) \text{ and } y - x_\mu \in \gamma\nabla f(x_\mu) \\
& \Leftrightarrow (\exists y \in \mathbf{E}) \ 2x_\mu - y \in (\mathbb{I} + \gamma\nabla^{\mu_0})(x_\mu) \text{ and } y \in (\mathbb{I} + \gamma\nabla f)(x_\mu) \\
& \Leftrightarrow (\exists y \in \mathbf{E}) \ \underbrace{(\mathbb{I} + \gamma\nabla^{\mu_0})^{-1}(2x_\mu - y)}_{=\mathbb{J}_{\gamma\nabla\mu_0}} \ni x \text{ and } \underbrace{(\mathbb{I} + \gamma\nabla f)^{-1}(y)}_{=\mathbb{J}_{\gamma\nabla f}} \ni x_\mu \\
& \stackrel{a)}{\Leftrightarrow} (\exists y \in \mathbf{E}) \ x_\mu \in \mathbb{J}_{\gamma\nabla\mu_0}(2x_\mu - y) \text{ and } x_\mu = \mathbb{J}_{\gamma\nabla f}(y) \\
& \stackrel{b)}{\Leftrightarrow} (\exists y \in \mathbf{E}) \ x_\mu = \mathbb{J}_{\gamma\nabla\mu_0}\mathbb{R}_{\gamma\nabla f}(y) \text{ and } x_\mu = \mathbb{J}_{\gamma\nabla f}(y), \tag{33}
\end{aligned}$$

where  $a)$  uses the facts that  $\mathbb{J}_{\gamma\nabla f}$  is a single-valued operator everywhere, whereas  $\mathbb{J}_{\gamma\nabla\mu_0}$  is a single-valued operator on the region of convexity  $B(\bar{x}; r_\mu)$  (Lemma 4), and  $b)$  uses the observation that  $x_\mu = \mathbb{J}_{\gamma\nabla f}(y)$  can be expressed as

$$x = \mathbb{J}_{\gamma\nabla f}(y) \Leftrightarrow 2x - y = (2\mathbb{J}_{\gamma\nabla f} - \mathbb{I})y = \mathbb{R}_{\gamma\nabla f}(y). \tag{34}$$

Also, using the last expression, we can write the first term of (33) as

$$\begin{aligned}
& \mathbb{J}_{\gamma\nabla\mu_0}\mathbb{R}_{\gamma\nabla f}(y) = x_\mu \\
& \Leftrightarrow 2\mathbb{J}_{\gamma\nabla\mu_0}\mathbb{R}_{\gamma\nabla f}(y) - y \stackrel{a)}{=} \mathbb{R}_{\gamma\nabla f}(y) \\
& \Leftrightarrow y = 2\mathbb{J}_{\gamma\nabla\mu_0}\mathbb{R}_{\gamma\nabla f}(y) - \mathbb{R}_{\gamma\nabla f}(y) \\
& \quad = (2\mathbb{J}_{\gamma\nabla\mu_0} - \mathbb{I})(\mathbb{R}_{\gamma\nabla f}(y)) \\
& \quad = \mathbb{R}_{\gamma\nabla\mu_0}\mathbb{R}_{\gamma\nabla f}(y) \\
& \Leftrightarrow y \in \mathbf{fix}(\mathbb{R}_{\gamma\nabla\mu_0}\mathbb{R}_{\gamma\nabla f}), \tag{35}
\end{aligned}$$

where  $a)$  uses (34). Using (33), (35), and  $\mathbb{J}_{\gamma\partial f} = \mathbf{prox}_{\gamma f}$  we have

$$\begin{aligned}
& x_\mu \in \mathbf{zer}(\nabla f + \nabla^{\mu_0}) \\
& \Leftrightarrow (\exists y \in \mathbf{E}) \ y \in \mathbf{fix}(\mathbb{R}_{\gamma\nabla\mu_0}\mathbb{R}_{\gamma\nabla f}) \text{ and } x_\mu = \mathbf{prox}_{\gamma f}(y) \\
& \Leftrightarrow x_\mu \in \mathbf{prox}_{\gamma f}(\mathbf{fix}(\mathbb{R}_{\gamma\nabla\mu_0}\mathbb{R}_{\gamma\partial f})).
\end{aligned}$$

Thus  $x_\mu$ , which is a locally optimal solution to the optimization problem  $(\mathcal{P}_\mu)$  over  $B(\bar{x}; r_\mu)$ , satisfies

$$x_\mu = \mathbf{zer}(\nabla f + \nabla^{\mu_0}) = \mathbf{prox}_{\gamma f}(\mathbf{fix}(\mathbb{R}_{\gamma\nabla\mu_0}\mathbb{R}_{\gamma\partial f})),$$

where the sets are singletons. Also, from (20)

$$\mathbf{fix} T_\mu = \mathbf{fix} R_\mu = \mathbf{fix}(\mathbb{R}_{\gamma\nabla\mu_0}\mathbb{R}_{\gamma\partial f}),$$

hence we have arrived at (10). Furthermore,  $f + \mu_0$  in  $(\mathcal{P}_\mu)$  is strongly-convex and smooth function over  $B(\bar{x}; r_\mu)$  due to Lemma 4(ii), so  $x_\mu$  will be the unique local minimum to  $f + \mu_0$  over  $B(\bar{x}; r_\mu)$ . So, the sets  $\mathbf{zer}(\nabla f + \nabla^{\mu_0})$ ,  $\mathbf{fix} T_\mu$ , and  $\mathbf{prox}_{\gamma f}(\mathbf{fix} T_\mu)$  are singletons.

## B.7 Proof to Proposition 2

To prove (i), we are going to use the following corollary, which follows directly from Lemma 6.

**Corollary 3.** *Let  $\bar{x} \in \mathcal{X}$  be a local minimum to  $(\mathcal{P})$ , where Assumptions 1, 2, and 3 hold. Define  $\mathfrak{M} = [\mu_{\min}, \mu_{\max}]$ , and let  $x_\mu$  be the local minimum of  $f + \mu \mathfrak{v}$  over the ball  $B(\bar{x}, \check{\mu})$ , where  $\mu_{\min}, \mu_{\max}, \check{\mu}$  are defined in Remark 1. Let  $\mu_{\min} < \mu_{\max}$ . Then for any  $\mu \in \mathfrak{M}$*

$$\|\mathbf{\Pi}(x_\mu) - \bar{x}\| < \alpha \min_{\mu \in \mathfrak{M}} r_\mu, \quad (36)$$

where  $\alpha \in \left(0, \frac{1}{\eta'} - \frac{1}{\eta}\right)$ ,  $\eta' \in (1, \eta)$  with  $\eta > 1$  being the constant defined in Assumption 2.

(i): For any  $\mu \in \mathfrak{M}$  we can express  $x_\mu$  as

$$x_\mu = \frac{1}{\beta\mu + 1} (\mathbf{\Pi}(x_\mu) - \mu \nabla f(x_\mu)), \quad (37)$$

due to (31). Now, for any  $\mu \in \mathfrak{M}$ ,

$$\begin{aligned} \|x_\mu - \bar{x}\| &\stackrel{a)}{=} \left\| \frac{1}{\beta\mu + 1} (\mathbf{\Pi}(x_\mu) - \mu \nabla f(x_\mu)) - \bar{x} \right\| \\ &= \frac{1}{\beta\mu + 1} \|\mathbf{\Pi}(x_\mu) - \bar{x} - \mu \nabla f(x_\mu) - \beta\mu \bar{x}\| \\ &\stackrel{b)}{\leq} \frac{1}{\beta\mu + 1} (\|\mathbf{\Pi}(x_\mu) - \bar{x}\| + \|\mu \nabla f(x_\mu) + \beta\mu \bar{x}\|) \\ &\stackrel{c)}{<} \frac{1}{\beta\mu + 1} \left( \alpha \min_{\mu \in \mathfrak{M}} r_\mu + \mu \|\nabla f(x_\mu)\| + \beta\mu \|\bar{x}\| \right) \\ &= \frac{\alpha}{\beta\mu + 1} \min_{\mu \in \mathfrak{M}} r_\mu + \frac{\beta\mu}{\beta\mu + 1} \left( \frac{1}{\beta} \|\nabla f(x_\mu)\| + \|\bar{x}\| \right) \\ &\stackrel{d)}{\leq} \frac{\alpha}{\beta\mu + 1} \min_{\mu \in \mathfrak{M}} r_\mu + \frac{\beta\mu}{\beta\mu + 1} \left( \frac{G}{\beta} + M \right) \\ &\stackrel{e)}{\leq} \frac{\alpha}{\beta\mu + 1} \min_{\mu \in \mathfrak{M}} r_\mu + \frac{1}{\eta} c_{\bar{x}} \frac{\beta\mu}{\beta\mu + 1} \\ &\stackrel{d)}{\leq} \frac{\alpha}{\beta\mu + 1} \min_{\mu \in \mathfrak{M}} r_\mu + \frac{1}{\eta} r_\mu \\ &\stackrel{e)}{\leq} \alpha \min_{\mu \in \mathfrak{M}} r_\mu + \frac{1}{\eta} r_\mu \\ &\leq \alpha r_\mu + \frac{1}{\eta} r_\mu \\ &\stackrel{f)}{<} \left( \frac{1}{\eta'} - \frac{1}{\eta} \right) r_\mu + \frac{1}{\eta} r_\mu \end{aligned} \quad (38)$$

$$= \frac{1}{\eta'} r_\mu, \quad (39)$$

where  $a)$  uses (37),  $b)$  uses triangle inequality,  $c)$  uses triangle inequality and (36) in Corollary 3,  $d)$  and  $e)$  use Assumption 2,  $e)$  uses  $1/(1 + \beta\mu) \leq 1$ ,  $f)$  applies  $\alpha \in \left(0, \frac{1}{\eta'} - \frac{1}{\eta}\right)$  with  $\eta' \in (1, \eta)$ . As, objective function  $f + \mu_0$  is strongly convex and smooth over  $B(\bar{x}; r_\mu)$ , from Lemma 7,  $x_\mu$  is the unique local minimum to the optimization problem  $(\mathcal{P}_\mu)$  over  $B(\bar{x}; r_\mu)$ . This completes (i).

(ii): In (i), we have shown that for any  $\mu \in \mathfrak{M}$ ,

$$\|x_\mu - \bar{x}\| \leq \frac{1}{\eta'} r_\mu,$$

where  $\eta' > 1$ . From (38), and recalling that  $\eta' > 1$ , for any  $\mu \in \mathfrak{M}$ ,

$$\begin{aligned} \|x_\mu - \bar{x}\| &\leq \frac{1}{\eta'} r_\mu \\ \Leftrightarrow r_\mu - \|x_\mu - \bar{x}\| &\geq \frac{\eta' - 1}{\eta'} r_\mu \\ \Rightarrow \min_{\mu \in \mathfrak{M}} r_\mu - \|x_\mu - \bar{x}\| &\geq \frac{\eta' - 1}{\eta'} \min_{\mu \in \mathfrak{M}} r_\mu \\ &\stackrel{a)}{\geq} \underbrace{\frac{\eta' - 1}{\eta'} \frac{c_{\bar{x}} \beta \mu_{\min}}{\beta \mu_{\min} + 1}}_{>0}, \end{aligned} \quad (40)$$

where  $a)$  uses (5) in Lemma 4. Thus, taking any  $\phi \in \left(0, \frac{\eta' - 1}{\eta'} \frac{c_{\bar{x}} \beta \mu_{\min}}{\beta \mu_{\min} + 1}\right)$ , we arrive at the first claim.

Next, from Lemma 7, the fixed point  $z_\mu$  corresponding to  $x_\mu$  satisfies

$$\begin{aligned} x_\mu &= \mathbf{prox}_{\gamma f}(z_\mu) \\ \Leftrightarrow z_\mu &= x_\mu + \gamma \nabla f(x_\mu) \end{aligned}$$

Hence, for any  $\mu \in \mathfrak{M}$ ,

$$\begin{aligned} \|z_\mu - \bar{x}\| &= \|x_\mu + \gamma \nabla f(x_\mu) - \bar{x}\| \\ &\leq \|x_\mu - \bar{x}\| + \gamma \|\nabla f(x_\mu)\| \\ \Leftrightarrow r_\mu - \|z_\mu - \bar{x}\| &\geq r_\mu - \|x_\mu - \bar{x}\| - \gamma \|\nabla f(x_\mu)\| \\ &\stackrel{a)}{\geq} \phi - \gamma \|\nabla f(x_\mu)\|, \end{aligned}$$

where  $a)$  uses (40). Because, for the strongly convex and smooth function  $f$ , its gradient is bounded over a bounded set  $B(\bar{x}; r_{\mu_{\max}})$  [53, Lemma 1, §1.4.2], for a sufficiently small  $\gamma$ , we can ensure that there exists a positive number  $\psi$  such that

$$r_\mu - \|z_\mu - \bar{x}\| > \psi,$$

for any  $\mu \in \mathfrak{M}$ . To be precise, if we take  $0 < \gamma < \frac{\phi}{\max_{\mu \in \mathfrak{M}} \|\nabla f(x_\mu)\|}$ , then for any  $\mu \in \mathfrak{M}$ ,

$$\phi - \gamma \|\nabla f(x_\mu)\| > \phi - \frac{\phi}{\max_{\mu \in \mathfrak{M}} \|\nabla f(x_\mu)\|} \|\nabla f(x_\mu)\|$$

$$\begin{aligned}
&= \phi \left( 1 - \frac{\|\nabla f(x_\mu)\|}{\max_{\mu \in \mathfrak{M}} \|\nabla f(x_\mu)\|} \right) \\
&\geq 0,
\end{aligned}$$

and by setting  $\psi = \phi - \gamma \|\nabla f(x_\mu)\|$  for  $0 < \gamma < \frac{\phi}{\max_{\mu \in \mathfrak{M}} \|\nabla f(x_\mu)\|}$ , we arrive at the last claim.

## B.8 Proof to Theorem 1

We use the following result from [66] in proving Theorem 1.

**Theorem 2** (Convergence of local contraction mapping [66, Theorem 1A.2]). *Let  $\mathbb{A} : \mathbf{E} \rightarrow \mathbf{E}$  be some operator. If there exist  $\tilde{x}$ ,  $\omega \in (0, 1)$ , and  $r > 0$  such that*

(a) *the operator  $\mathbb{A}$  is  $\omega$ -contractive on  $B(\tilde{x}; r)$ , i.e., for all  $x_1, x_2$  in  $B(\tilde{x}; r)$ :*

$$\|\mathbb{A}(x_1) - \mathbb{A}(x_2)\| \leq \omega \|x_1 - x_2\|,$$

and

(b)

$$\|\mathbb{A}(\tilde{x}) - \tilde{x}\| \leq (1 - \omega)r.$$

*Then  $\mathbb{A}$  has a unique fixed point in  $B(\tilde{x}; r)$  and the iteration scheme  $x_{n+1} = \mathbb{A}(x_n)$  with the initialization  $x_0 := \tilde{x}$  linearly converges to that unique fixed point.*

*Proof.* The proof of this theorem can be found in [66, pp. 313-314]. □

Furthermore, recall that NExOS (Algorithm 1) can be compactly represented using (Compact-OI) in §3.1 as follows. For any  $m \in \{1, 2, \dots, N\}$  (equivalently for each  $\mu_m \in \{\mu_1, \dots, \mu_N\}$ ),

$$z_{\mu_m}^{n+1} = \mathbb{T}_{\mu_m}(z_{\mu_m}^n), \tag{41}$$

where  $z_{\mu_m}^0$  is initialized at  $z_{\mu_{m-1}}$ .

Now we start the proof. First, we provide the proof when we consider exact fixed point, and then we present the proof for the case where we consider approximate fixed point. The proof for approximate fixed point is structurally very similar to the exact case but somewhat more cumbersome, hence we present it later.

**Proof for exact fixed point.** From Proposition 1, for any  $\mu \in \mathfrak{M}$ , the operator  $\mathbb{T}_\mu$  is a  $\kappa'$ -contraction mapping over the region of convexity  $B(\bar{x}; r_\mu)$ . From Lemma 4 there will be a unique local minimum  $x_\mu$  of over  $B(\bar{x}; r_\mu)$ . Suppose, we have computed the unique fixed point  $z_{\mu_{m-1}} \in \mathbf{fix} \mathbb{T}_{\mu_{m-1}}$  by solving the outer iteration corresponding to  $\mu_{m-1}$ . Now we select the new penalty parameter

$$\mu_m = \mu_{m-1} - \Delta_{m-1}, \tag{42}$$

where

$$0 < \Delta_{m-1} \leq \frac{(1 - \kappa')}{\ell} \psi, \tag{43}$$

where  $\psi > 0$  is a constant that was defined in Proposition 2(ii), and from Lemma 5,  $\ell$  is the Lipschitz constant of the Douglas-Rachford operator in  $\mu$  for fixed argument, which does not change as we are operating in the bounded set  $B(\bar{x}; r_{\mu_{\max}})$ . So the right-hand side in (43) is a strictly positive constant, and we can always reduce  $\mu_m$  by that amount (until we are close to  $\mu_{\min}$ , when we just reduce the necessary amount to reach  $\mu_{\min}$ ). We claim that, if we reduce  $\mu_m$  by the aforementioned rule, then for any  $\mu_m \in \mathfrak{M}$ , each outer iteration scheme (41) will converge linearly to the corresponding fixed point of the operator  $\mathbb{T}_{\mu_m}$ , which we prove now.

We initialize the compact form of the outer iteration scheme (41) for  $\mu_m$  at the previously found fixed point  $z_{\mu_{m-1}}$ , i.e.,  $z_{\mu}^{n+1} = \mathbb{T}_{\mu_m}(z_{\mu}^n)$  at  $z_{\mu_m}^0 := z_{\mu_{m-1}}$ . Around this initial point, let us construct the open ball  $B(z_{\mu_{m-1}}; \psi)$ . Set  $r_{\mu_m} := \psi + \|z_{\mu_{m-1}} - \bar{x}\|$ . Then  $B(z_{\mu_{m-1}}; \psi) \subseteq B(\bar{x}; r_{\mu_m}) \subseteq B(\bar{x}; r_{\mu_{m-1}})$  because for any  $x \in B(z_{\mu_{m-1}}; \psi)$ , we have

$$\begin{aligned} \|x - \bar{x}\| &\leq \underbrace{\|x - z_{\mu_{m-1}}\|}_{< \psi} + \|z_{\mu_{m-1}} - \bar{x}\| \\ &< \psi + \|z_{\mu_{m-1}} - \bar{x}\| \quad (\text{this is equal to } r_{\mu_m} \text{ by construction}) \\ &\stackrel{a)}{<} r_{\mu_{m-1}} - \|z_{\mu_{m-1}} - \bar{x}\| + \|z_{\mu_{m-1}} - \bar{x}\| \\ &= r_{\mu_{m-1}}, \end{aligned}$$

where in *a)* we have used Proposition 2(ii). So, from Proposition 1, on  $B(z_{\mu_{m-1}}; \psi) \subseteq B(\bar{x}; r_{\mu_m})$  the Douglas-Rachford operator  $\mathbb{T}_{\mu_m}$  is contractive for  $\mu_m$  selected using (42). Also,

$$\begin{aligned} \|\mathbb{T}_{\mu_m}(z_{\mu_{m-1}}) - z_{\mu_{m-1}}\| &= \|\mathbb{T}_{\mu_m}(z_{\mu_{m-1}}) - \mathbb{T}_{\mu_{m-1}}(z_{\mu_{m-1}})\| \\ &\stackrel{a)}{\leq} \ell \|\mu_m - \mu_{m-1}\| \\ &\stackrel{b)}{=} \ell \Delta_{m-1} \\ &\stackrel{c)}{\leq} (1 - \kappa')\psi, \end{aligned}$$

where *a)* uses Lemma 5, with  $\ell$  being the Lipschitz constant of  $\mathbb{T}_{\mu}$ , *b)* uses (42), and *c)* uses (43). Hence, both conditions of Theorem 2 are satisfied, and the iterates  $z_{\mu_m}^n$  in (41) will linearly converge to the unique fixed point  $z_{\mu_m}$  of the operator  $\mathbb{T}_{\mu_m}$ , and  $x_{\mu_m}^{n+1} = \mathbf{prox}_{\gamma f}(z_{\mu_m}^n)$  will linearly converge to the corresponding locally optimal solution  $x_{\mu_m} = \mathbf{prox}_{\gamma}(z_{\mu_m})$  due to the continuity of  $\mathbf{prox}_{\gamma f}$ . Furthermore,

$$\begin{aligned} \mathbb{T}_{\mu_m}(z_{\mu_m}^n) - z_{\mu_m}^n &= \left( \overbrace{2\mathbf{prox}_{\gamma \mu_0}(2\mathbf{prox}_{\gamma f}(z_{\mu_m}^n) - z_{\mu_m}^n)}^{=y_{\mu_m}^{n+1}} - \overbrace{\mathbf{prox}_{\gamma f}(z_{\mu_m}^n)}^{=x_{\mu_m}^{n+1}} \right) \\ &= y_{\mu_m}^{n+1} - x_{\mu_m}^{n+1}, \end{aligned}$$

so  $\mathbb{T}_{\mu_m}(z_{\mu_m}^n) - z_{\mu_m}^n \rightarrow 0$  is equivalent to  $y_{\mu_m}^{n+1} - x_{\mu_m}^{n+1} \rightarrow 0$ . Adding this to  $x_{\mu_m}^{n+1} \rightarrow x_{\mu_m}$  we have  $y_{\mu_m}^{n+1} \rightarrow x_{\mu_m}$ .

Finally,  $x_{\mu_{\min}} \rightarrow \bar{x}$  as  $\mu_{\min} \rightarrow 0$ , which follows from Lemma 6(ii). This completes our proof.

**Proof for approximate fixed point.** Now suppose that, in place of an exact fixed point  $z_{\mu_{m-1}}$ , we have  $\tilde{z}$ , which is an approximate fixed point of  $\mathbb{T}_{\mu_{m-1}}$  in  $B(\bar{x}; r_\mu)$ , *i.e.*,  $\|z_{\mu_{m-1}} - \tilde{z}\| \leq \epsilon$  where  $\epsilon$  is a small positive number. Then

$$\|\mathbb{T}_{\mu_{m-1}}(\tilde{z}) - \mathbb{T}_{\mu_{m-1}}(z_{\mu_{m-1}})\| \stackrel{a)}{\leq} \kappa' \overbrace{\|\tilde{z} - z_{\mu_{m-1}}\|}^{\leq \epsilon} \leq \epsilon, \quad (44)$$

where *a)* uses  $\kappa'$ -contractive nature of  $\mathbb{T}_{\mu_{m-1}}$  over  $B(\bar{x}; r_\mu)$ . Hence, using triangle inequality,

$$\begin{aligned} \|\tilde{z} - \bar{x}\| &\stackrel{a)}{\leq} \|\tilde{z} - \mathbb{T}_{\mu_{m-1}}(\tilde{z})\| + \|\mathbb{T}_{\mu_{m-1}}(\tilde{z}) - z_{\mu_{m-1}}\| + \|z_{\mu_{m-1}} - \bar{x}\| \\ &\stackrel{b)}{\leq} 2\epsilon + \|z_{\mu_{m-1}} - \bar{x}\|, \end{aligned}$$

where *a)* uses triangle inequality and *b)* uses (44). Hence, using the last inequality, for a sufficiently small  $\epsilon$ , *e.g.*, by picking

$$\epsilon \in \left(0, \frac{1}{2} \min_{\mu \in \mathfrak{M}} (r_\mu - \|z_\mu - \bar{x}\|) - \psi\right), \quad (45)$$

which will work for all  $\mu \in \{\mu_1, \dots, \mu_N\}$ , we can ensure that

$$r_{\mu_{m-1}} - \|\tilde{z} - \bar{x}\| > \psi, \quad (46)$$

where we used Proposition 2(ii). In this case, the penalty parameter is set as:

$$\mu_m = \mu_{m-1} - \Delta_{m-1}, \quad (47)$$

where

$$0 < \Delta_{m-1} \leq \frac{(1 - \kappa')\psi - \epsilon}{\ell}, \quad (48)$$

where the right hand side can be kept positive for sufficiently small  $\epsilon$ . Now, we initialize the iteration scheme  $z_{\mu_m}^{n+1} = \mathbb{T}_{\mu_m}(z_{\mu_m}^n)$  at  $z_{\mu_m}^0 := \tilde{z}$ . Around this initial point, let us construct the open ball  $B(\tilde{z}, \psi)$ . Set  $r_{\mu_m} := \psi + \|\tilde{z} - \bar{x}\|$ . Then we can again show that  $B(\tilde{z}; \psi) \subseteq B(\bar{x}; r_{\mu_m}) \subseteq B(\bar{x}; r_{\mu_{m-1}})$ . Hence, from Proposition 1, on  $B(\tilde{z}; \psi)$ , the Douglas-Rachford operator  $\mathbb{T}_{\mu_m}$  is contractive. Similarly,  $\|\mathbb{T}_{\mu_m}(\tilde{z}) - \tilde{z}\| \leq (1 - \kappa')\psi$ . Thus, both conditions of Theorem 2 are satisfied, and  $z_{\mu_m}^n$  in (41) will linearly converge to the unique fixed point  $z_{\mu_m}$  of the operator  $\mathbb{T}_{\mu_m}$ , and  $x_{\mu_m}^n, y_{\mu_m}^n$  will linearly converge to  $x_{\mu_m}$ . Also, as we have decreased the penalty parameter strictly, *i.e.*,  $\mu_m < \mu_{m-1}$ , the new locally optimal solution  $x_{\mu_m}$  will be different than  $x_{\mu_{m-1}}$  due to Assumption 3. Finally, invoking Lemma 6(ii), we have  $x_{\mu_{\min}} \rightarrow \bar{x}$  as  $\mu_{\min} \rightarrow 0$ , which completes our proof.

## B.9 Proof to Proposition 3

From Proposition 1, we know that the operator  $\mathbb{T}_\mu$  is  $\kappa'$ -contractive on  $B(x; r_\mu)$ . First, we show that, for the given initialization of  $z_\mu^0$ , the iterates  $z_\mu^n$  stay in  $\overline{B}(z_\mu; \|z_\mu^0 - z_\mu\|)$  for any  $n \in \mathbf{N}$ . The base case is true, *i.e.*,  $z_\mu^0 \in \overline{B}(z_\mu; \|z_\mu^0 - z_\mu\|)$ . Let,  $z_\mu^n \in \overline{B}(z_\mu; \|z_\mu^0 - z_\mu\|)$ , *i.e.*,

$$\|z_\mu^n - z_\mu\| \leq \|z_\mu^0 - z_\mu\|. \quad (49)$$

Then

$$\|z_\mu^{n+1} - z_\mu\| \stackrel{a)}{=} \|\mathbb{T}_\mu(z_\mu^n) - \mathbb{T}_\mu(z_\mu)\|$$

$$\begin{aligned}
& \stackrel{b)}{\leq} \kappa' \|z_\mu^n - z_\mu\|, \\
& \stackrel{c)}{\leq} \kappa' \|z_\mu^0 - z_\mu\| \\
& \leq \|z_\mu^0 - z_\mu\|,
\end{aligned} \tag{50}$$

where  $a)$  uses  $z_\mu \in \mathbf{fix} \mathbb{T}_\mu$ , and  $b)$  uses Proposition 1, and  $c)$  uses (49). So, the iterates  $z_\mu^n$  stay in  $\overline{B}(z_\mu; \|z_\mu^0 - z_\mu\|)$  for all  $n \in \mathbf{N}$ . As,  $\kappa' \in (0, 1)$ , (50) also implies that  $z_\mu^n$  linearly converges to  $z_\mu$  with the rate of at least  $\kappa'$ . Then using similar reasoning presented in the proof to Theorem 1, we have  $x_\mu^n$  and  $y_\mu^n$  linearly converge to the unique local minimum  $x_\mu$  of  $(\mathcal{P}_\mu)$ . Finally, from Lemma 6(ii),  $x_\mu \rightarrow \bar{x}$  as  $\mu \rightarrow 0$ . This completes our proof.

## C Convergence results when Assumption 1 regarding smoothness and strong convexity of $f$ is removed

In this section, we remove Assumption 1 and instead assume that  $f$  is closed (its epigraph is a closed set), proper (it is finite somewhere and  $-\infty$  nowhere), and convex, but, unless specified, all the other setups in §3.1-§3.4 stay the same.

In this extended setup, Lemma 2 is not applicable anymore, and the operator  $2\mathbf{prox}_{\gamma f} - \mathbb{I}$  is just nonexpansive on  $\mathbf{E}$  and not contractive in general [46, Example 23.3 and Corollary 23.10].

Nonexpansiveness of  $2\mathbf{prox}_{\gamma f} - \mathbb{I}$  changes part of Lemma 4 as follows. Lemma 4(i) and (iii) stay intact as they do not involve  $f$ , but Lemma 4(ii) changes as follows: the objective function  $f + \mu_0$  is just convex now on the open ball  $B(x; r_\mu)$ , where this ball is the same one defined in Lemma 4.

This difference in the nature of  $f + \mu_0$  in turn changes Proposition 1: the operator  $\mathbb{R}_\mu$  will now be nonexpansive on  $B(x; r_\mu)$  due to (20) in B.3, and  $\mathbb{T}_\mu = (1/2)\mathbb{I} + (1/2)\mathbb{R}_\mu$  will now be firmly nonexpansive on  $B(x; r_\mu)$  due to [46, Definition 4.23 and Remark 4.24(iii)].

On the other hand, Lemma 5, which shows the Lipschitz continuity of  $\mathbb{T}_\mu(x)$  and  $\mathbb{R}_\mu(x)$  in the penalty parameter  $\mu$  for a fixed  $x$ , will still be the same because the proof does not depend on the nature of  $\mathbb{T}_\mu(x)$  or  $\mathbb{R}_\mu(x)$  with respect to  $x$ .

In Assumption 2,  $G$  will correspond to an upper bound on the norm of subgradient of  $f$  on  $B(\bar{x}; r)$  rather than gradient norm as the function is not necessarily differentiable anymore.

In Lemma 6(i), exterior point minimization function  $f + \mu_0$  in  $(\mathcal{P}_\mu)$  will not be differentiable in the open ball  $B(\bar{x}; \tilde{r})$  anymore, but will attain a local minimum of  $f + \mu_0$  in this ball. Lemma 6(ii) and Lemma 6(iii) will stay the same.

Under the new setup, Lemma 7 changes to the following. Any local minimum  $x_\mu$  to  $(\mathcal{P}_\mu)$  over some  $B(\bar{x}; r_\mu)$  will satisfy

$$x_\mu \in \mathbf{zer}(\partial f + \nabla \mu_0) = \mathbf{prox}_{\gamma f}(\mathbf{fix} \mathbb{T}_\mu),$$

where the sets  $\mathbf{zer}(\nabla f + \nabla \mu_0)$ ,  $\mathbf{fix} \mathbb{T}_\mu$ , and  $\mathbf{prox}_{\gamma f}(\mathbf{fix} \mathbb{T}_\mu)$  are not necessarily singletons over  $B(\bar{x}; r_\mu)$  anymore.

In Proposition 2(i), a local minimum  $x_\mu$  to  $(\mathcal{P}_\mu)$  over  $B(\bar{x}; r_\mu)$  will not be unique anymore as we do not have strong convexity of  $f + \mu_0$  on  $B(\bar{x}; r_\mu)$ , but rest of the results will hold. In the proof

to Proposition 2, we can consider any  $x_\mu$  arbitrarily and working with subgradient  $u \in \partial f(x_\mu)$  we can show again that as  $\mu \rightarrow 0$ ,  $x_\mu \rightarrow \bar{x}$  and  $(f + \mu \mathfrak{q})(x_\mu) \rightarrow f(\bar{x}) + \frac{\beta}{2} \|\bar{x}\|^2$ . Proposition 2(ii) stays the same.

Results in Theorem 1 and Proposition 3 will stay the same except the convergence rate will be sublinear. This is due to the fact that, under our new setup, the iteration scheme described by (41) will correspond to a locally firmly nonexpansive operator  $\mathbb{T}_{\mu_m}$ , rather than a locally contractive one in our previous setup. The resulting iteration scheme (**Compact-OI**) would correspond to the Krasnosel'skiĭ–Mann or averaged iteration [46, §5.2]. A straightforward application of [67, Theorem 1, Chapter 2] shows that,  $z_{\mu_m}^n$  converges to some  $z_{\mu_m} \in \mathbf{fix} \mathbb{T}_{\mu_m}$  with the rate

$$\|z_{\mu_m}^{n+1} - z_{\mu_m}^n\|^2 \leq \frac{1}{n+1} d_{\mathbf{fix} \mathbb{T}_{\mu_m}}^2(z_{\mu_m}^0)$$

and the iterates  $x_{\mu_m}^n, y_{\mu_m}^n$  converge to  $x_{\mu_m} = \mathbf{prox}_{\gamma f}(z_{\mu_m})$ . Finally,  $x_{\mu_{\min}} \rightarrow \bar{x}$  as  $\mu_{\min} \rightarrow 0$ , where the proof stays the same. Similarly, in Algorithm 2,  $z_\mu^n$  converges to  $z_\mu \in \mathbf{fix} \mathbb{T}_\mu$  with rate

$$\|z_\mu^{n+1} - z_\mu^n\|^2 \leq \frac{1}{n+1} d_{\mathbf{fix} \mathbb{T}_\mu}^2(z_\mu^0)$$

and both  $x_\mu^n$  and  $y_\mu^n$  converge to corresponding local minimum  $x_\mu = \mathbf{prox}_{\gamma f}(z_\mu)$  of  $(\mathcal{P}_\mu)$ , and  $x_\mu \rightarrow \bar{x}$  as  $\mu \rightarrow 0$ .